

WHITE MICAS IN THE LAKE LEWIS LEUCOGRANITE,
NOVA SCOTIA

Patrick Andrzej Bogutyn

Submitted in Partial Fulfillment of the Requirements
for the Degree of Bachelor of Science, Honours
Department of Earth Sciences
Dalhousie University, Halifax, Nova Scotia
March 2001



Dalhousie University

Department of Earth Sciences
Halifax, Nova Scotia
Canada B3H 3J5
(902) 494-2358
FAX (902) 494-6889

DATE

JULY 7, 2001

AUTHOR

PATRICK BOGUTYN

TITLE

WHITE Micas in THE

LAKE LEWIS LEUCOGRANITE

Nova Scotia

Degree

BSc

Convocation

FALL

Year

2001

Permission is herewith granted to Dalhousie University to circulate and to have copied for non-commercial purposes, at its discretion, the above title upon the request of individuals or institutions.

THE AUTHOR RESERVES OTHER PUBLICATION RIGHTS, AND NEITHER THE THESIS NOR EXTENSIVE EXTRACTS FROM IT MAY BE PRINTED OR OTHERWISE REPRODUCED WITHOUT THE AUTHOR'S WRITTEN PERMISSION.

THE AUTHOR ATTESTS THAT PERMISSION HAS BEEN OBTAINED FOR THE USE OF ANY COPYRIGHTED MATERIAL APPEARING IN THIS THESIS (OTHER THAN BRIEF EXCERPTS REQUIRING ONLY PROPER ACKNOWLEDGEMENT IN SCHOLARLY WRITING) AND THAT ALL SUCH USE IS CLEARLY ACKNOWLEDGED.

ABSTRACT

The South Mountain Batholith, a peraluminous granitic complex, ranges in composition from biotite granodiorite to muscovite-topaz leucogranite. Leucogranitic rocks form minor and late components of the batholith. The Lake Lewis Leucogranite belongs to the late-stage magmatic evolution of the batholith, and this thesis presents a new textural and chemical investigation of its white micas. Texturally the white micas form two groups: 1) primary micas that are coarse-grained, dimensionally compatible with other minerals, euhedral to subhedral with well-defined, sharp boundaries, and have muscovite-phengite epitaxial overgrowths; and 2) secondary micas that are also coarse-grained and dimensionally compatible with other minerals, but are anhedral with ragged edges, cataastically deformed (bent, kinked, and sheared), and altered with fluorite crystallization along cleavage planes. Chemically, these groups correspond to muscovite, phengite, protolithionite, and siderophyllite, respectively. Lithium may constitute an essential component required for the complete calculation of structural formulae and classification of the white micas, and the application of regression equations based on F and SiO₂ appear valid for the estimation of lithium contents. Classification of the micas, without calculated lithium using cation proportions, and with calculated lithium using the Mg–Li–Fe+Mn+Ti–Al^{VI} diagram, produces nearly identical nomenclature. Oscillatory zoning of muscovite(K₂Al₄[Si₆Al₂O₂₀])(OH, F)₄–phengite(K₂FeAl₃[Si₇AlO₂₀])(OH, F)₄) in some of the undeformed micas is consistent with the build-up and release of fluid pressures in the late stages of crystallization of the Lake Lewis Leucogranite. Textural and chemical evidence support the primary magmatic nature of the undeformed white micas, and the secondary hydrothermal nature of the deformed and chemically altered micas. Chemical substitution in the primary magmatic white micas is a combination of Tschermak substitution (Mg, Fe²⁺)^{VI}, Si^{IV} ↔ Al^{IV}, Al^{VI} and biotitic substitution 2/3 Al^{VI}, 1/3 □^{VI} ↔ (Fe²⁺)^{VI} (where □ stands for a vacant octahedral site) exchange mechanisms. Chemical substitution in the secondary and primary hydrothermal aplitic white micas produces zinnwaldite(K₂Fe_{3.1}Li_{1.3}(Al, Fe)₂[Si_{5.7}Al_{3.1}O₂₀])(F, OH)₄). Texturally, the plagioclases and K-feldspars are euhedral and unaltered, and appear to be primary magmatic phases. Chemically, the plagioclases are An₀₋₅ and the K-feldspars are Or₈₅₋₁₀₀. In high-fluorine magmas, complexing of calcium with fluorine may force the crystallization of nearly pure albite from the magma. The primary nature of the feldspars is consistent with the deduced primary nature of the white micas. Magmatic fluids expelled from the Lake Lewis Leucogranite probably carried Ca, F, and metallic elements that formed mineralized greisens, such as the nearby Walker Moly deposit. The epitaxially zoned muscovite-phengite grains have implications for tracing the magmatic evolution of the late leucogranite magma, and the reliability of ⁴⁰Ar/³⁹Ar dating.

Key Words: leucogranite, white mica, muscovite, phengite, zinnwaldite, lithium, fractional crystallization, fluido-magmatic, cation substitution, albite

ACKNOWLEDGEMENTS

I would like to extend my sincere thanks and gratitude to Professor D. Barrie Clarke for giving me the opportunity to experience the ups and downs of research, and whose knowledge of micas and the South Mountain Batholith was invaluable. He was very generous with his time and resources. I thank Sarah Carruzzo for discussions that helped flesh out ideas about the white micas. I must thank Bob MacKay for his expert assistance with the electron microprobe and kindly allowing me to share his office. I thank Gordon Brown for his speedy thin-section preparation and advice.

I thank Marcos Zentilli and Martin Gibling for their assistance through the 4200 class and critical reviews of parts of this thesis. Thanks to Norma Keeping and Darlene Van De Rijt for their administrative assistance. I am grateful to my elves, Jamel Joseph, for making a couple of last minute trips to the library and scanning of figures, and Melanie Purves, for helping me out with my feldspar summary table and cleaning up figures for Chapter 2, in the two weeks prior to the deadline. I must thank all my friends for all the laughs and keeping me sane during my thesis! I cannot finish this without the utmost gratefulness to my family. To my dad, for the constant reminders that this is only a project and financial assistance throughout my schooling, and to my mom, for all those home cooked meals left in my apartment when I was spending my days, and nights, in the LSC, I am forever indebted.

TABLE OF CONTENTS

ABSTRACT.....	i
ACKNOWLEDGEMENTS	ii
TABLE OF CONTENTS	iii
TABLE OF FIGURES.....	vi
TABLE OF TABLES.....	viii
CHAPTER 1 INTRODUCTION.....	1
1.1 Introduction.....	1
1.2 Leucogranites in general	1
1.3 Micas	1
<i>1.3.1 Chemistry of micas.....</i>	3
<i>1.3.2 Structure of micas</i>	4
<i>1.3.3 Muscovite</i>	7
1.4 Textural and chemical criteria for recognizing primary and secondary muscovite	9
1.5 Statement of purpose, objectives, and scope	12
1.6 Claim	13
1.7 Organization.....	13
CHAPTER 2 LAKE LEWIS LEUCOGRANITE.....	15
2.1 Leucogranites in the South Mountain Batholith.....	15
2.2 Relationship of Lake Lewis Leucogranite to South Mountain Batholith	17
2.3 Ages of the South Mountain Batholith and Lake Lewis Leucogranite	19
2.4 Geochemistry of leucogranite in the South Mountain Batholith.....	20
2.5 Relationship between leucogranites and mineral deposits in the South Mountain Batholith.....	24
2.6 Summary.....	25
CHAPTER 3 METHODOLOGY.....	26
3.1 Introduction.....	26
3.2 Field Investigation.....	26
3.3 Petrographic methods.....	27
<i>3.3.1 Optical mineralogy techniques</i>	27
<i>3.3.2 Roycroft method</i>	27

3.4 Electron microprobe analysis	28
3.4.1 Sample preparation.....	29
3.4.2 Microprobe operating techniques.....	29
3.4.3 Backscattered electron images	30
3.5 Summary.....	30
CHAPTER 4 OBSERVATIONS AND RESULTS	31
 4.1 Petrographic observations.....	31
4.1.1 Thin sections	31
4.1.2 Thick sections.....	41
 4.2 Mineral chemical data	45
4.3 Summary.....	45
CHAPTER 5 DISCUSSION.....	57
 5.1 Introduction.....	57
 5.2 Lithium content of white micas	57
5.2.1 Mass balance method.....	60
5.2.2 Distribution coefficient method	61
5.2.3 Lithium estimates from electron microprobe analyses	61
5.2.4 Comparison of analyzed and calculated lithium	62
5.2.5 Summary	65
 5.3 Classification and nomenclature of white micas	65
5.3.1 Classification without lithium.....	65
5.3.2 Classification with lithium	66
5.3.3 Summary of mica classification	72
 5.4 Are the white micas primary or secondary?	72
5.4.1 Physical evidence.....	73
5.4.2 Chemical evidence	73
5.4.3 Coexisting feldspars.....	79
5.4.4 Evidence from Roycroft method.....	82
5.4.5 Summary	83
 5.5 Chemical substitution processes in the white micas	83
 5.6 Systematic spatial variation in composition of white micas.....	87
 5.7 Implications for $^{40}\text{Ar}/^{39}\text{Ar}$ dating of white micas	87
 5.8 Summary.....	89
CHAPTER 6 CONCLUSIONS.....	90
 6.1 Conclusions.....	90
 6.2 Recommendations for future work	92

REFERENCES.....	.93
APPENDIX A RAW MICA DATA.....	A1
APPENDIX B RAW FELDSPAR DATA.....	B1

TABLE OF FIGURES

CHAPTER 1

1.1	Graphical depiction of the principal variations in compositions of micas.....	5
1.2	Three-dimensional model of muscovite	6

CHAPTER 2

2.1	Simplified geological map of the eastern part of the SMB.....	16
2.2	Conventional argon release plots for two muscovite separates from the Lake Lewis Leucogranite.....	20
2.2	Major and trace element chemical variation diagrams of leucogranitic rocks from the South Mountain Batholith	21
2.3	Variation diagrams for rare earth elements of leucogranitic rocks from the South Mountain Batholith.....	22
2.4	Whole-rock $\delta^{18}\text{O}$ values variation diagrams for leucogranitic rocks from the South Mountain Batholith.....	23

CHAPTER 4

4.1	Geological map of the Lake Lewis Leucogranite with sample locations	32
4.2	Thin section photomicrographs of undeformed white micas.....	39
4.3	Backscattered electron image enlargement of epitaxial overgrowth	40
4.4	Thin section photomicrographs of deformed white micas	42
4.5	Thick mica photomicrographs	43

CHAPTER 5

5.1	Plot of octahedral site occupancies with and without lithium estimates	63
5.2	Comparison of calculated Li and analyzed Li	64
5.3a	Mica grouping of based on end-member mica cation proportion of Si and Al.....	67
5.3b	Mica grouping based on end-member mica cation proportion of Fe+Mn+Mg and Al	68
5.4	Diagram of principal components of biotite compositions.....	69
5.5	Compositional fields of natural micas on mgli-feal diagram.....	70
5.6	Mgli-feal diagram of Lake Lewis Leucogranite micas.....	71
5.7	Plot of Fe against Na/(Na+K)	75
5.8	Plot of Na_2O against Al_2O_3	76
5.9	Plot of SiO_2 against MgO	77
5.10	Miscibility gap between muscovite and biotite	78
5.11	Ternary plot of Lake Lewis Leucogranite feldspar compositions	80

5.12	Lake Lewis Leucogranite feldspar thin section photomicrographs	81
5.13a	Chemical substitution plot of Si against Fe+Mg.....	85
5.13b	Chemical substitution plot of Fe+Mn+Mg against Al	86
5.14a	Different ages given by the muscovite-phengite zones.....	88
5.14b	Similar ages given by the muscovite-phengite zones	88

TABLE OF TABLES**CHAPTER 1**

1.1	Definitions of various terms	2
1.2	Principal constituents in the categories X, Y, and Z depicted with approximate formulae	4
1.3	Physical and chemical criteria to distinguish primary from secondary muscovite	10

CHAPTER 2

2.1	Summary comparison of petrographic data for leucogranitic rocks in the eastern South Mountain Batholith	18
-----	--	----

CHAPTER 4

4.1	Petrographic descriptions.....	33
4.2	Mica group averages and standard deviations	46
4.3	Averages and standard deviations of feldspar analyses.....	48

CHAPTER 5

5.1	Summary of methods for calculating lithium	58
5.2	Granitic mineral/melt distribution coefficients for lithium.....	60
5.3	Cation proportions for end-member micas	65

CHAPTER 1

INTRODUCTION

1.1 Introduction

Mineral deposits in the South Mountain Batholith belong to the latest magmatic stages of evolution, and to various stages of its subsolidus history. Primary magmatic and secondary hydrothermal white micas bridge these stages, and a better understanding of these micas could contribute to a better understanding of the origin and timing of mineral deposits. Table 1.1 defines various terms used in this thesis.

1.2 Leucogranites in general

This thesis uses the Streckeisen (1976) definition of “leuco” referring to igneous rocks with 0-6% ferromagnesian minerals. “Leucogranitic rocks” and “leucogranite” is used as a general name for leucocratic monzogranite or leucogranite.

The heterogeneity of the South Mountain Batholith results from extensive convective fractional crystallization from a more primitive magma to produce more evolved central leucogranitic rocks. Iron and magnesium were preferentially removed from the magma first, and used to create biotite. Calcium was partitioned into plagioclase. Both biotite and plagioclase decrease in abundance towards the center of the batholith producing rocks of lighter color (Clarke and Chatterjee 1988).

1.3 Micas

Mica minerals show considerable variation in their chemical compositions and physical structures (Tischendorf et al. 1997). A platy morphology and perfect basal

Table 1.1. Definitions of various terms used in this thesis. Definitions taken from Bates and Jackson (1987).

Term	Definition
Biotite	A widely distributed and important rock-forming mineral of the mica group: $K_2(Mg, Fe^{2+})_6(Al, Fe^{3+})Si_6O_{20}(OH)_4$. It is generally black, dark brown, or dark green, and forms a constituent of crystalline rocks (either as an original crystal in igneous rocks of all kinds or a product of metamorphic origin in gneisses and schists) or a detrital constituent of sandstones and other sedimentary rocks. Biotite is useful in the potassium-argon method of age determination.
Cataclasis	Rock deformation accomplished by fracture and rotation of mineral grains or aggregates without chemical reconstitution.
Cataclastic	Pertaining to the structure produced in a rock by the action of severe mechanical stress during dynamic metamorphism; characteristic features include bending, breaking, and granulation of the minerals. Also, said of the rocks exhibiting such structures.
Dioctahedral	Said of a layered-mineral structure in which only two of the three available octahedrally coordinated positions are occupied.
Epitaxial	Adjective of epitaxy.
Epitaxy	Orientation of one crystal with that of the crystalline substrate on which it grew. It is a type of overgrowth in which the two nets in contact share a common mesh.
Greisen	A pneumatolytically altered granitic rock composed largely of quartz, mica, and topaz. The mica is usually muscovite or lepidolite. Tourmaline, fluorite, rutile, cassiterite, and wolframite are common accessory minerals.
Greisenization	A process of hydrothermal alteration in which feldspar and muscovite are converted to an aggregate of quartz, topaz, tourmaline, and lepidolite (i.e., greisen) by the action of water vapor containing fluorine.
Muscovite	A mineral of the mica group: $K_2Al_4(Al, Si_6)O_{20}(OH)_4$. It is colorless to yellowish or pale brown, and is a common mineral in gneisses and schists, in most acid igneous rocks (such as granites and pegmatites), and in many sedimentary rocks (esp. sandstones).
Peraluminous	Said of an igneous rock in which the molecular proportion of aluminum oxide is greater than that of sodium and potassium oxides combined.

Table 1.1 continued

Phengite	A dioctahedral K-mica, of ideal composition $K_2[(Fe^{2+}, Mg)Al_3](Si_6Al)O_{20}(OH, F)_4$.
Trioctahedral	Pertaining to a layered-mineral structure in which all possible octahedral positions are occupied.
Zinnwaldite	A mineral of the mica group: $K_4(Li, Fe, Al)_6(Si, Al)_8O_{20}(OH, F)_4$. It is a pale-violet, yellowish, brown, or dark-gray variety of lepidolite containing iron, and is the characteristic mica of greisens.

cleavage characterizes micas as a result of their layered atomic structure (Deer et al. 1992).

1.3.1 Chemistry of micas

Deer et al. 1992 described the chemical composition of micas by the general formula $X_2Y_{4-6}Z_8O_{20}(OH, F)_4$ where

X is commonly K, Na, or Ca, but can also be Ba, Rb, Cs, among others;

Y is commonly Al, Mg, or Fe, but can also be Mn, Cr, Ti, Li, among others; and

Z is commonly Si or Al, but can also be Fe^{3+} and Ti.

Micas can be subdivided into dioctahedral and trioctahedral classes where the number of Y ions is 4 and 6 respectively. Further subdivisions are made according to the nature of the principal X constituent. X is largely K or Na in the common micas.

Table 1.2 shows further subdivisions according to the principal constituents in the categories X, Y, and Z, with approximate formulae. For muscovite, equivalent substitution of divalent ions for Al in Y sites can balance a ratio of Si:Al greater than 6:2

(Deer et al. 1992). Figure 1.1 graphically depicts the principal variations in compositions of micas.

A common feature among micas is their water content. Analyses show approximately 4-5 per cent H₂O⁺, except for those with high fluorine content (Deer et al. 1992). Table 26 in Deer et al. (1992) gives examples of mica chemical analyses.

Table 1.2. Principal constituents in the categories X, Y, and Z depicted with approximate formulae (Deer et al. 1992).

Di-octahedral				
	X	Y	Z	
Common micas	Muscovite	K ₂	Al ₄	Si ₆ Al ₂
	Paragonite	Na ₂	Al ₄	Si ₆ Al ₂
Brittle micas	Glaucophane	(K,Na) _{1.2-2.0}	(Fe,Mg,Al) ₄	Si _{7-7.6} Al _{1.0-0.4}
	Margarite	Ca ₂	Al ₄	Si ₄ Al ₄
Tri-octahedral				
	X	Y	Z	
Common micas	Phlogopite	K ₂	(Mg,Fe ²⁺) ₆	Si ₆ Al ₂
	Biotite	K ₂	(Mg,Fe,Al) ₆	Si ₆₋₅ Al ₂₋₃
Brittle micas	Zinnwaldite	K ₂	(Fe,Li,Al) ₆	Si ₆₋₇ Al ₂₋₁
	Lepidolite	K ₂	(Li,Al) ₅₋₆	Si ₆₋₅ Al ₂₋₃
	Clintonite	Ca ₂	(Mg,Al) ₆	Si _{2.5} Al _{3.5}

1.3.2 Structure of micas

Two identical layers of linked tetrahedra of (Si, Al)O₄, with a composite layer of octahedrally coordinated Y cations between the two layers, is the basic structural feature of micas (Deer et al. 1992). Figure 1.2 shows the three-dimensional structure of muscovite. Additional hydroxyl, fluoride, or chloride anions together with the apical oxygens complete the octahedral coordination of these cations. In muscovite, the structure has a central gibbsite layer Al₂(OH)₆, where apical oxygens of the tetrahedral layers (two on each side) replace four of the six hydroxyl ions. The centers of the

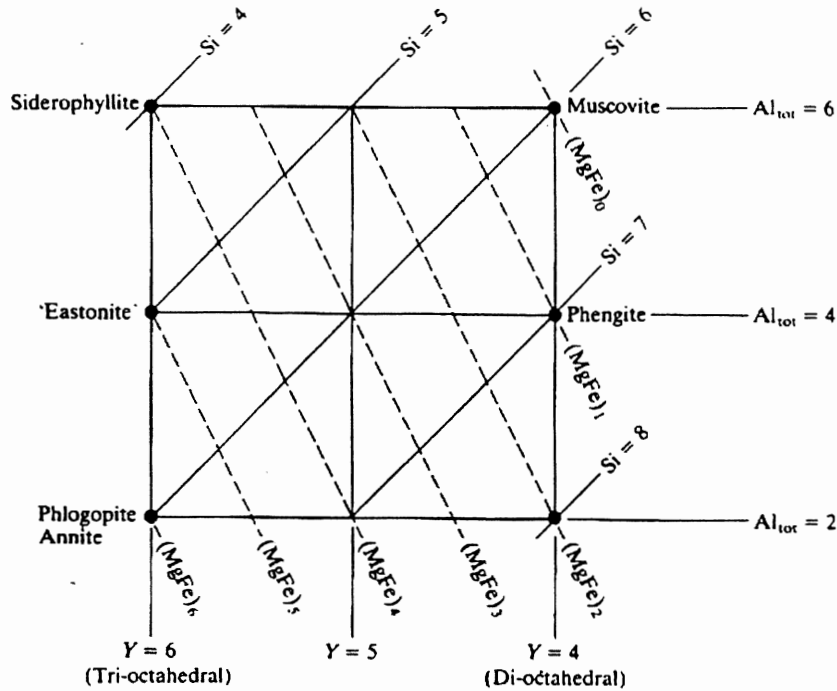


Figure 1.1. A graphical depiction of the principal variations in compositions of micas showing the number of octahedral sites filled (dioctahedral, 4; trioctahedral, 6), and Si, Al, and M^{2+} atoms per formula unit (Deer et al. 1992).

hexagons formed by the tetrahedral vertices hold the remaining hydroxyl ions

(Deer et al. 1992).

The tetrahedral layers have a net negative charge in micas that is balanced by planes lying between them composed of cations (X), such as K and Na. Because the cations lie centrally on the line joining the centers of hexagons formed by the basal oxygens of tetrahedral layers, they are in approximately 12-fold coordination. Going from the basal oxygens of one composite sheet to the analogous oxygens of its neighbor does not introduce lateral displacement. The hexagons can be superimposed in six

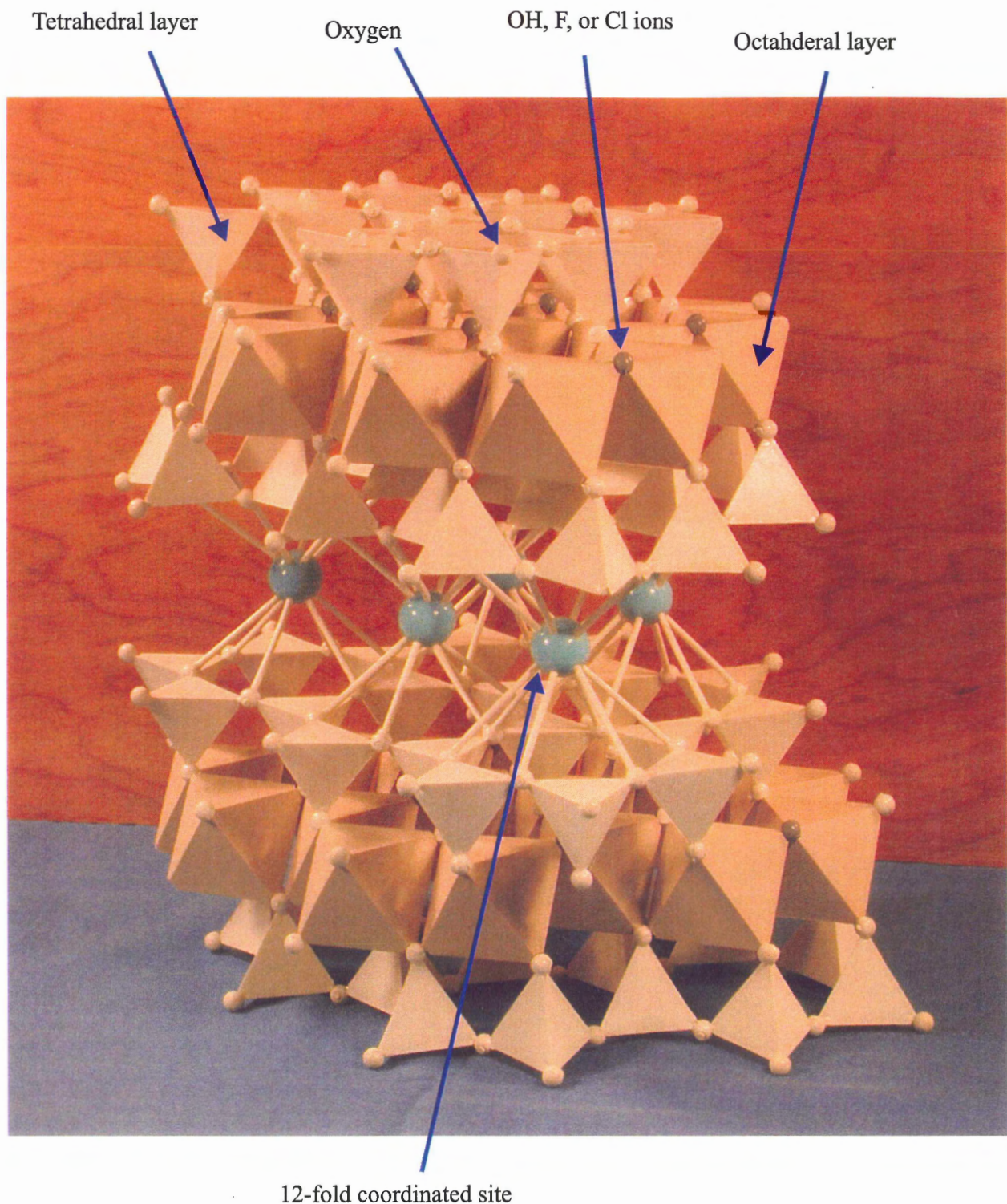


Figure 1.2. Three-dimensional model of muscovite.

different ways, so that one hexagon may be related to the next by a rotation through 0° or by a multiple of 60° (Deer et al. 1992).

This discussion describes an idealized mica layer. The true mica structure has twisted tetrahedra so that $(\text{Si}, \text{Al})_2\text{O}_5$ sheets have ditrigonal rather than hexagonal symmetry. These distortions achieve a dimensional match between the octahedral and larger ideal tetrahedral components, and are greater in dioctahedral micas than in trioctahedral micas (Deer et al. 1992).

There does not appear to be any ordering of the different cation species in the common micas (muscovite, biotite, and phlogopite) in octahedral and (Si, Al) in tetrahedral sites. In some other micas, distinct site preferences do occur (Deer et al. 1992).

1.3.3 Muscovite

Aluminum ions randomly occupy one quarter of the tetrahedral sites in muscovite ($\text{K}_2\text{Al}_4(\text{Si}_6\text{Al}_2\text{O}_{20})(\text{OH}, \text{F})_4$) and silicon ions occupy the rest. Potassium ions occupy the approximately 12-fold coordinated positions between composite layers. In muscovite, the main isomorphous replacements are:

For K: Na, Rb, Cs, Ca, and Ba

For octahedral Al: Mg, Fe^{2+} , Fe^{3+} , Mn, Li, Cr, Ti, and V

For OH: F

(Si_6Al_2) can vary to (Si_7Al) .

Muscovites have a low iron content. White micas with a high iron content are called phengites (Deer et al. 1992).

White micas with a high lithium content are known as lepidolites. Up to about 3.6 percent Li₂O may enter without changing the muscovite structure. Rather than replacing aluminum, lithium enters vacant octahedral sites, as in lepidolites, but other substitutions must occur to maintain charge balance. Natural muscovites have an average fluorine content of about 0.6 per cent. It is possible to synthesize fluor-muscovite, in which (OH) is replaced by fluorine (Deer et al. 1992).

Pink muscovites owe their color to the small amount of Mn³⁺ present, its preponderance over Fe²⁺, and the absence of Fe³⁺. Brown, pale green, or red muscovites owe their colors to varying amounts of Fe²⁺ and Fe³⁺, whereas the presence of Cr³⁺ leads to green colorations (Deer et al. 1992).

Lithian muscovites have lower refraction indices, but their optical properties are more influenced by the iron and manganese content rather than by the percentage of Li₂O. The refractive indices of phengites, illites, and hydrous muscovites are higher than normal muscovite because of the replacement of Al^{IV} (Al in the tetrahedral site) by Si and of Al^{VI} (Al in the octahedral site) by Fe²⁺ or Mg (Deer et al. 1992).

An increase in the substitution of Na for K and in Ti content correlates with higher temperature conditions, but at the highest temperatures, muscovite becomes enriched in potassium, and albite is formed. The muscovites of peraluminous granites are generally fluorine-rich and have greater thermal stability than most quartz-rich muscovite-bearing granites containing both potassium feldspar and plagioclase. In these granites, muscovite occurs in interstitial crystals and as small dispersed flakes within feldspar (Deer et al. 1992).

The P-T stability curve for synthetic end-member muscovite intersects the P-T minimum melting curve of granite at approximately 3.5 kbar and 700°C. Such muscovite can thus crystallize from a liquid of granitic composition at pressures above 3.5 kbar, but below this pressure, it can only form in the solid state (the position of the stability curve for natural muscovite compositions will, however, be different). Larger interstitial muscovite crystals in granites could, therefore, have formed in equilibrium with the liquid, or have crystallized in the solid state at any pressure or temperature below the stability curve of muscovite. Smaller flakes of muscovite commonly dispersed within feldspar most likely crystallized by leaching of K and Si from the feldspar at temperatures below the granite solidus (Deer et al. 1992).

1.4 Textural and chemical criteria for recognizing primary and secondary muscovite

Table 1.3 presents a variety of physical and chemical criteria for distinguishing between primary magmatic and secondary non-magmatic muscovite. Distinctions between different types of muscovite based on chemical criteria must first be made using physical criteria. Even though individual textural criteria can be challenged (Zen 1988), together with chemical differences between the different types of muscovite, they provide the only means of distinguishing between magmatic and non-magmatic muscovite. Several studies show that the textural and chemical criteria of Table 1.3 are not always adequate to distinguish between different types of muscovite (Fallon 1998). In the South Mountain Batholith, Ham and Kontak (1988) did not find a difference in TiO₂ contents between magmatic and non-magmatic muscovite.

Table 1.3. Physical and chemical criteria to distinguish primary from secondary muscovite (after Fallon 1998, criteria adapted from Miller et al. 1981, Speer 1984, Ham and Kontak 1988, Zen 1988, and Roycroft 1991).

Physical Criteria	
Primary Magmatic Muscovite	Secondary Post-Magmatic Muscovite
Muscovite must be:	
1. coarse grained, comparable to other magmatic phases, especially biotite	1. Muscovite may be subhedral or euhedral in shape and of comparable grain size to other magmatic phases, but is normally enclosed within mineral from which it has formed.
2. subhedral or euhedral in habit with sharp, well-defined grain boundaries	2. Muscovite altering plagioclase or K-feldspar usually takes the form of a fine-grained dense mass concentrated in the core of the host mineral; subhedral-euhedral grains along cleavage traces or in fractures; and larger isolated subhedral grains with sharp or spongy grain edges, typically in the core of plagioclase.
3. not enclose or be enclosed by a mineral from which it may have formed, e.g. plagioclase	3. Muscovite replacing biotite usually takes the form of fine-grained clusters or subhedral grains enclosing or enclosed within larger biotite grains or mantling the edges of the biotite.
4. relatively abundant in a clean, unaltered granitoid rock	4. Inclusions of groundmass minerals are common and grains should have ragged outlines.
5. optically zoned in a manner identical to other magmatic minerals, specifically plagioclase	
6. when intergrown with biotite, contacts between the two minerals should be well defined and euhedral, and both minerals should have different cleavage orientations.	
Chemical Criteria	
Primary Magmatic Muscovite	Secondary Post-Magmatic Muscovite
Magmatic muscovite may have $TiO_2 > 1$ wt%, be richer in Al_2O_3 and Na_2O , and poorer in SiO_2 , MgO , and Fe compared to obvious secondary muscovite, such as that replacing plagioclase or biotite.	TiO_2 contents < 1 wt% are considered typical of non-magmatic muscovite, which also have higher SiO_2 , MgO , and Fe contents than their primary equivalents.
$Na/(Na + K) > 0.06$	$Na/(Na + K) < 0.06$

The first physical criterion to distinguish between magmatic and non-magmatic muscovite is grain size and dimensional compatibility with other rock-forming minerals such as quartz, potassium feldspar, and plagioclase. Magmatic muscovites should be on the same order of grain size as other magmatic rock-forming minerals. The second physical criterion is grain shape. Euhedral to subhedral grains are a sign of magmatic muscovite, but non-magmatic muscovite can also have a euhedral shape. The third physical criterion is the textural relation of muscovite grains with other grains. Magmatic muscovite must be in textural equilibrium with other minerals, and the grain boundaries must be straight and sharp. The fourth physical criterion set out is the inclusion relationship of muscovite with other minerals. Euhedral inclusions of muscovite in other magmatic minerals suggest that the muscovite inclusions are magmatic. Inclusions of magmatic minerals in muscovite are inconclusive.

Muscovite has a wide range of chemical substitutions. A distinctive feature of magmatic muscovite is a TiO_2 content greater than that of non-magmatic muscovite (Miller et al. 1981). Zen (1988) suggests that muscovite with TiO_2 content greater than 0.60 weight percent (wt%) is likely to be of magmatic origin. Miller et al. (1981) further distinguished magmatic and non-magmatic muscovites using other major element indicators. Magmatic muscovite is richer in Al_2O_3 and Na_2O than non-magmatic muscovite, and magmatic muscovite is poorer in SiO_2 , MgO , and Fe compared with non-magmatic muscovite. Monier et al. (1984) used $\text{Na}/(\text{Na} + \text{K})$ ratios to differentiate between magmatic (greater than 0.06) and non-magmatic muscovite (less than 0.06). Ham and Kontak (1988) used the second chemical criterion, that is the equilibrium distribution of trace elements between muscovite and magmatic biotite, to distinguish

between magmatic and non-magmatic muscovite. The third chemical criterion is the use of chemical zoning by the Roycroft thick section method. Chemical zoning in muscovite must be analogous to that shown by unequivocal magmatic minerals such as plagioclase (Roycroft 1991). The fourth and final chemical criterion is chemical equilibrium with other magmatic rock-forming minerals (the principle of mutual saturation). The systematic disposition of tie lines is consistent with magmatic equilibrium, and any departure from these constraints suggests non-equilibrium conditions. The useful elements are Al, Fe, F, P, and Ba. Chemical equilibrium is easier to reach at high temperature than at low temperature (Deer et al. 1992), thus magmatic muscovites can signify chemical equilibrium.

The inability to differentiate between different types of muscovite based on chemical parameters may result from an inability to differentiate between magmatic and non-magmatic muscovite based only on textural criteria (Miller et al. 1981).

Magmatically-zoned muscovite can have a low TiO_2 content which is considered a characteristic of non-magmatic muscovite (Ding 1995). Chemical zoning, analogous to that shown by unequivocal magmatic minerals such as plagioclase, may provide the only sure way of recognizing magmatic muscovite (Roycroft 1991). With these uncertainties, any separation of magmatic from non-magmatic muscovite based on the criteria from Table 1.3 may be subjective.

1.5 Statement of purpose, objectives, and scope

The general purpose of this thesis is to study the white micas in the Lake Lewis Leucogranite, and to test the usefulness of muscovite as an indicator mineral to locate mineral deposits.

The specific objectives of this thesis are:

- (i) to study the chemical compositions and textures of micas in the Lake Lewis Leucogranite;
- (ii) to classify the white micas on the basis of their structural formulae;
- (iii) to determine the primary or secondary nature of the white micas in the Lake Lewis Leucogranite;
- (iv) to understand the substitution mechanisms in the white micas;
- (v) to use primary muscovite compositions as indicators of magmatic differentiation;
- (vi) to use secondary white micas as indicators of the type of deposits; and
- (vii) to comment on the usefulness of white mica to yield reliable $^{40}\text{Ar}/^{39}\text{Ar}$ radiometric ages.

The scope of this thesis is to principally study the geochemistry of white micas. A very brief examination of the geochemistry of K-feldspar and plagioclase, as a comparison with the geochemistry of the white micas, is also a part of this study.

1.6 Claim

Most of the white micas in the Lake Lewis Leucogranite are primary magmatic, and their chemical compositions contain information about the late stages of crystallization of the leucogranite. The secondary white micas have distinctive textures and chemical compositions that contain information about the subsolidus alteration processes in the Lake Lewis Leucogranite.

1.7 Organization

Following this Introduction, Chapter 2 examines the relationship of the leucogranites to the rest of the South Mountain Batholith (SMB). Chapter 3 describes the methodology

used including petrography, microprobe, and the Roycroft thick section method. Chapter 4 presents the results of petrographic observations, mineral chemical data, and calculation of structural formulae. Chapter 5 provides chemical plots to classify white micas and a discussion of magmatic processes, subsolidus processes, and implications for getting good ages from muscovite. Chapter 6 presents the conclusions achieved and recommendations for future work.

CHAPTER 2

LAKE LEWIS LEUCOGRANITE

2.1 Leucogranites in the South Mountain Batholith

The South Mountain Batholith is a peraluminous granitic complex ranging in composition from biotite granodiorite to muscovite-topaz leucogranite (MacDonald et al. 1992). The batholith underlies approximately 7300 km² of southwestern Nova Scotia (Clarke et al. 1993), and intrudes predominantly metawackes and metapelites of the Cambrian-Ordovician Meguma Group (Taylor 1969). The emplacement and crystallization occurred during the waning stages of Acadian deformation (Horne et al. 1988). Leucogranitic rocks form minor and late components of the South Mountain Batholith (Fig. 2.1).

Clarke et al. (1993) classified the leucogranitic rocks of the South Mountain Batholith into two principal categories. ‘Associated leucogranites’ occur as small zones in fine-grained leucomonzogranites, are everywhere hosted by fine-grained leucomonzogranite, and comprise < 1% of the areal extent of the batholith. Associated leucogranitic rocks are fine- to medium-grained with porphyritic and equigranular textures, and resemble their host leucomonzogranite in texture and grain size.

‘Independent leucogranites’ (Clarke et al. 1993) form larger bodies without any particular spatial associations with other rock types. Independent leucogranitic rocks occur as discrete bodies in the central portion of the South Mountain Batholith, ranging in area from a few tens of square meters to 5 km², and account for approximately 0.7% of the batholith area. Contacts with their host rocks (granodiorite, monzogranite, and

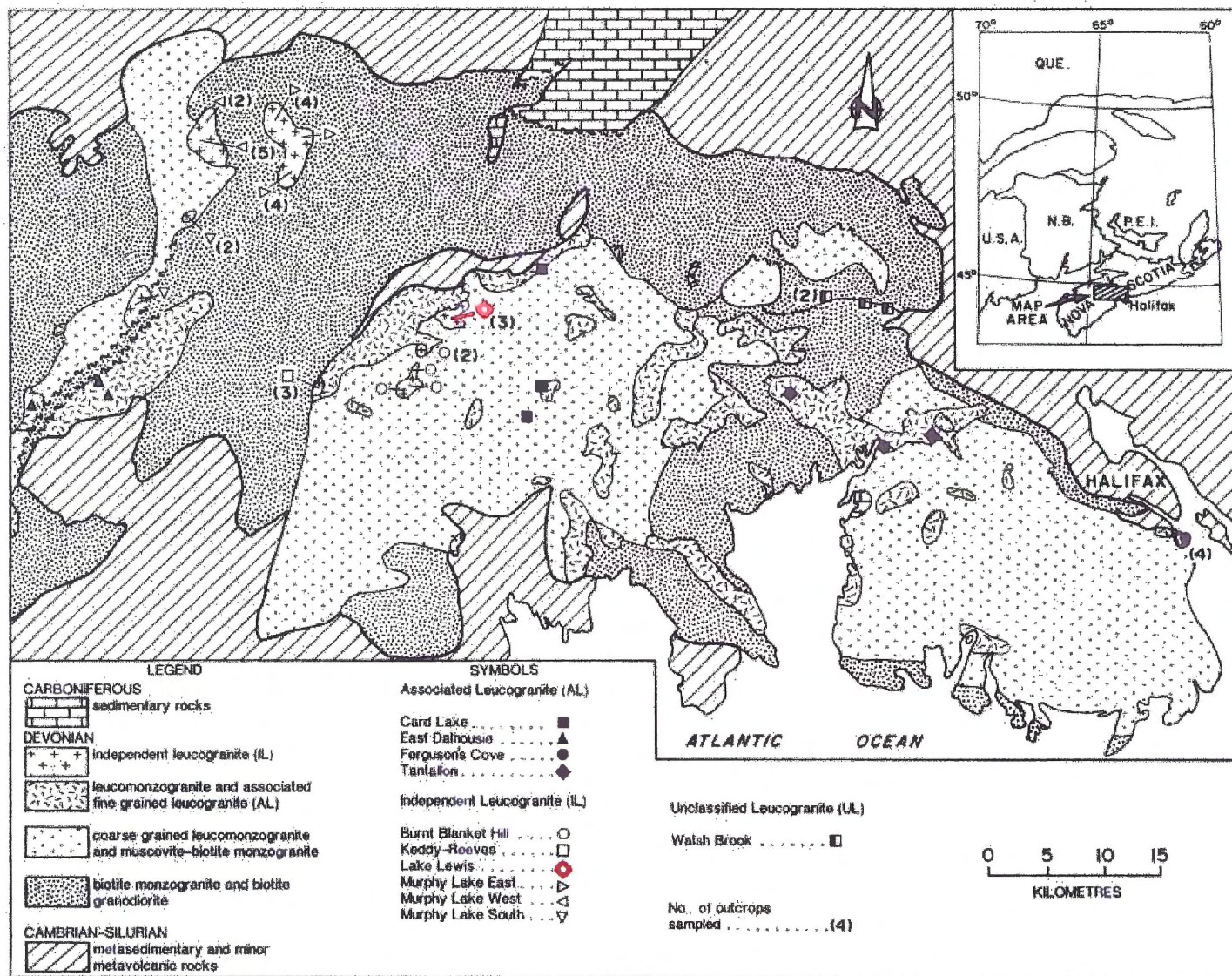


Figure 2.1. Simplified geological map of the eastern part of the South Mountain Batholith with distribution of leucogranitic bodies (Clarke et al. 1993). Lake Lewis Leucogranite = ◊.

leucomonzogranite) are sharp and intrusive. Independent leucogranitic rocks range from fine- to very coarse-grained, and have equigranular, porphyritic, pegmatitic, and aplitic textures, all of which can occur in a single outcrop (Clarke et al. 1993).

Table 2.1 compares petrographic data for leucogranitic rocks in the eastern portion of the South Mountain Batholith. The composition and zoning of the plagioclase feldspars, habit and modal abundance of muscovite, modal abundance and degree of alteration of biotite, and modal abundance of minor phases such as topaz, andalusite, and fluorite are the principal petrographic differences between the two types of leucogranitic rocks (Clarke et al. 1993).

2.2 Relationship of Lake Lewis Leucogranite to South Mountain Batholith

Clarke et al. (1993) classified the Lake Lewis Leucogranite as an independent leucogranitic body located in the central portion of the South Mountain Batholith near New Ross. The Lake Lewis Leucogranite is a small body of leucocratic porphyry, < 1 km² in areal extent, intruded into the equigranular New Ross Leucomonzogranite on South Canoe Lake (Ham 1991). The best exposure of the Lake Lewis Leucogranite is along the New Ross-Vaughan Road.

Ham (1991) gives the following description of the body. The Lake Lewis Leucogranite is a white to cream colored, fine- to medium-grained, equigranular body, although locally porphyritic with phenocrysts of quartz and feldspar, and contains < 2% mafic minerals. This leucogranitic body has a modal percentage of muscovite of 2-3%, and a modal percentage of biotite of < 2%. The groundmass may contain minor muscovite and biotite clots, and small, rounded, bluish quartz eyes. Minor pegmatite and aplite dykes and quartz-vein stockworks are common within the unit. Intrusive contacts

Table 2.1. Summary comparison table of petrographic data for leucogranitic rocks in the eastern portion of the South Mountain Batholith (Clarke et al. 1993).

Grain size	Texture		Mineralogy										Mineralization				Ref.				
	Comp.	Textural types	Plagioclase			K-feldspar			Muscovite (%)			Biotite (%)			Topaz	Andal.	Tour.	Fluor.	Type	Commodities	
			Zoning	An	Host	Primary	Lamellae	Repl.	Range	Av.	Type	Range	Av.	Alt.							
<i>Associated leucogranitoids</i>																					
Card Lake	F-M	PO+EQ>AP+PG+MA	0-1	U												0	0	0	G	U,Sn,Cu,Mo,Pb,Zn	1,2
East Dalhousie	F-M	PO+EQ>MG	0-11	N,R>U	O,M	R>P	x	3.6-12.3	7.5	A>E	1.3-1.6	1.5	F,C,M	0	0-tr.	0	0	D	U	3,4	
Ferguson's Cove	F-M	PO>MG	1-12	R,N>U	O>M	R,P	x	5.5-9.8	6.9	A>E	1.6-2.2	1.9	C>F,M	0	0-tr.	0	0	G	As,Cu	5	
Tantallon	F-M	PO+EQ+AP+GR>PG+MG+SE+MA	1-10	N,R>U	O>M	R		2.2-12.5	6.8	A>E	1.4-2.6	1.8	C>M>F	0	0-tr.	0	0	G	As,Cu	5	
<i>Independent leucogranitoids</i>																					
Burnt Blanket Hill	F-M	PO+EQ>PG	0-2	U>R	O>M	P	x	7.2-19.8	12.3	E>A	0-2.0	0.6	M>F,H	0-tr.	0-0.6	0	0	P	W,Cu	1,2	
Keddy-Reeves	M	EQ	0-2	U	O			6.0-16.8	10.5	E>A	tr.-0.1	0.1	F	0-0.7	0	0	P	Sn,W,Li,Ta,U	3		
Lake Lewis	F-M	EQ>PO>PG+AP	0-6	U	O>M	R,P	x	9.8-17.7	14.7	E>A	tr.-1.3	0.4	M>F	0-tr.	0-0.5	0	tr.	P	Mo	2	
Murphy Lake East	F-VC	PO+EQ+PG>AP+MG+SE+GR+MA	1-14	N>U	O		x	3.2-16.7	10.3	E>A	0-3.9	1.7	H>M>F	0	0	0	0	D	U,F	4	
Murphy Lake South	F-VC	PO+EQ>PG+AP	n.d.	U,N	O	R,P	x	2.5-10.5	5.8		0.7-2.3	1.6	H,M,F	0	0	0	0-tr.			4	
Murphy Lake West	F-VC	PO+EQ+PE>AP+MG+SE+GR+MA	0-1	U	O>M		x	8.8-28.5	16.4		0-1.4	0.3	H>M>F	0-tr.	0	0	0	D	U,F,P,Ba	4	
<i>Unclassified leucogranitoids</i>																					
Walsh Brook	F-M	EQ>GR	2-14	N>R>U	O	P	x	5.8-12.4	8.7	A>E	1.0-2.0	1.5	C>F	0	0-tr.	0-0.1	0			6	

Texture

Grain size: F—fine (<0.1 cm); M—medium (0.1–0.5 cm); C—coarse (0.5–3.0 cm); VC—very coarse (>3.0 cm).

Texture: AP—aplite; EQ—equigranular; GR—graphic; MA—mica aplite (coarse phenocrysts of muscovite±biotite±quartz) in aplitic matrix; MG—megacrystic; PG—pegmatitic; PO—porphyritic; SE—seriate.

Mineralogy

Plagioclase: Comp. An—anorthite content; Zoning—N, normal; R, reverse; U, unzoned.

K-feldspar: M—microcline; O—orthoclase; P—patch; R—rod and bead; Repl.—replacement of plagioclase.

Muscovite: Av.—arithmetic mean; Type—A, anhedral replacement product of K-feldspar, plagioclase±andalusite±biotite; E, euhedral (primary?) habit.

Biotite: Alt.—type of alteration (C, chlorite; F, fresh; H, hematite; M, muscovite).

Topaz—modal abundance.

Andal. (andalusite)—modal abundance.

Tour. (tourmaline)—modal abundance

Fluor. (fluorite)—modal abundance.

Mineralization

Type: D—disseminations and fracture fillings, mostly U, F±Mo±W; G—greisen±quartz vein with polymetallic mineralization; P—pegmatite-hosted polymetallic mineralization.

Ref.—references: (1) Corey (1991); (2) Ham (1991); (3) Horne (1987); (4) MacDonald & Ham (1992); (5) MacDonald & Horne (1987); (6) Corey (1987).

with the New Ross Leucomonzogranite and the Sherwood Monzogranite outcrop on South Canoe Lake. Shea and Wallace (1963) noted sharp intrusive contacts with the Panuke Lake Leucomonzogranite in drill core.

Within the Lake Lewis Leucogranite, pegmatite, with minor black tourmaline, and aplite occur parallel to the contact with the New Ross Leucomonzogranite, exposed on South Canoe Lake. At the contact, the Lake Lewis Leucogranite truncates megacrysts of alkali feldspar within the Sherwood Monzogranite. A gradational contact between the Lake Lewis Leucogranite and the New Ross Leucomonzogranite occurs west of South Canoe Lake. Fluorine, uranium, and molybdenum mineralization occurs within the Lake Lewis Leucogranite along hematized fractures and shear planes, and as disseminations throughout the groundmass (Ham 1991).

2.3 Ages of the South Mountain Batholith and Lake Lewis Leucogranite

Whole-rock Rb-Sr dating by Clarke and Halliday (1980) for different facies of the batholith yielded the following ages: 371.8 ± 2.2 Ma for the early biotite granodiorite, 364.3 ± 1.3 Ma for a later monzogranite, and 361.2 ± 1.4 Ma for aplites and a suite of late porphyries. Harper (1988) reproduced the Rb-Sr age of the monzogranite and also determined a muscovite primary crystallization age of 371 ± 5 Ma. Harper also obtained an age for the leucomonzogranite of 361 ± 2 Ma, but estimated a muscovite primary crystallization age of 369.6 ± 1 Ma. He also determined U-Pb monazite ages of 372.8 ± 2.1 Ma for the leucomonzogranite and 374.3 ± 1.9 Ma for the monzogranite. Reynolds et al. (1981) reported an average biotite and muscovite $^{40}\text{Ar}/^{39}\text{Ar}$ age from granodiorite, “adamellite”, and late intrusive rocks from the South Mountain Batholith of 367 Ma.

Clarke et al. (1993) reported $^{40}\text{Ar}/^{39}\text{Ar}$ ages ranging from 369 ± 2 Ma to 375 ± 4 Ma for independent leucogranite bodies in the South Mountain Batholith. Figure 2.2 shows $^{40}\text{Ar}/^{39}\text{Ar}$ age spectra for muscovite separates from the Lake Lewis Leucogranite that give ages of 370 ± 2 Ma and 370 ± 4 Ma. These results are in agreement with previous age determinations for the South Mountain Batholith. Both primary and secondary muscovites in leucogranite samples have ages close to the intrusion age of the South Mountain Batholith, and no age below 370 Ma appears to be primary. The agreement of muscovite and monazite age determinations by different methods suggests that all isotopic systems in the South Mountain Batholith, within analytical uncertainty, closed at approximately 370 Ma (Clarke et al. 1993).

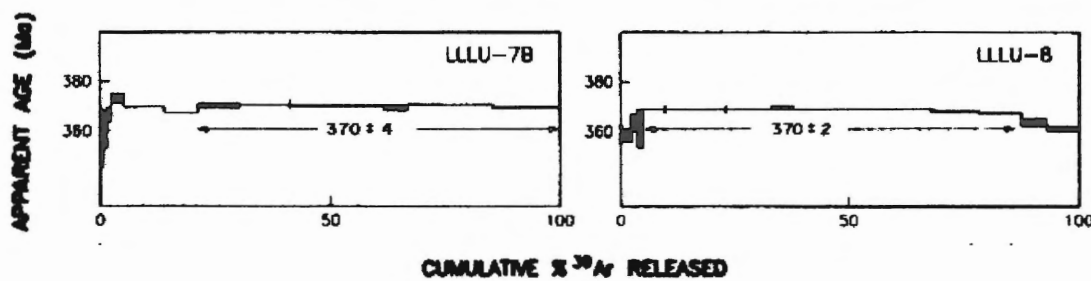


Figure 2.2. Conventional argon release plots for two muscovite separates from the Lake Lewis Leucogranite. Double-ended arrows define the plateau extent for each stated age, and vertical tick marks on the spectra indicate separate heating steps. Half-heights of black bars represent relative uncertainties at the 1σ level (from Clarke et al. 1993).

2.4 Geochemistry of leucogranites in the South Mountain Batholith

In chemical diagrams reported by Clarke et al. (1993), leucogranitic rocks from the South Mountain Batholith form an extension of the magmatic trend of the batholith

towards more evolved compositions, with the Lake Lewis Leucogranite plotting at the most evolved end of the trend (Figs. 2.3-2.5). The most significant diagram is the K-Rb plot. Taylor (1965) and Shaw (1968) reported that K/Rb ratios < 160 are unattainable by crystal-melt processes, and such ratios indicate the involvement of an aqueous fluid phase which stabilizes abundant primary or secondary muscovite with low K/Rb. The leucogranites of the South Mountain Batholith show very low K/Rb values (Fig. 2.3b) that may have been reached by fluid-rock interaction, with the Lake Lewis Leucogranite plotting at the low end with K/Rb < 50. Clarke et al. (1993) concluded that the high A/CNK, F, P₂O₅, Na₂O/K₂O, Gd_N/Yb_N, the low Ti, Zr, Ba, and Th, and the variable U and δ¹⁸O values are the effects of two kinds of fluid-rock interaction: (1) late-stage fluido-magmatic interaction and (2) subsolidus hydrothermal alteration. The association with pegmatites, lower K/Rb ratio, strong fractionation of HREE, and fairly constant δ¹⁸O, suggest involvement of closed-system, late-stage fluid-magmatic processes for independent leucogranites.

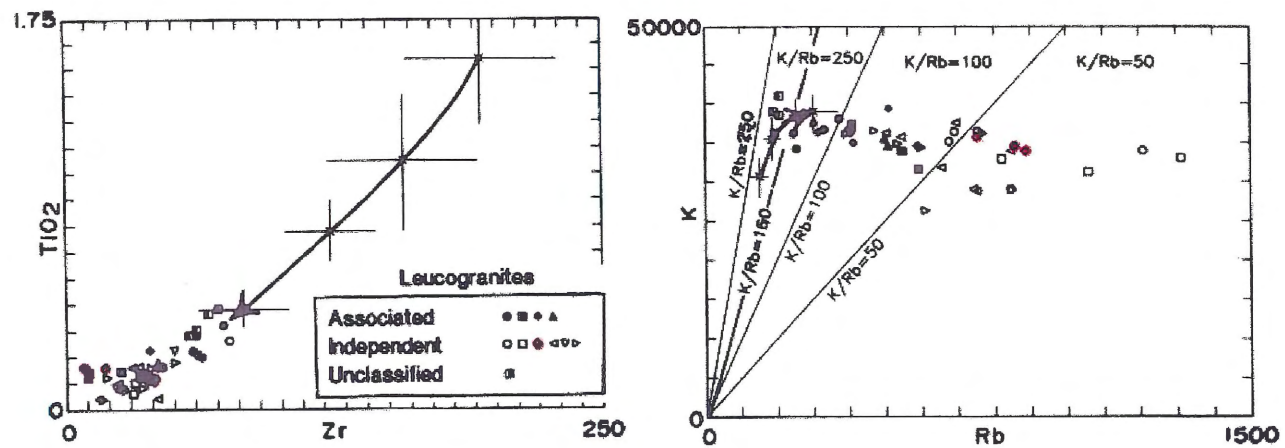


Figure 2.3. Major and trace element chemical variation diagrams of leucogranitic rocks from the South Mountain Batholith. The South Mountain Batholith magmatic trend follows the arrow on each graph. Symbols are the same as in Figure 2.1 where the Lake Lewis Leucogranite = ◊ (from Clarke et al. 1993).

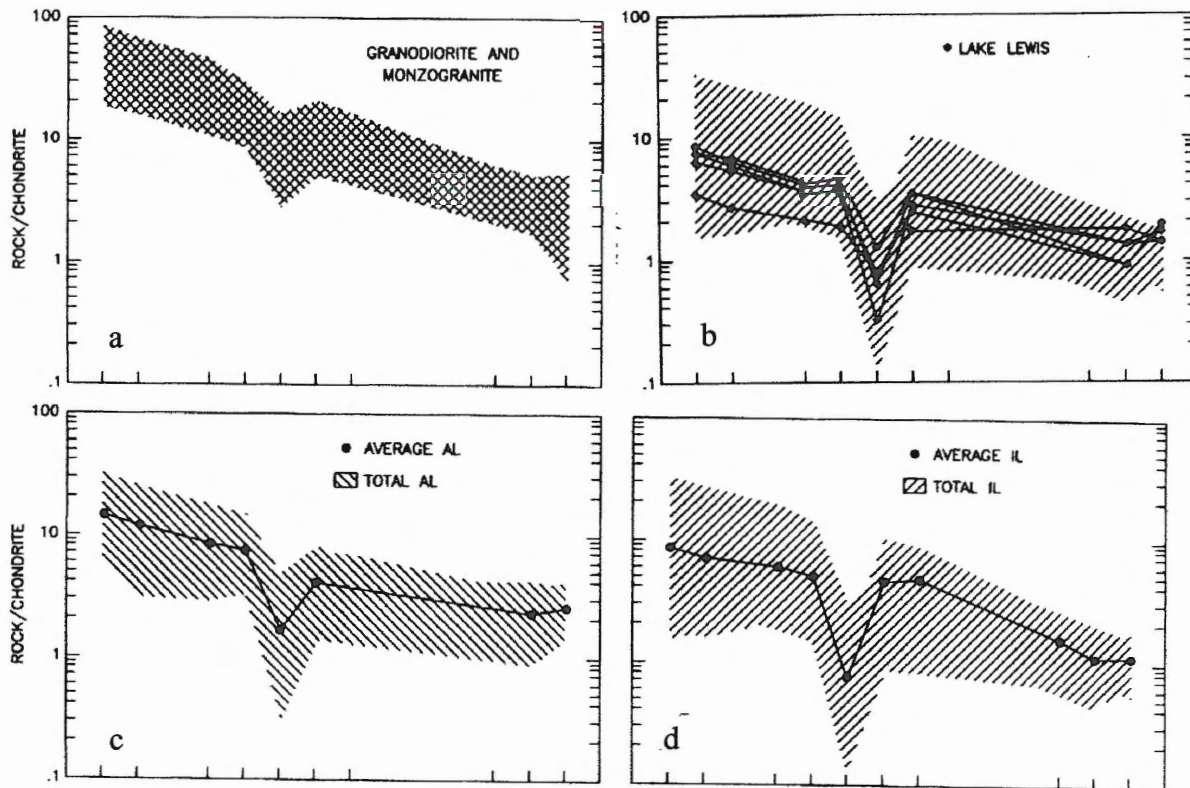


Figure 2.4. Variation diagrams for rare earth elements of leucogranitic rocks from the South Mountain Batholith. (a) Averages and ranges for the South Mountain Batholith. (b) Lake Lewis Leucogranite with shaded area representing the range of associated leucogranite compositions in the South Mountain Batholith. (c) Associated leucogranitic rocks with the shaded area representing the range of associated leucogranite compositions in the South Mountain Batholith. (d) Independent leucogranitic rocks with the shaded area representing the range of associated leucogranite compositions in the South Mountain Batholith (from Clarke et al. 1993).

Associated and independent leucogranites show compositional overlap for every element. Associated leucogranites have compositional trends where $\text{SiO}_2 > 75\%$ and $\delta^{18}\text{O}$ values are outside 10.0-12.8%. Diagnostic chemical characteristics of independent leucogranite include $\text{Na}_2\text{O} > 4.10\%$, $\text{K}_2\text{O} < 3.75\%$, $\text{P}_2\text{O}_5 > 0.45\%$, $\text{F} > 3500 \text{ ppm}$,

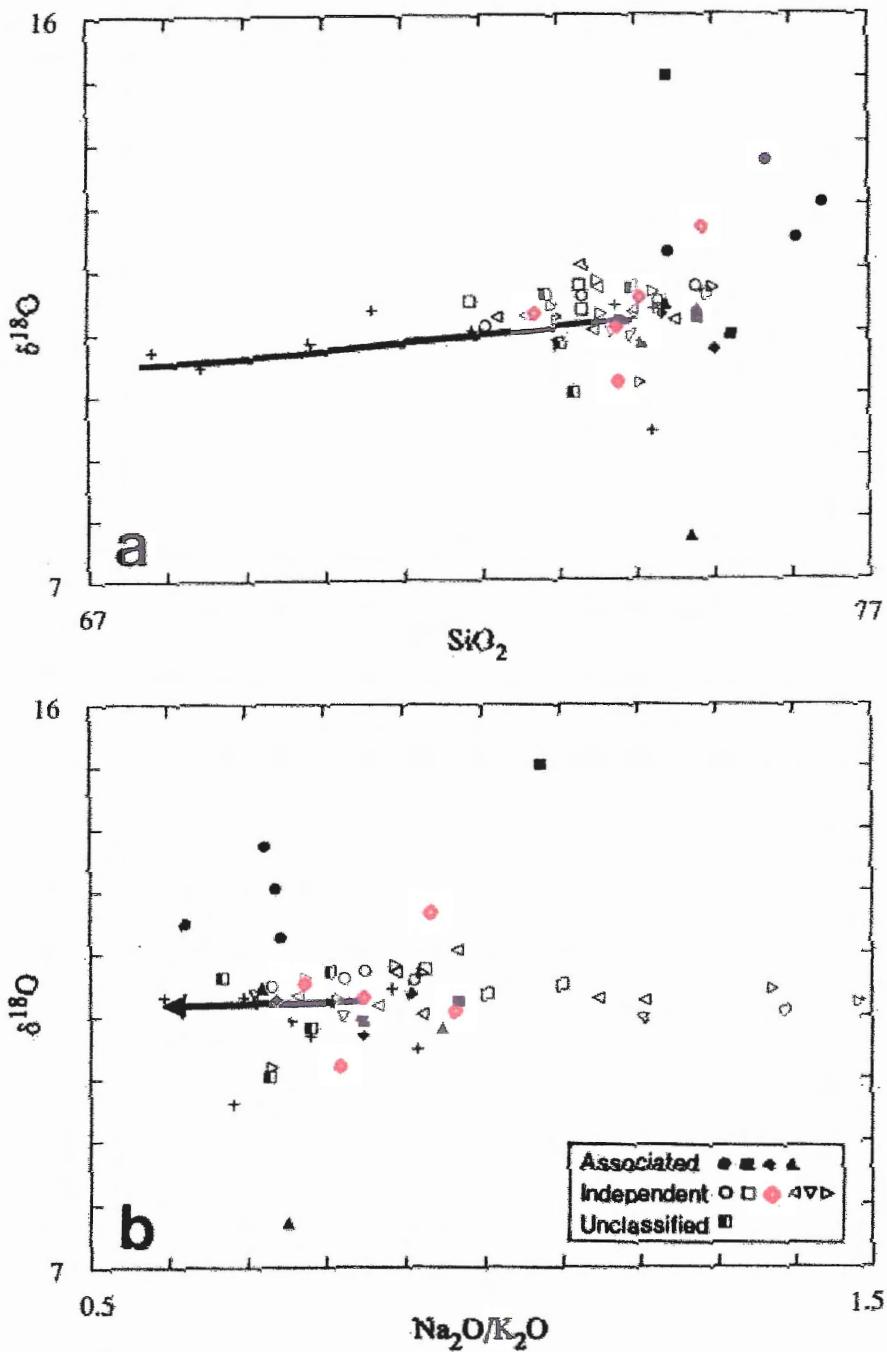


Figure 2.5. Whole-rock $\delta^{18}\text{O}$ values (in ‰ relative to Standard Mean Ocean Water) variation diagrams for leucogranitic rocks in the South Mountain Batholith. Symbols are defined in Figure 2.1 (Lake Lewis Leucogranite = \diamond) and arrows are defined in Figure 2.3. + symbols represent samples used to define magmatic trend. (a) $\delta^{18}\text{O}$ - SiO_2 plot skewed toward high silica values. (b) $\delta^{18}\text{O}$ - $\text{Na}_2\text{O}/\text{K}_2\text{O}$ plot showing that the alteration [increasing albitization ($\text{Na}_2\text{O}/\text{K}_2\text{O}$)] responsible for producing some of the associated leucogranites affected their oxygen isotopic composition, and did not affect the oxygen isotopic composition of the independent leucogranites (Clarke et al. 1993).

Rb > 600 ppm, Ta > 7 ppm, Nb > 20 ppm, Li > 350 ppm, and Gd_N/Yb_N > 4. Whole-rock δ¹⁸O values suggest that the associated leucogranites formed as open systems, possibly involving more than one fluid (Clarke et al. 1993).

2.5 Relationship between leucogranites and mineral deposits in the South Mountain Batholith

Fluorine-rich leucogranitic rocks are of interest because of their economic potential (Weidner and Martin 1987). Quartz-rich leucocratic granitoid rocks enriched in granophile elements typically host Sn-W-U-Mo and Be-B-Li-P deposits. Granophile deposits are commonly associated with pegmatites and greisens. Greisens form by alteration of either the granitic or country rock by the addition or depletion of elements to produce assemblages with variable combinations of white mica, quartz, fluorite, tourmaline, and topaz (Strong 1981).

Mineralization associated with leucogranites in the South Mountain Batholith is diverse. The two types of leucogranite bodies have spatially associated polymetallic mineral occurrences, but have different styles of mineralization. The independent leucogranite bodies tend to be of the closed-system pegmatite style of mineralization. The associated leucogranite bodies tend to have an open-system greisen style of mineralization (Clarke et al. 1993).

Pegmatite-type mineral occurrences in the independent bodies host Sn, W, U, Mo, Li, Ta, and Cu mineralization, whereas dissemination- and/or fracture-type mineral occurrences host U, F, Mo, and W mineralization. Greisen or quartz vein-type mineral occurrences in the associated leucogranite bodies host Cu, As, U, Sn, Mo, Pb, and Zn mineralization, and the disseminated types host U mineralization (Clarke et al. 1993).

Many of these occurrences are small, but economically significant deposits of uranium and tin occur at Millet Brook (Chatterjee et al. 1982) and near East Kemptville (Richardson et al. 1982), respectively.

Mineral occurrences in the independent leucogranites may represent local concentrations of incompatible components deposited by a volatile-rich fluid phase. The $\delta^{18}\text{O}$ values reported by Clarke et al. (1993) suggest that the magmatic-fluid system was essentially closed to external inputs. In contrast, the $\delta^{18}\text{O}$ data from associated leucogranites suggests that the mineral occurrences probably formed from open-system fluid circulation.

2.6 Summary

In the South Mountain Batholith, leucogranitic bodies classify as either associated or independent leucogranites. These leucogranites differ in field relations, mineralogy, and chemical composition. The Lake Lewis Leucogranite, following the classification of Clarke et al. (1993), is an independent leucogranitic body that follows the geochemical extension of the magmatic trend in the South Mountain Batholith. Radiometric dating ($^{40}\text{Ar}/^{39}\text{Ar}$ on muscovite) shows that the South Mountain Batholith and its leucogranites have identical ages of 372 ± 3 Ma. Leucogranites in the South Mountain Batholith are spatially related to mineralization.

CHAPTER 3

METHODOLOGY

3.1 Introduction

Research for this thesis employs several techniques on the macroscopic to microscopic scale, ranging from field sampling to basic petrography and chemical analyses using the electron microprobe. The objective is to distinguish primary magmatic features and secondary alteration features with particular reference to white micas and feldspars, and to determine how much of the mineralogical, textural, and chemical features of the Lake Lewis Leucogranite results from primary magmatic processes, how much results from secondary alteration processes, and what these micas can tell us about late-stage crystallization and mineral deposits forming in the Lake Lewis Leucogranite.

3.2 Field investigation

Field investigation of the Lake Lewis Leucogranite in the New Ross area used the geological map of Windsor by Ham (1991). Outcrop locations marked on the Windsor map were visited and representative rock samples of the leucogranite were taken. Eleven fresh representative samples were collected by the author (LL99 series), and two samples from the leucogranite (LLL2 and LLL3) and one from the Walker Moly deposit (SC-20W) were collected by others on previous excursions. Where possible, large samples were taken so that future work requiring crushed samples could be done.

3.3 Petrographic methods

The petrographic microscope is an essential tool providing information about mineral assemblages and textures.

3.3.1 Optical mineralogy techniques

Mineral identification follows the systematic collection of optical properties set out by the undergraduate optical properties checklist. Rock textures can be readily assessed with the petrographic microscope. Primary magmatic features include hypidiomorphic granular texture, interlocking grains, equigranular grain size, euhedral grain shape, and epitaxial overgrowths. Secondary features include textural and chemical changes such as subsolidus exsolution, pseudomorphic replacements, sericitization and kaolinization of feldspars, chloritization of biotites, and mechanical changes such as cataclasis.

3.3.2 Roycroft method

At a normal thin section thickness of 30 microns, primary magmatic zoning in white micas is difficult to see, and may have been overlooked in many granites (Roycroft 1989). The Roycroft method involves the use of a sharp blade to separate white mica cleavage flakes approximately 0.3 mm thick. Optical zoning is best observed under a petrographic microscope in slices that give middle-first-order to upper-second-order interference colors in basal sections, whereas normal thin sections give lower interference colors.

Compositionally zoned white mica textures, which result from magmatic evolution, provide criteria that distinguish primary and secondary white micas

(Roycroft 1991). Unzoned white micas, on the other hand, do not necessarily imply secondary origin.

3.4 Electron microprobe analysis

The electron microprobe laboratory at Dalhousie University operates a fully automated JEOL 733 electron microprobe X-ray microanalyzer equipped with four wavelength dispersive spectrometers (WDS) and an Oxford Link eXL 131 eV energy dispersive system (EDS). The method is rapid, non-destructive, and can provide fully quantitative chemical analyses of solid materials as small as 1 to 3 microns in diameter on an elemental weight percent basis. The microprobe is fully computer controlled, capable of high-efficiency and accurate analysis, and is capable of unattended overnight operation (R. MacKay, written comm).

The technique of X-ray microanalysis consists of detecting characteristic X-rays produced by bombarding a solid sample with high-energy electrons. X-rays emitted from excited atoms have an energy characteristic of the elements producing them. Detection of these X-rays can be achieved by an energy dispersive spectrometer, a solid-state device that discriminates among X-ray energies, or by wavelength dispersive spectroscopy, a crystal spectrometer that uses a diffracting crystal to select the wavelength of interest. Provided that a suitable light element X-ray window is used, both spectroscopic methods are capable of analyzing elements beginning with beryllium or boron in the periodic table (Friel 1995). The Dalhousie laboratory can provide fully quantitative analyses for elements ranging from oxygen and fluorine up the periodic table in terms of atomic number to uranium (R. MacKay, written comm).

3.4.1 Sample preparation

Samples were mounted on a glass thin section, ground, and polished to achieve a flat surface. To provide a ground path for the electron beam, samples were coated with a thin coating of carbon film. Carbon is highly conductive, does not heavily absorb X-rays, and can be easily evaporated, thus making it an excellent choice for coating non-conductive samples (Friel 1995).

3.4.2 Microprobe operating conditions

Micas and feldspars were analyzed on the Dalhousie University JEOL 733 electron microprobe. The energy dispersive system was used for all elements, with the exception of barium in the feldspar analyses, and fluorine in the mica analyses, that were both measured using the wavelength dispersive system. The operating resolution of the energy dispersive system was 137 eV at 5.9 keV. Acquisition of each spectrum lasted 20 seconds with an accelerating voltage of 15 kV and a beam current of 15 nA, with the exception of barium in the feldspar analyses which lasted 80 seconds and fluorine in the mica analyses which lasted 40 seconds. The probe spot size was approximately 1 micron for feldspar analyses and 10 microns for mica analyses. The raw data were corrected using the Link ZAF matrix correction program (R. MacKay, personal comm).

The electron microprobe calibration was performed on cobalt metal and the instrument precision on cobalt metal ($n = 10$) was $\pm 0.5\%$ at one standard deviation. The accuracy for major elements was ± 1.5 to 2.0 relative %. Detection limits using the energy dispersive system for most elements range from approximately 0.1 to 0.3%, whereas using the wavelength dispersive system the detection limits range from 0.01 to 0.03% (R. MacKay, personal comm).

The mineral analyses were carried out using the following geological standards: sanidine for Si, Al, K; Kakanui kaersutite amphibole for Ti, Mg, Ca; garnet 12442 for Fe; jadeite for Na; MnO₂ for Mn; barite for Ba; and F-apatite for F. Mica and sanidine controls were used for mica and feldspar analyses (R. MacKay, personal comm).

3.4.3 Backscattered electron images

Backscattered electron images (BEI) provide gray-scale compositional maps of phases based on their average atomic number (R. MacKay written comm). Areas with higher atomic numbers show lighter shades of gray. The complete set of microprobe data is available on disk in CSV format.

3.5 Summary

Through the use of petrographic observations and electron microprobe work, I attempt to distinguish between primary magmatic minerals and processes, and secondary minerals and alteration processes in the Lake Lewis Leucogranite, with particular reference to white micas and feldspars. The next chapter presents all the observations and analytical data.

CHAPTER 4

OBSERVATIONS AND RESULTS

4.1 Petrographic observations

Figure 4.1 shows the sample locations from the Lake Lewis Leucogranite and Walker Moly deposit. Samples LL99-9 and LL99-12 are aplitic samples.

4.1.1 Thin sections

Table 4.1 summarizes basic petrographic features of the Lake Lewis Leucogranite and Walker Moly deposit samples. These samples show typical igneous interlocking crystalline textures with sharp grain boundaries, although some of the samples have been cataastically deformed. The leucogranite samples show complex intergrowths of muscovite and phengite. The leucogranite samples have similar modal percentages of quartz ($25 \pm 5\%$), K-feldspar ($25 \pm 5\%$), plagioclase ($35 \pm 5\%$), white mica ($15 \pm 5\%$) and trace (1-3%) amounts of biotite. Some leucogranite samples have small amounts of accessory minerals such as fluorite and topaz. Zircon halos are common in the brown micas.

The Lake Lewis Leucogranite has a complex intergrowth of brown and white micas. Figures 4.2 a and b show a white mica core with a brown mica overgrowth, but the opposite mica relationship is also present with brown mica cores and white mica overgrowths. A close-up backscattered electron image of this epitaxial overgrowth of phengite on a muscovite core in sample LL99-7 (Fig. 4.3) shows the sharpness of the contact between the two varieties of mica, and the cleavage planes are continuous through the contact. Feldspars are generally unaltered and are not zoned (Fig. 4.2c).

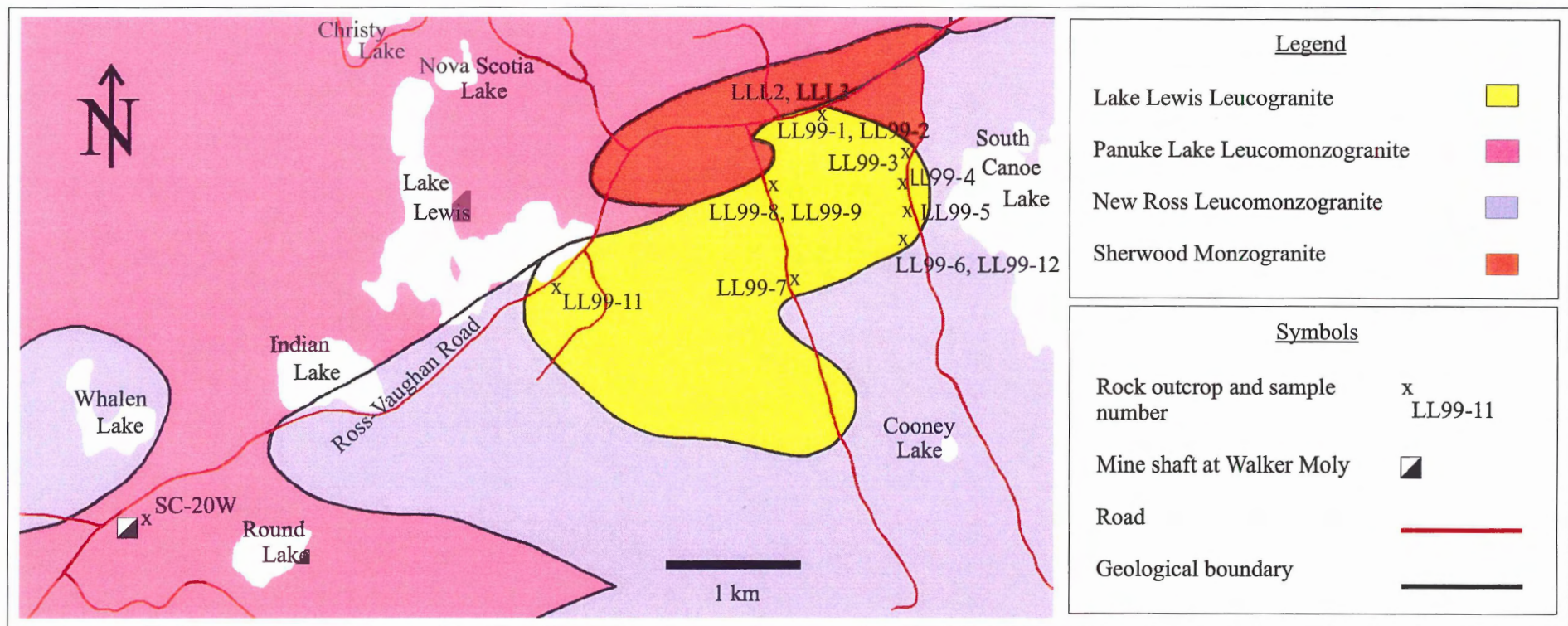


Figure 4.1 Geological map of the Lake Lewis Leucogranite and surrounding area with sample locations. Geology is simplified after Ham (1991).

Table 4.1. Petrographic observations of Lake Lewis Leucogranite and Walker Moly deposit samples. This table is continued on the following pages.

Plagioclase	K-feldspar	White Mica	Biotite
LLL2 and LLL3; fine-grained samples; bands of grain size reduction by cataclastic deformation; fluorite veins			
0.1-2mm; euhedral to subhedral grains; undulose extinction in some grains; albite twinning > Carlsbad twinning; feldspars undeformed; inclusions of white mica and quartz; most grains cloudy, but some unaltered grains present	0.1-2mm; euhedral to subhedral grains; undulose extinction in some grains; Carlsbad twinning in some grains; feldspars undeformed; perthitic exsolution lamellae in some grains; inclusions of white mica, quartz, and plagioclase; inclusions in quartz; most grains cloudy, but some unaltered grains present	0.1-2mm; euhedral to subhedral grains; undulose extinction in some grains; replacement of biotite; inclusions in quartz; some micas kinked and bent, and contain dark patches; similar to LL99-1, LL99-2, and SC-20W	absent
LL99-1 and LL99-2; fine-grained samples; bands of grain size reduction by cataclastic deformation			
0.1-2mm; euhedral to subhedral grains; undulose extinction in some grains; albite twinning > Carlsbad twinning; mostly undeformed; inclusions of white mica and quartz; most grains cloudy, but some unaltered grains present	0.1-2mm; euhedral to subhedral grains; undulose extinction in some grains; Carlsbad twinning in some grains; mostly undeformed; perthitic exsolution lamellae in some grains; inclusions of white mica, quartz, and plagioclase; inclusions in quartz; most grains cloudy, but some unaltered grains present	0.1-2mm; euhedral to subhedral grains; undulose extinction in some grains; replacement of biotite; inclusions in quartz; micas kinked and bent, contain dark patches and fluorite inclusions; similar to LLL2, LLL3, and SC-20W	absent

Table 4.1 continued

Plagioclase	K-feldspar	White Mica	Biotite
LL99-3; medium-coarse-grained sample; topaz present			
0.5-4mm; euhedral to subhedral grains; undulose extinction in some grains; albite twinning > Carlsbad twinning; inclusions of white mica and quartz; unaltered grains	0.5-3mm; euhedral to subhedral grains; undulose extinction in some grains; Carlsbad twinning in some grains; perthitic exsolution lamellae in some grains; inclusions of white mica, quartz, and plagioclase; inclusions in quartz; unaltered grains	0.2-2mm; euhedral to subhedral grains; undulose extinction in some grains; replacement of biotite; inclusions in quartz	0.5-2mm; euhedral to subhedral grains; inclusions in quartz; replacement by white mica
LL99-4; medium-coarse-grained sample; hypidiomorphic texture			
0.5-5mm; euhedral to subhedral grains; undulose extinction in some grains; albite twinning > Carlsbad twinning; inclusions of white mica and quartz; generally unaltered	0.5-4mm; euhedral to subhedral grains; undulose extinction in some grains; Carlsbad twinning in some grains; large grains with perthitic exsolution lamellae common; inclusions of white mica, quartz, and plagioclase; inclusions in quartz; unaltered grains	0.5-4mm; euhedral to subhedral grains; undulose extinction in some grains; replacement of biotite; inclusions in quartz	0.5-2mm; euhedral to subhedral grains; inclusions in quartz; replacement by white mica

Table 4.1 continued

Plagioclase	K-feldspar	White Mica	Biotite
LL99-5; medium-coarse-grained sample; topaz (~2%) with inclusions of biotite present			
0.5-5mm; euhedral to subhedral grains; undulose extinction in some grains; albite twinning > Carlsbad twinning; poikilitic texture; inclusions of white mica and quartz; generally unaltered	0.5-4mm; euhedral to subhedral grains; undulose extinction in some grains; Carlsbad twinning in some grains; perthitic exsolution lamellae in some grains; poikilitic texture; inclusions of white mica, quartz, and plagioclase; inclusions in quartz; varying degrees of alteration	0.5-4mm; euhedral to subhedral grains; undulose extinction in some grains; replacement of biotite; inclusions in quartz	0.5-2mm; euhedral to subhedral grains; inclusions in quartz; replacement by white mica
LL99-6; coarse-grained sample			
0.5-6mm; euhedral to subhedral grains; undulose extinction in some grains; albite twinning > Carlsbad twinning; inclusions of white mica and quartz; grains generally unaltered	0.5-8mm; euhedral to subhedral grains; undulose extinction in some grains; Carlsbad twinning in some grains; perthitic exsolution lamellae in some grains; inclusions of white mica, quartz, and plagioclase; inclusions in quartz; varying degrees of alteration	0.5-3mm; euhedral to subhedral grains; undulose extinction in some grains; replacement of biotite; inclusions in quartz	0.5-1.5mm; euhedral to subhedral grains; inclusions in quartz; replacement by white mica

Table 4.1 continued

Plagioclase	K-feldspar	White Mica	Biotite
LL99-7; medium-coarse-grained sample			
0.5-4mm; euhedral to subhedral grains; undulose extinction in some grains; albite twinning > Carlsbad twinning; inclusions of white mica and quartz; inclusions in quartz; some grains with varying degrees of alteration	0.5-3mm; euhedral to subhedral grains; undulose extinction in some grains; Carlsbad twinning in some grains; perthitic exsolution lamellae common; inclusions of white mica, quartz, and plagioclase; some grains with varying degrees of alteration	0.5-3mm; euhedral to subhedral grains; undulose extinction in some grains; replacement of biotite; inclusions in quartz, K-feldspar, and plagioclase	0.5-2mm; euhedral to subhedral grains; inclusions in quartz; replacement by white mica
LL99-8; coarse-grained sample; unaltered sample			
1-8mm; euhedral to subhedral grains; undulose extinction in some grains; albite twinning = Carlsbad twinning; inclusions of white mica and biotite; generally unaltered	1-8mm; euhedral to subhedral grains; undulose extinction in some grains; Carlsbad twinning very common; perthitic exsolution lamellae very common; inclusions of white mica, quartz, and plagioclase; unaltered	0.5-4mm; euhedral to subhedral grains; undulose extinction in some grains; replacement of biotite; inclusions in quartz, K-feldspar, and plagioclase	1-4mm; subhedral grains; inclusions in quartz and plagioclase; replacement by white mica
LL99-9; medium-grained sample; grain size reduction by cataclastic deformation; unaltered sample; topaz present			
0.5-5mm; euhedral to subhedral grains; undulose extinction in some grains; albite twinning > Carlsbad twinning; inclusions of white mica, quartz, and biotite; generally unaltered	0.5-4mm; euhedral to subhedral grains; undulose extinction in some grains; Carlsbad twinning in some grains; perthitic exsolution lamellae common; inclusions of white mica, biotite, quartz, and plagioclase; unaltered	0.2-2mm; mostly euhedral to subhedral grains, but some anhedral grains present; very little undulose extinction; nearly complete replacement of biotite; inclusions in quartz	0.2-2mm; euhedral to subhedral grains; inclusions in quartz and plagioclase; nearly complete replacement by white mica

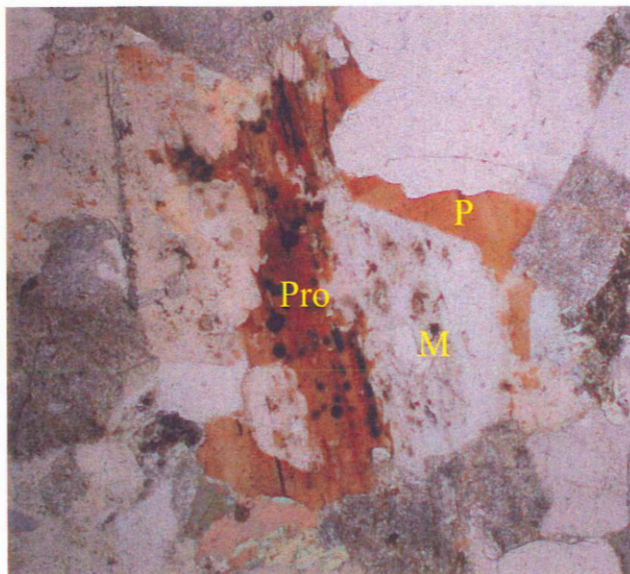
Table 4.1 continued

Plagioclase	K-feldspar	White Mica	Biotite
LL99-11; medium-coarse-grained sample			
1-4mm; euhedral to subhedral grains; undulose extinction in some grains; albite twinning > Carlsbad twinning; inclusions of white mica, quartz, and biotite; grains generally unaltered	1-4mm; euhedral to subhedral grains; undulose extinction in some grains; Carlsbad twinning in some grains; perthitic exsolution lamellae common; inclusions of white mica, quartz, and plagioclase (in larger grains)	0.5-3mm; euhedral to subhedral grains; undulose extinction in some grains; replacement of biotite; inclusions in feldspars and mica quartz	0.1-1mm; euhedral to subhedral grains; inclusions in quartz and plagioclase; replacement by white mica
LL99-12; medium-coarse-grained sample; some grain size reduction by cataclastic deformation; topaz present			
0.5-2 mm; euhedral to subhedral grains; undulose extinction in some grains; albite twinning > Carlsbad twinning; inclusions of white mica and quartz; generally unaltered	0.5-3mm; euhedral to subhedral grains; undulose extinction in some grains; Carlsbad twinning in some grains; large perthitic exsolution lamellae common; inclusions of white mica, quartz, and plagioclase in larger grains; some grains with varying degrees of alteration	0.2-2mm; mostly subhedral, but some are euhedral or anhedral grains present; undulose extinction in some grains; replacement of biotite; inclusions in feldspars and quartz	0.2-1mm; euhedral to subhedral grains; most common as inclusions in quartz; replacement by white mica

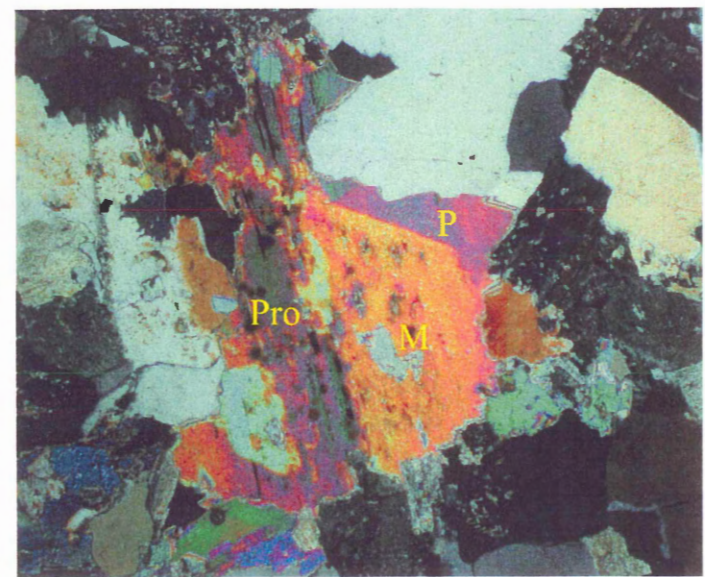
Table 4.1 continued

Plagioclase	K-feldspar	White Mica	Biotite
SC-20W; very coarse-grained sample; large blue tourmalines 1-12mm in size 45%; topaz 8%; quartz 5%			
0.2-2mm; subhedral grains; undulose extinction common; albite twinning; deformed feldspars; unaltered grains; 2%	0.2-3mm; euhedral to subhedral grains; undulose extinction common; occurs as replacement of biotite; mica splays; micas are kinked and bent, contain dark patches, and have fluorite inclusions with zinnwaldite replacement cores; similar to LL99-1, LL99-2, LLL2, and LLL3; 40%		absent

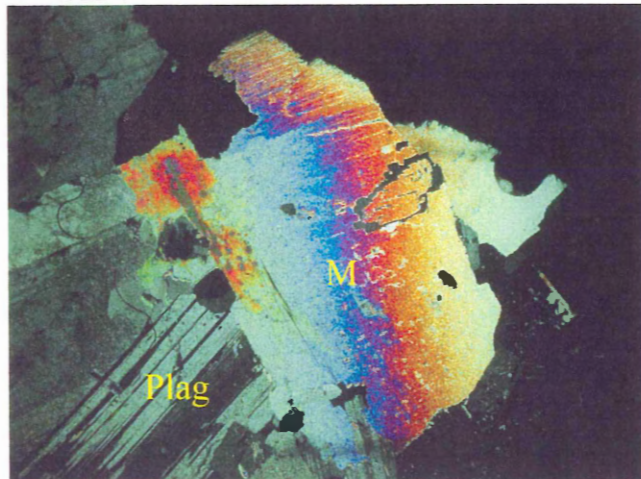
a PPL



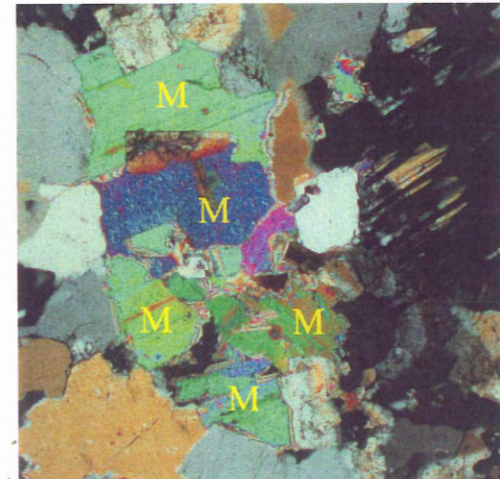
b XN



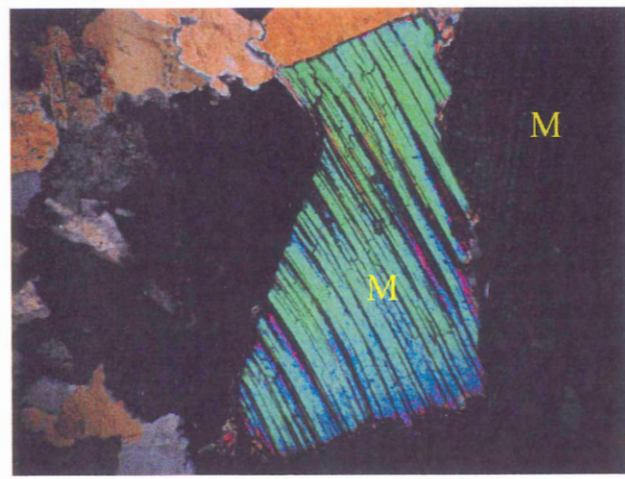
c XN



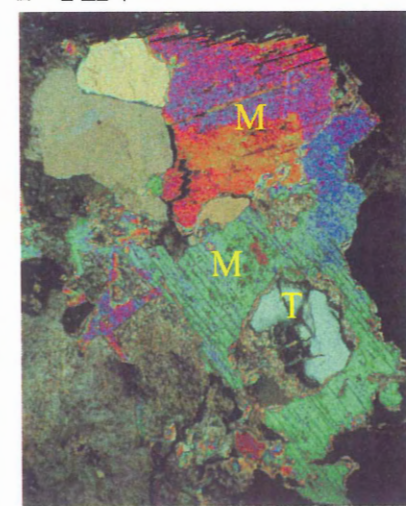
d XN



e XN



f XN



2 mm

Figure 4.2. Thin section photomicrographs of representative white micas from the Lake Lewis Leucogranite. (a-b) Sample LL99-7 shows epitaxial overgrowth of phengite (P) on a muscovite core (M) with a coexisting protolithionite (Pro) grain. (c-f) Samples LL99-8, LL99-9 (aplitic sample), LLL3, and LL99-3, respectively. These micas are undeformed and texturally primary examples of muscovite from the Lake Lewis Leucogranite. Sample LL99-8 also shows an undeformed plagioclase (Plag) grain. The mica from sample LL99-3 (f) has grown around a topaz (T) grain.

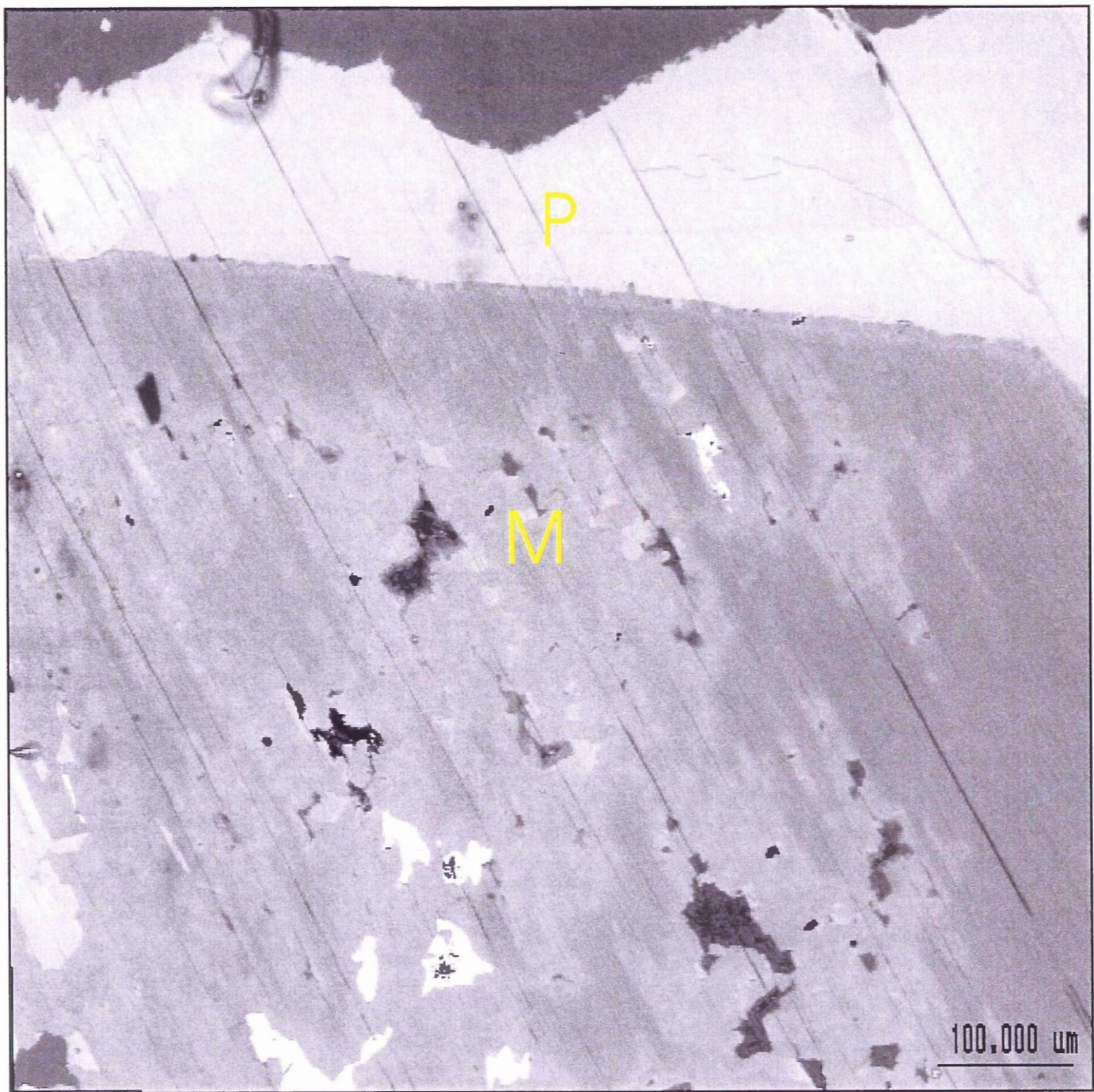


Figure 4.3. Backscattered electron image enlargement of muscovite(M)-phengite(P) overgrowth from Figure 4.2 a and b. The boundary between the muscovite core and phengite overgrowth is well-defined, sharp, and straight. Note that the cleavage continues through the boundary uninterrupted.

Topaz is associated with mica and is present in both the Walker deposit and the leucogranite (Fig. 4.2f). Topaz grains contain inclusions of biotite suggesting a magmatic origin, and thus suggest the magma was rich in fluorine.

Micas from the Lake Lewis Leucogranite and Walker Moly deposit look similar. The micas are deformed, have inclusions of fluorite, and are altered throughout the grain (Fig. 4.4). The deformation was associated with a fluid and is discussed in more detail in Chapter 5. These sample locations have many fluorite veins indicating a late-stage injection of fluid. The fluids penetrated the micas along cleavage planes and created deformation in the form of shearing, kinking, and bending.

4.1.2 Thick sections

Figure 4.5 shows several thick white mica grains that display epitaxial overgrowth between a colorless muscovite and a light brown phengite. The contacts between the two types of mica are sharp crystal growth faces. These grains extinguish as a whole meaning these two varieties of mica are in optical continuity and crystallographically aligned where the orientation of one mica determines the orientation of the other mica. These overgrowths are primary textural features. The basal grain sections of the grain photographed in Figures 4.5 a and b yield perfect biaxial Bxa figures. These figures give a $2V$ angle of approximately 40° , equivalent with a white mica and too high for biotite, a dispersion of $r > v$, also equivalent with a white mica and opposite to biotite. The low absorption colors of the brown bands are too low for biotite. This evidence shows that these are indeed varieties of white mica, with the brown bands being a higher iron variety (phengite) than the colorless bands (muscovite). Undulose extinction is very common in these thick mica grains suggesting growth from a silicate melt.

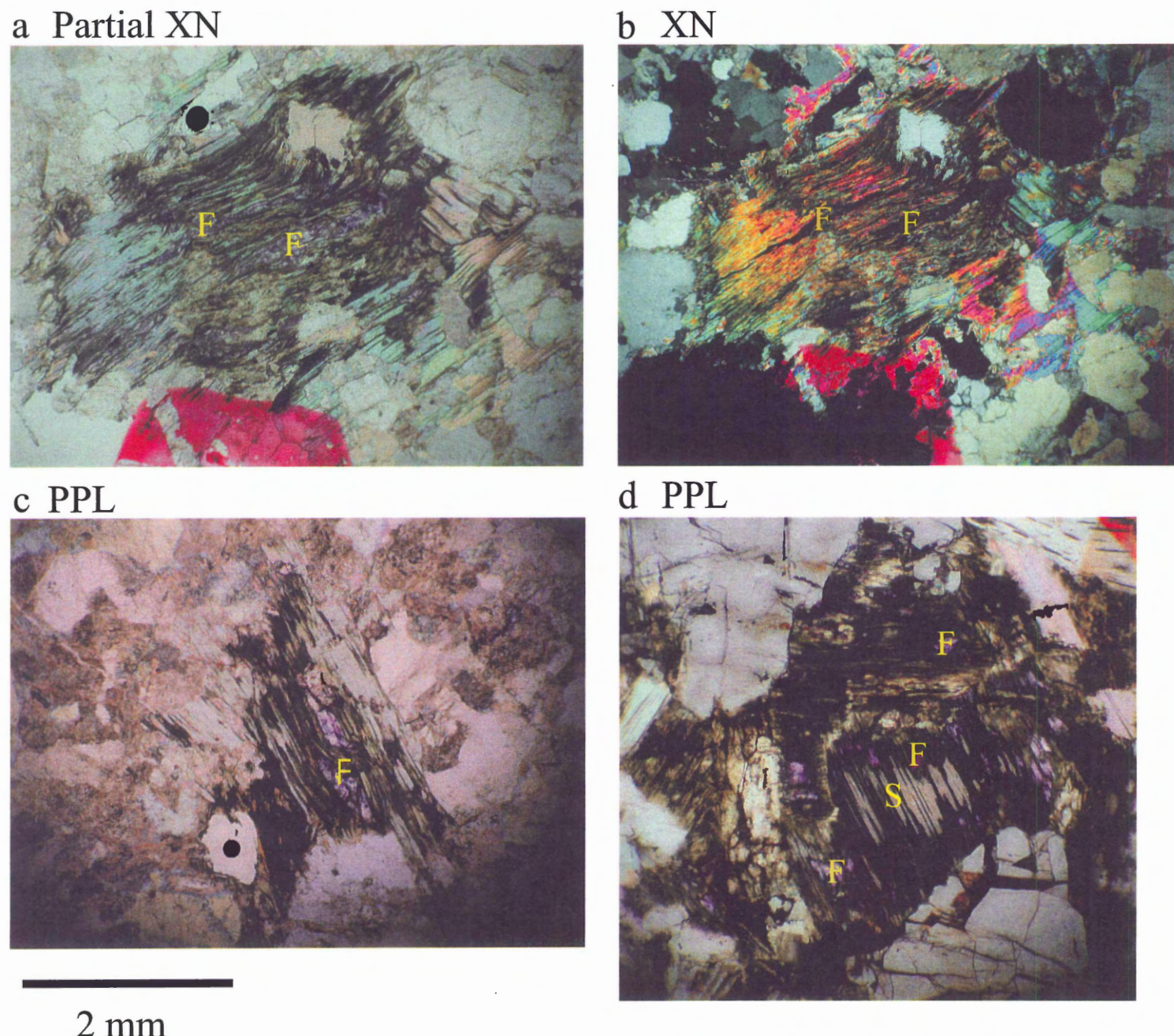
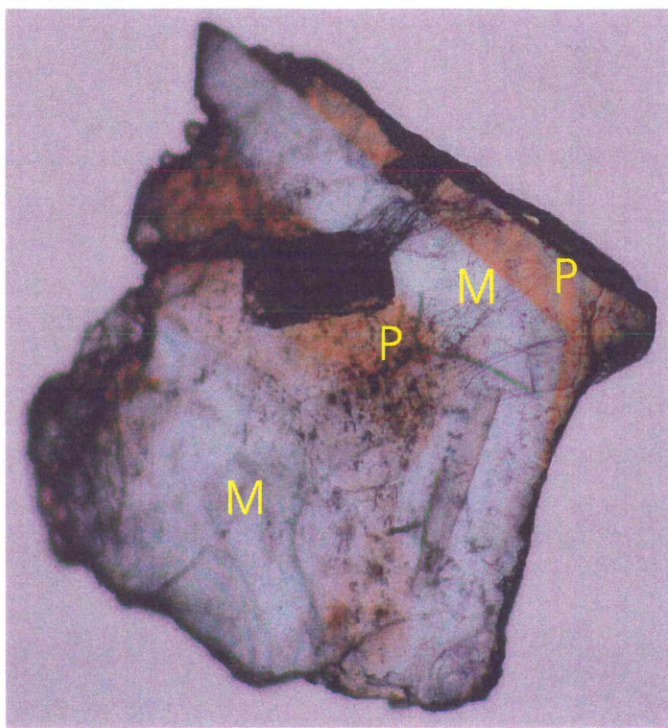
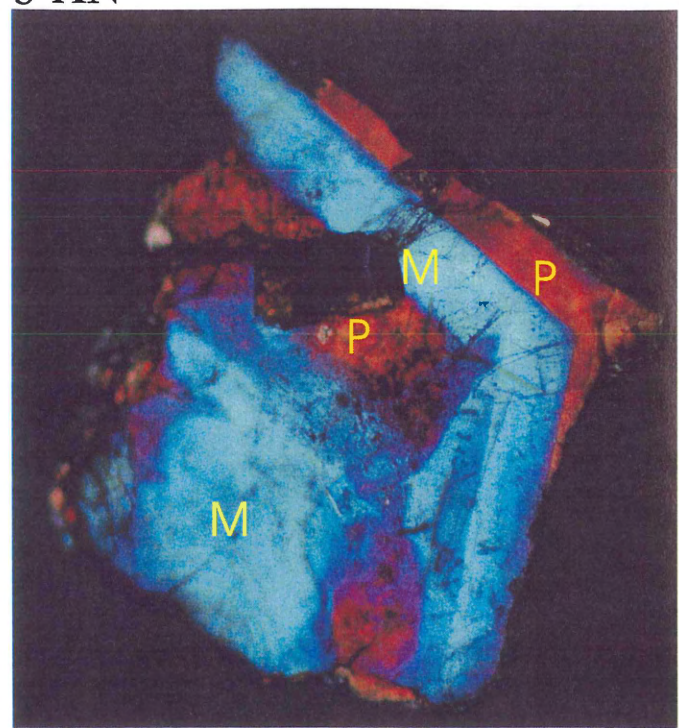


Figure 4.4. Thin section photomicrographs of representative deformed white micas from the Lake Lewis Leucogranite and Walker Moly deposit. These deformed white micas are bent, sheared, and kinked. The micas also have fluorite crystallization (F) along cleavage planes. (a-c) Lake Lewis Leucogranite sample LLL3. (d) Walker Moly deposit sample SC-20W. Central core is altered to chemically determined siderophyllite (S).

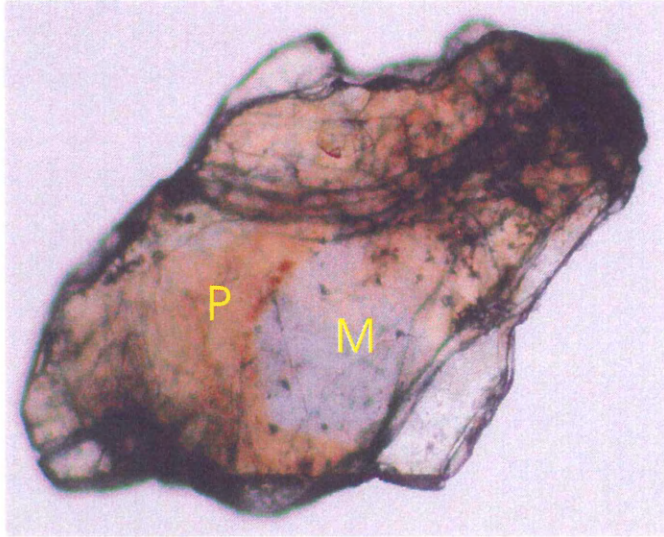
a PPL



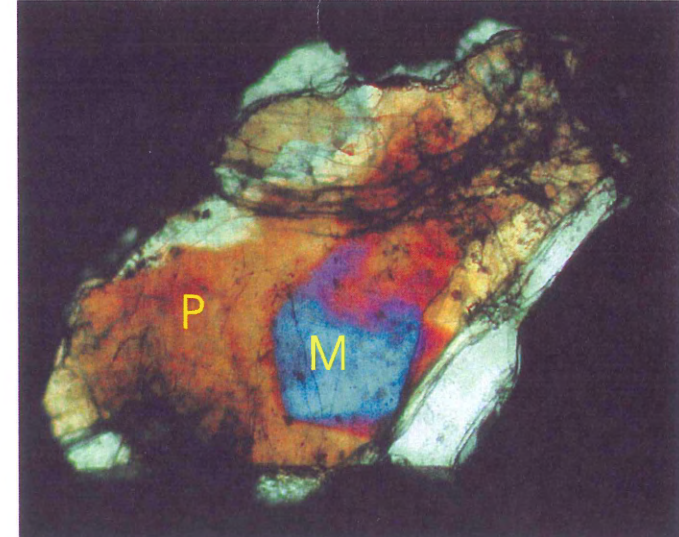
b XN



c PPL



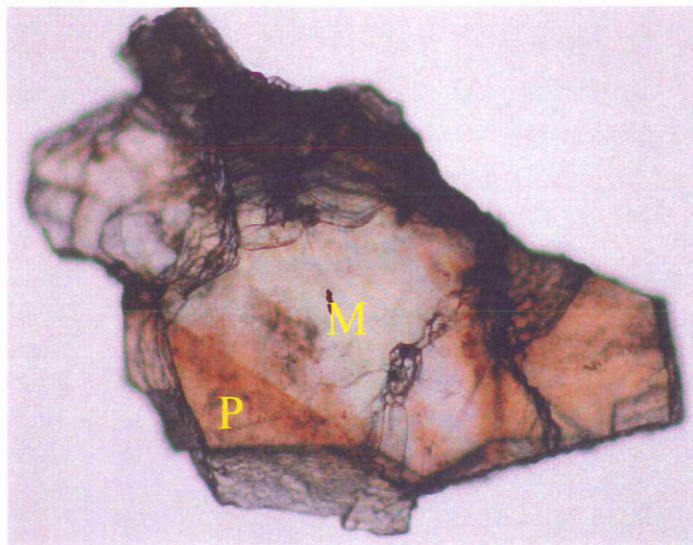
d XN



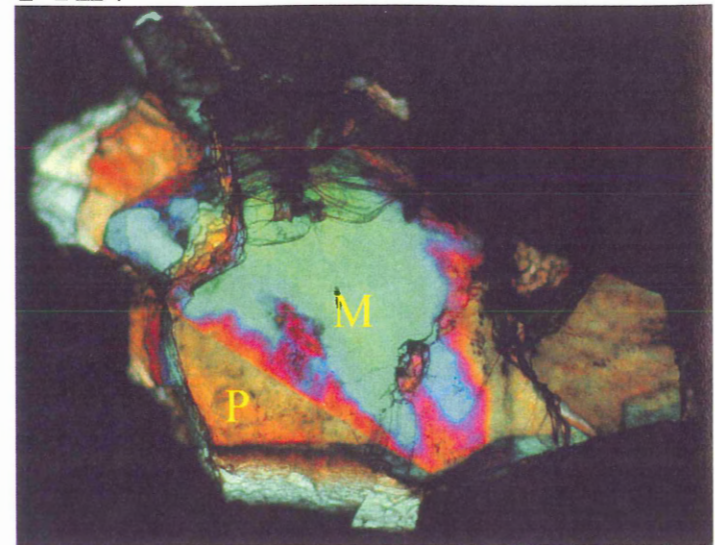
2 mm

Figure 4.5. Photomicrographs of Lake Lewis Leucogranite white mica grains, approximately 0.3 mm thick, showing epitaxial overgrowths of brown phengite (P) on colorless muscovite (M) and vice-versa. (a-b) Sample LL99-8 mica shows two separate overgrowth bands of phengite on a muscovite core and muscovite band. (c-d) Sample LL99-6 mica shows a pseudohexagonal muscovite core with a phengite overgrowth. This figure is continued on the following page.

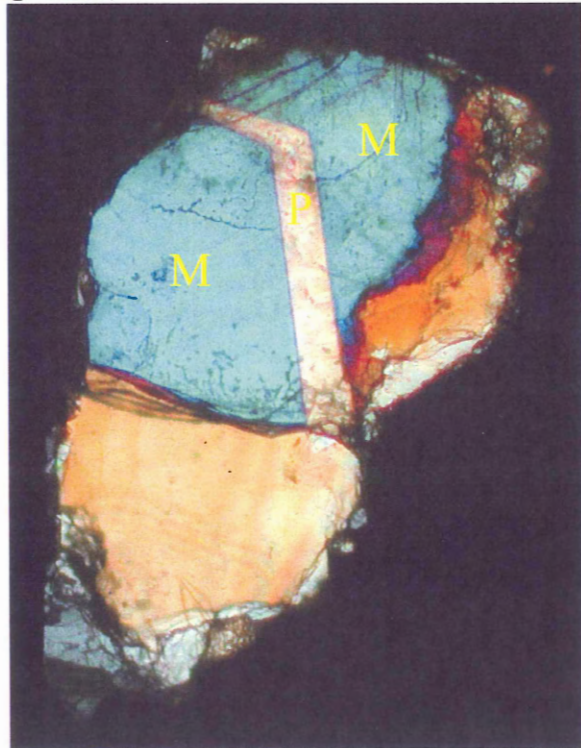
e PPL



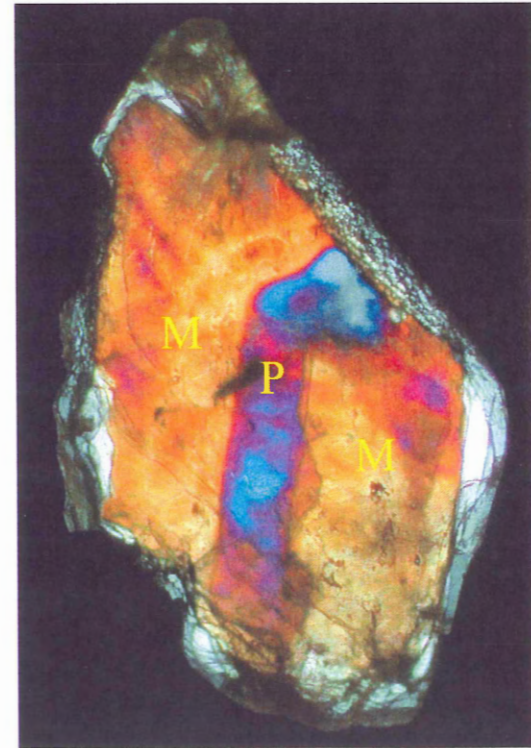
f XN



g XN



h XN



2 mm

Figure 4.5. continued.. (e-f) Sample LL99-6 mica shows an overgrowth of phengite on muscovite. (g-h) Samples LL99-6 and LL99-8, respectively, micas also show overgrowths of phengite on muscovite.

4.2 Mineral chemical data

Table 4.2 summarizes the results of mica structural formulae calculations. The calculations, based on 22 oxygens, use the molecular proportions method described in Appendix 1 of Deer et al. (1992) to recalculate the raw microprobe data. The calculations can be found, with more detailed explanations, in the Microsoft Excel 97 file Mica struc form.xls on the included disk. Also included on this disk, in the Microsoft Excel 97 file Li struc form.xls, are the lithium estimate calculations using regression equations based on F and SiO₂ from Tischendorf et al. (1997). These calculations, also based on 22 oxygens, use the charge balance method to recalculate the raw microprobe data to mica structural formulae.

Table 4.3 summarizes the results of feldspar structural formulae calculations. The raw microprobe data were recalculated, based on 32 oxygens, using the Minpet version 2.0 program by L. Richard. The K-feldspars have chemical compositions that range from Or₈₅₋₁₀₀. The plagioclases show very low anorthite contents that range from An₀₋₅. These compositions can result from perfect fractional crystallization, from re-equilibration with a fluid with decreasing pressure or temperature conditions, or from alteration by a sodic fluid replacement. The Lake Lewis Leucogranite feldspars are not altered, thus favoring fractional crystallization hypothesis. This problem is dealt with in more detail in Chapter 5.

4.3 Summary

Through textural observations, two different kinds of white micas are present in the Lake Lewis Leucogranite. The first is coarse-grained, dimensionally compatible with other minerals, euhedral to subhedral with sharp, well-defined, and straight grain

Table 4.2. Mica group averages and standard deviations of mica microprobe data for Lake Lewis Leucogranite and Walker Moly samples. This table is continued on the next page.

Mineral n	Muscovite		Phengite I		Phengite II		Zinnwaldite	
	54		91		27		12	
Location	average	σ	average	σ	average	σ	average	σ
SiO ₂	49.83	1.95	45.79	1.14	45.51	1.29	39.01	1.61
TiO ₂	0.44	0.60	0.17	0.17	0.39	0.23	0.76	0.54
Al ₂ O ₃	26.03	1.87	33.85	1.25	29.89	1.56	23.51	0.56
FeO	5.58	1.80	3.25	0.90	6.85	1.69	19.18	2.97
MnO	0.06	0.06	0.07	0.07	0.13	0.08	0.39	0.08
MgO	0.97	0.52	0.32	0.24	0.52	0.35	0.55	0.30
CaO	0.06	0.06	0.02	0.03	0.02	0.03	0.02	0.03
Na ₂ O	0.12	0.09	0.59	0.20	0.49	0.16	0.42	0.09
K ₂ O	10.01	0.88	10.38	0.67	10.44	0.34	9.75	0.26
Cr ₂ O ₃	0.03	0.04	0.03	0.04	0.03	0.04	0.02	0.03
Cl	0.01	0.02	0.01	0.02	0.01	0.01	0.03	0.03
P ₂ O ₅	0.06	0.05	0.08	0.07	0.06	0.05	0.07	0.06
BaO	0.03	0.05	0.05	0.06	0.04	0.06	0.04	0.05
F	2.15	1.58	1.33	0.63	2.55	0.67	2.72	0.91
Total	95.37	1.51	95.94	1.00	96.93	1.04	96.46	0.98
Si	6.34	0.19	6.40	0.18	6.74	0.42	6.37	0.48
Ti	0.02	0.02	0.07	0.04	0.04	0.04	0.02	0.02
Al Total	5.31	0.32	4.85	0.35	4.77	0.57	4.71	0.45
Al IV	1.66	0.19	1.60	0.18	1.26	0.42	1.63	0.48
Al VI	3.65	0.16	3.25	0.50	3.51	0.22	3.07	0.65
Fe	0.54	0.36	1.19	0.74	0.76	0.40	1.41	1.28
Mn	0.01	0.01	0.02	0.02	0.02	0.02	0.03	0.03
Mg	0.08	0.04	0.13	0.05	0.13	0.10	0.09	0.08
Ca	0.00	0.00	0.00	0.00	0.01	0.01	0.00	0.01
Na	0.15	0.04	0.13	0.04	0.11	0.07	0.10	0.06
K	1.87	0.07	1.91	0.07	1.84	0.16	1.93	0.09
Cr	0.00	0.00	0.00	0.00	0.00	0.00	0.00	0.00
Cl	0.00	0.00	0.00	0.00	0.00	0.00	0.01	0.01
P	0.01	0.01	0.01	0.01	0.01	0.01	0.01	0.01
Ba	0.00	0.00	0.00	0.00	0.00	0.00	0.00	0.00
F	0.73	0.62	1.20	0.39	1.24	0.83	0.81	0.43
OH	3.26	0.62	2.80	0.39	2.75	0.83	3.18	0.44
Tet	8.00	0.00	8.00	0.00	8.00	0.00	8.00	0.00
Oct	4.31	0.26	4.66	0.35	4.46	0.28	4.62	0.64
Dodec	2.03	0.05	2.06	0.08	1.96	0.19	2.05	0.13

Table 4.2 continued

Mineral n	Protolithonite		Siderophyllite	
	18	7		
Location	average	σ	average	σ
SiO ₂	38.86	1.50	35.59	0.20
TiO ₂	0.84	0.53	0.06	0.06
Al ₂ O ₃	23.46	0.53	23.13	0.19
FeO	19.70	2.95	24.80	0.42
MnO	0.38	0.08	0.50	0.09
MgO	0.63	0.33	0.12	0.04
CaO	0.02	0.02	0.01	0.01
Na ₂ O	0.43	0.09	0.49	0.10
K ₂ O	9.74	0.24	9.80	0.12
Cr ₂ O ₃	0.02	0.03	0.02	0.03
Cl	0.03	0.03	0.06	0.02
P ₂ O ₅	0.06	0.06	0.11	0.09
BaO	0.06	0.08	0.05	0.07
F	2.65	0.84	2.77	0.11
Total	96.90	1.36	97.51	0.73
Si	6.29	0.48	6.15	0.25
Ti	0.02	0.02	0.00	0.00
Al Total	4.72	0.46	5.17	0.55
Al IV	1.71	0.48	1.85	0.25
Al VI	3.01	0.69	3.32	0.78
Fe	1.58	1.35	1.34	1.33
Mn	0.03	0.03	0.02	0.03
Mg	0.07	0.08	0.02	0.02
Ca	0.00	0.01	0.00	0.00
Na	0.11	0.06	0.17	0.04
K	1.94	0.08	1.92	0.05
Cr	0.00	0.00	0.01	0.01
Cl	0.01	0.01	0.01	0.01
P	0.01	0.01	0.00	0.00
Ba	0.00	0.00	0.00	0.00
F	0.86	0.44	1.01	0.22
OH	3.13	0.44	2.99	0.22
Tet	8.00	0.00	8.00	0.00
Oct	4.71	0.67	4.71	0.59
Dodec	2.06	0.13	2.10	0.06

Table 4.3. Averages and standard deviations of feldspar microprobe analyses for Lake Lewis Leucogranite samples. This table is continued on the following pages.

Sample Mineral Location	LL99-1 K-feldspar core n		LL99-1 K-feldspar rim 4		LL99-1 plagioclase core 4		LL99-1 plagioclase rim 2		LL99-2 K-feldspar core 4		LL99-2 K-feldspar rim 4	
	average	σ	average	σ	average	σ	average	σ	average	σ	average	σ
SiO ₂	64.22	0.86	63.46	0.98	67.60	2.13	69.08	0.13	64.43	0.18	64.96	0.69
TiO ₂	0.04	0.03	0.01	0.01	0.02	0.04	0.00	0.00	0.01	0.01	0.03	0.03
Al ₂ O ₃	18.53	0.33	19.26	1.02	19.89	0.96	19.69	0.06	18.52	0.27	18.35	0.20
FeO	0.00	0.00	0.18	0.35	0.02	0.03	0.00	0.00	0.04	0.03	0.07	0.05
MnO	0.07	0.07	0.05	0.04	0.01	0.01	0.03	0.04	0.04	0.05	0.02	0.02
MgO	0.01	0.01	0.11	0.14	0.06	0.04	0.05	0.07	0.02	0.03	0.04	0.05
BaO	0.01	0.01	0.00	0.01	0.00	0.00	0.00	0.00	0.00	0.00	0.03	0.07
CaO	0.01	0.03	0.03	0.04	0.34	0.42	0.09	0.13	0.04	0.05	0.01	0.01
Na ₂ O	0.37	0.21	0.81	0.53	10.42	1.18	10.97	1.51	0.45	0.42	0.27	0.12
K ₂ O	16.16	0.39	15.11	0.36	0.44	0.56	0.08	0.09	16.00	1.00	16.43	0.28
Total	99.77	0.76	99.63	1.03	99.07	1.92	100.14	1.08	99.84	0.47	100.44	0.83
Si	11.95	0.08	11.82	0.15	11.93	0.21	12.02	0.06	11.96	0.02	12.00	0.02
Al	4.06	0.08	4.23	0.22	4.14	0.24	4.04	0.04	4.05	0.06	3.99	0.02
Ti	0.01	0.00	0.00	0.00	0.00	0.01	0.00	0.00	0.00	0.00	0.00	0.00
Fe	0.00	0.00	0.03	0.05	0.00	0.00	0.00	0.00	0.01	0.01	0.01	0.01
Mn	0.01	0.01	0.01	0.01	0.00	0.00	0.01	0.01	0.01	0.01	0.00	0.00
Mg	0.00	0.00	0.03	0.04	0.02	0.01	0.01	0.02	0.00	0.01	0.01	0.01
Ba	0.00	0.00	0.00	0.00	0.00	0.00	0.00	0.00	0.00	0.00	0.00	0.01
Ca	0.00	0.01	0.01	0.01	0.06	0.08	0.02	0.02	0.01	0.01	0.00	0.00
Na	0.13	0.08	0.29	0.19	3.56	0.35	3.70	0.48	0.16	0.15	0.10	0.04
K	3.84	0.11	3.59	0.09	0.10	0.13	0.02	0.02	3.79	0.23	3.87	0.06
Ab	3.30	1.80	7.40	4.60	95.60	5.60	99.00	1.30	4.10	3.90	2.40	1.00
An	0.10	0.10	0.20	0.20	1.70	2.20	0.50	0.70	0.20	0.30	0.10	0.10
Or	96.70	1.90	92.50	4.50	2.70	3.50	0.60	0.60	95.70	4.20	97.50	1.10

Table 4.3 continued

Sample Mineral Location n	LL99-2 plagioclase core 4		LL99-2 plagioclase rim 4		LL99-3 K-feldspar core 3		LL99-3 K-feldspar rim 3		LL99-3 plagioclase core 3		LL99-3 plagioclase rim 3	
	average	σ	average	σ	average	σ	average	σ	average	σ	average	σ
SiO ₂	68.48	0.30	68.39	0.12	64.12	0.77	64.08	0.23	68.85	0.31	69.00	0.39
TiO ₂	0.00	0.00	0.01	0.02	0.02	0.03	0.04	0.04	0.00	0.00	0.04	0.02
Al ₂ O ₃	19.36	0.06	19.30	0.09	18.84	0.11	18.58	0.07	19.82	0.14	19.74	0.05
FeO	0.04	0.07	0.02	0.02	0.02	0.02	0.05	0.04	0.01	0.02	0.00	0.00
MnO	0.02	0.05	0.01	0.01	0.01	0.02	0.01	0.01	0.02	0.03	0.02	0.04
MgO	0.05	0.05	0.06	0.07	0.03	0.03	0.00	0.01	0.03	0.01	0.05	0.04
BaO	0.13	0.24	0.00	0.01	0.01	0.01	0.24	0.16	0.15	0.26	0.10	0.10
CaO	0.03	0.01	0.03	0.02	0.00	0.00	0.00	0.01	0.23	0.18	0.08	0.07
Na ₂ O	11.61	0.48	11.23	0.63	0.28	0.15	0.37	0.09	9.63	0.64	10.01	0.87
K ₂ O	0.12	0.07	0.08	0.07	16.36	0.12	16.22	0.23	0.11	0.03	0.12	0.12
Total	99.93	0.72	99.24	0.67	100.49	0.38	100.30	0.22	99.19	0.52	99.35	1.11
Si	11.99	0.04	12.02	0.04	11.90	0.06	11.93	0.01	12.07	0.07	12.07	0.04
Al	3.99	0.02	4.00	0.02	4.12	0.03	4.07	0.03	4.09	0.01	4.07	0.04
Ti	0.00	0.00	0.00	0.00	0.00	0.00	0.01	0.01	0.00	0.00	0.01	0.00
Fe	0.01	0.01	0.00	0.00	0.00	0.00	0.01	0.01	0.00	0.00	0.00	0.00
Mn	0.00	0.01	0.00	0.00	0.00	0.00	0.00	0.00	0.00	0.00	0.00	0.01
Mg	0.01	0.01	0.02	0.02	0.01	0.01	0.00	0.00	0.01	0.00	0.01	0.01
Ba	0.01	0.02	0.00	0.00	0.00	0.00	0.02	0.01	0.01	0.02	0.01	0.01
Ca	0.01	0.00	0.01	0.00	0.00	0.00	0.00	0.00	0.04	0.03	0.02	0.01
Na	3.94	0.16	3.83	0.20	0.10	0.06	0.14	0.03	3.27	0.21	3.39	0.27
K	0.03	0.02	0.02	0.02	3.88	0.06	3.85	0.05	0.02	0.01	0.03	0.03
Ab	99.20	0.40	99.40	0.50	2.50	1.40	3.40	0.90	98.00	1.00	98.80	1.00
An	0.10	0.10	0.10	0.10	0.00	0.00	0.00	0.10	1.30	0.80	0.50	0.40
Or	0.70	0.40	0.50	0.40	97.50	1.40	96.60	0.90	0.70	0.20	0.80	0.80

Table 4.3 continued

Sample Mineral Location	LL99-4 K-feldspar core n		LL99-4 K-feldspar rim 3		LL99-4 plagioclase core 4		LL99-4 plagioclase rim 2		LL99-5 K-feldspar core 4		LL99-5 K-feldspar rim 4	
	average	σ	average	σ	average	σ	average	σ	average	σ	average	σ
SiO ₂	64.25	0.45	63.96	0.90	67.84	0.50	68.78	0.62	63.83	0.69	63.70	0.44
TiO ₂	0.03	0.03	0.01	0.02	0.05	0.06	0.06	0.05	0.00	0.00	0.04	0.04
Al ₂ O ₃	18.80	0.15	18.78	0.32	20.13	0.33	19.86	0.23	18.69	0.12	18.70	0.20
FeO	0.06	0.08	0.02	0.02	0.00	0.00	0.10	0.01	0.01	0.01	0.04	0.04
MnO	0.00	0.01	0.00	0.00	0.01	0.01	0.00	0.00	0.00	0.00	0.02	0.03
MgO	0.04	0.07	0.03	0.03	0.05	0.05	0.04	0.02	0.02	0.05	0.02	0.02
BaO	0.01	0.02	0.01	0.01	0.01	0.01	0.00	0.00	0.00	0.01	0.03	0.05
CaO	0.01	0.02	0.03	0.05	0.26	0.17	0.00	0.00	0.01	0.02	0.00	0.00
Na ₂ O	1.60	0.17	0.75	0.32	11.66	0.17	11.58	0.44	1.23	0.52	0.77	0.33
K ₂ O	15.13	0.17	16.19	0.53	0.19	0.07	0.17	0.07	14.97	0.86	15.31	0.37
Total	100.63	0.63	100.53	1.11	100.84	0.40	101.00	0.21	99.50	0.70	99.37	1.01
Si	11.88	0.00	11.88	0.04	11.85	0.08	11.95	0.08	11.91	0.03	11.91	0.04
Al	4.09	0.01	4.11	0.03	4.14	0.07	4.06	0.06	4.11	0.03	4.12	0.02
Ti	0.01	0.00	0.00	0.00	0.01	0.01	0.01	0.01	0.00	0.00	0.01	0.01
Fe	0.01	0.01	0.00	0.00	0.00	0.00	0.01	0.00	0.00	0.00	0.01	0.01
Mn	0.00	0.00	0.00	0.00	0.00	0.00	0.00	0.00	0.00	0.00	0.00	0.01
Mg	0.01	0.02	0.01	0.01	0.01	0.01	0.01	0.01	0.01	0.01	0.01	0.01
Ba	0.00	0.00	0.00	0.00	0.00	0.00	0.00	0.00	0.00	0.00	0.00	0.00
Ca	0.00	0.00	0.01	0.01	0.05	0.03	0.00	0.00	0.00	0.00	0.00	0.00
Na	0.57	0.06	0.27	0.11	3.95	0.06	3.90	0.16	0.44	0.19	0.28	0.12
K	3.57	0.05	3.84	0.17	0.04	0.01	0.04	0.02	3.56	0.22	3.65	0.07
Ab	13.80	1.40	6.50	2.80	97.70	0.90	99.10	0.40	11.10	4.70	7.10	2.80
An	0.00	0.10	0.10	0.20	1.20	0.70	0.00	0.00	0.10	0.10	0.00	0.00
Or	86.10	1.40	93.30	2.60	1.10	0.40	1.00	0.40	88.80	4.80	92.90	2.80

Table 4.3 continued

Sample Mineral Location n	LL99-5 plagioclase core 3		LL99-5 plagioclase rim 3		LL99-6 K-feldspar core 3		LL99-6 K-feldspar rim 3		LL99-6 plagioclase core 4		LL99-6 plagioclase rim 4	
	average	σ	average	σ	average	σ	average	σ	average	σ	average	σ
SiO ₂	67.85	1.23	67.97	0.71	63.24	0.64	63.60	0.23	67.61	0.94	67.82	0.76
TiO ₂	0.02	0.03	0.02	0.03	0.02	0.03	0.02	0.03	0.00	0.00	0.02	0.04
Al ₂ O ₃	19.46	0.15	19.69	0.46	18.70	0.19	18.70	0.32	19.86	0.73	19.76	0.29
FeO	0.01	0.01	0.01	0.02	0.01	0.02	0.04	0.06	0.02	0.04	0.00	0.00
MnO	0.00	0.00	0.00	0.00	0.01	0.01	0.00	0.00	0.01	0.01	0.01	0.02
MgO	0.05	0.06	0.04	0.04	0.02	0.02	0.00	0.01	0.03	0.02	0.01	0.02
BaO	0.01	0.01	0.15	0.24	0.00	0.00	0.01	0.02	0.00	0.00	0.00	0.00
CaO	0.12	0.11	0.12	0.09	0.00	0.00	0.00	0.00	0.41	0.36	0.30	0.30
Na ₂ O	11.84	0.31	11.20	0.56	1.11	0.60	0.68	0.53	11.04	0.78	10.97	0.71
K ₂ O	0.08	0.05	0.12	0.05	15.68	0.54	16.09	0.88	0.18	0.16	0.17	0.06
Total	99.76	0.96	99.76	0.74	99.63	0.99	100.01	0.19	99.71	0.63	99.42	0.67
Si	11.94	0.08	11.95	0.12	11.86	0.03	11.88	0.04	11.91	0.13	11.94	0.07
Al	4.03	0.07	4.08	0.09	4.13	0.02	4.12	0.07	4.12	0.17	4.10	0.09
Ti	0.00	0.00	0.00	0.00	0.00	0.00	0.00	0.00	0.00	0.00	0.00	0.01
Fe	0.00	0.00	0.00	0.00	0.00	0.00	0.01	0.01	0.00	0.01	0.00	0.00
Mn	0.00	0.00	0.00	0.00	0.00	0.00	0.00	0.00	0.00	0.00	0.00	0.00
Mg	0.01	0.01	0.01	0.01	0.01	0.00	0.00	0.00	0.01	0.01	0.00	0.00
Ba	0.00	0.00	0.01	0.02	0.00	0.00	0.00	0.00	0.00	0.00	0.00	0.00
Ca	0.02	0.02	0.02	0.02	0.00	0.00	0.00	0.00	0.08	0.07	0.06	0.06
Na	4.04	0.12	3.82	0.19	0.40	0.21	0.25	0.19	3.77	0.25	3.75	0.22
K	0.02	0.01	0.03	0.01	3.75	0.17	3.84	0.22	0.04	0.04	0.04	0.01
Ab	99.00	0.70	98.70	0.40	9.60	5.10	6.00	4.70	96.90	2.60	97.50	1.90
An	0.60	0.50	0.50	0.40	0.00	0.00	0.00	0.00	2.00	1.80	1.50	1.50
Or	0.40	0.30	0.70	0.30	90.40	5.10	94.00	4.70	1.10	0.90	1.00	0.40

Table 4.3 continued

Sample Mineral Location	LL99-7 K-feldspar core n		LL99-7 K-feldspar rim 3		LL99-7 plagioclase core 4		LL99-7 plagioclase rim 3		LL99-8 K-feldspar core 4		LL99-8 K-feldspar rim 4	
	average	σ	average	σ	average	σ	average	σ	average	σ	average	σ
SiO ₂	63.81	0.09	63.48	0.65	67.88	0.49	67.68	0.45	64.62	0.16	63.61	1.30
TiO ₂	0.02	0.03	0.01	0.01	0.02	0.03	0.03	0.03	0.02	0.03	0.03	0.05
Al ₂ O ₃	18.67	0.16	18.54	0.12	19.96	0.21	20.16	0.23	18.86	0.29	18.76	0.51
FeO	0.02	0.03	0.03	0.03	0.02	0.05	0.00	0.00	0.05	0.05	0.04	0.03
MnO	0.04	0.04	0.03	0.05	0.01	0.02	0.00	0.00	0.03	0.05	0.04	0.05
MgO	0.07	0.01	0.05	0.05	0.02	0.02	0.05	0.08	0.03	0.04	0.01	0.02
BaO	0.00	0.00	0.00	0.01	0.06	0.08	0.00	0.00	0.08	0.06	0.13	0.15
CaO	0.00	0.00	0.01	0.01	0.14	0.13	0.21	0.09	0.01	0.01	0.06	0.10
Na ₂ O	1.51	0.19	0.79	0.40	11.00	0.48	10.89	0.67	1.33	0.26	0.55	0.32
K ₂ O	14.80	0.44	15.14	0.24	0.11	0.04	0.12	0.02	14.98	0.25	15.74	0.47
Total	99.50	0.50	98.74	1.18	99.64	0.34	99.49	0.95	100.38	0.35	99.48	1.28
Si	11.89	0.02	11.93	0.02	11.93	0.06	11.90	0.05	11.91	0.04	11.89	0.06
Al	4.10	0.02	4.10	0.03	4.13	0.04	4.18	0.06	4.09	0.06	4.13	0.07
Ti	0.00	0.00	0.00	0.00	0.00	0.00	0.00	0.00	0.00	0.01	0.00	0.01
Fe	0.00	0.01	0.01	0.01	0.00	0.01	0.00	0.00	0.01	0.01	0.01	0.01
Mn	0.01	0.01	0.00	0.01	0.00	0.00	0.00	0.00	0.01	0.01	0.01	0.01
Mg	0.02	0.00	0.01	0.01	0.00	0.01	0.01	0.02	0.01	0.01	0.00	0.01
Ba	0.00	0.00	0.00	0.00	0.00	0.01	0.00	0.00	0.01	0.00	0.01	0.01
Ca	0.00	0.00	0.00	0.00	0.03	0.02	0.04	0.02	0.00	0.00	0.01	0.02
Na	0.55	0.07	0.29	0.14	3.75	0.17	3.71	0.20	0.48	0.10	0.20	0.12
K	3.52	0.10	3.63	0.03	0.03	0.01	0.03	0.01	3.52	0.06	3.76	0.16
Ab	13.50	1.80	7.20	3.30	98.70	0.70	98.20	0.50	11.80	2.20	5.00	3.00
An	0.00	0.00	0.00	0.10	0.70	0.60	1.10	0.50	0.00	0.10	0.30	0.50
Or	86.50	1.80	92.70	3.40	0.70	0.20	0.70	0.10	88.20	2.20	94.70	2.60

Table 4.3 continued

Sample Mineral Location	LL99-8 plagioclase core n		LL99-8 plagioclase rim 14		LL99-9 K-feldspar core 3		LL99-9 K-feldspar rim 3		LL99-9 plagioclase core 3		LL99-9 plagioclase rim 3	
	average	σ	average	σ	average	σ	average	σ	average	σ	average	σ
SiO ₂	67.18	1.88	68.89	0.80	64.28	0.70	64.48	0.16	67.38	0.73	68.16	0.39
TiO ₂	0.03	0.04	0.01	0.02	0.03	0.04	0.01	0.02	0.04	0.04	0.00	0.01
Al ₂ O ₃	20.70	1.35	19.85	0.42	19.19	0.25	19.34	0.02	20.78	0.17	20.23	0.07
FeO	0.03	0.04	0.02	0.04	0.00	0.00	0.04	0.06	0.04	0.04	0.01	0.02
MnO	0.02	0.04	0.03	0.05	0.01	0.02	0.05	0.02	0.02	0.04	0.00	0.01
MgO	0.03	0.03	0.04	0.04	0.06	0.05	0.02	0.03	0.03	0.04	0.07	0.04
BaO	0.01	0.03	0.01	0.04	0.05	0.08	0.05	0.06	0.09	0.12	0.00	0.00
CaO	1.04	1.46	0.08	0.09	0.00	0.00	0.00	0.01	0.21	0.09	0.06	0.07
Na ₂ O	9.78	1.05	10.55	0.72	0.75	0.38	0.93	0.15	10.13	1.43	10.25	1.43
K ₂ O	0.20	0.08	0.14	0.07	15.00	0.54	14.69	0.05	0.11	0.06	0.12	0.05
Total	99.20	0.56	99.78	0.51	100.16	0.85	100.53	0.19	99.67	0.55	99.41	1.21
Si	11.82	0.30	12.02	0.11	11.89	0.03	11.89	0.03	11.86	0.11	11.97	0.08
Al	4.29	0.29	4.08	0.10	4.18	0.03	4.20	0.00	4.31	0.03	4.18	0.05
Ti	0.00	0.01	0.00	0.00	0.00	0.01	0.00	0.00	0.01	0.01	0.00	0.00
Fe	0.00	0.01	0.00	0.01	0.00	0.00	0.01	0.01	0.01	0.01	0.00	0.00
Mn	0.00	0.01	0.01	0.01	0.00	0.00	0.01	0.00	0.00	0.01	0.00	0.00
Mg	0.01	0.01	0.01	0.01	0.02	0.01	0.01	0.01	0.01	0.01	0.02	0.01
Ba	0.00	0.00	0.00	0.00	0.00	0.01	0.00	0.01	0.01	0.01	0.00	0.00
Ca	0.20	0.28	0.01	0.02	0.00	0.00	0.00	0.00	0.04	0.02	0.01	0.01
Na	3.34	0.36	3.57	0.24	0.27	0.14	0.33	0.06	3.46	0.49	3.49	0.46
K	0.05	0.02	0.03	0.02	3.54	0.16	3.45	0.01	0.02	0.01	0.03	0.01
Ab	93.40	7.10	98.80	0.70	7.10	3.60	8.80	1.30	98.20	0.30	98.80	0.60
An	5.40	7.10	0.40	0.40	0.00	0.00	0.00	0.10	1.20	0.50	0.40	0.40
Or	1.20	0.50	0.90	0.40	92.90	3.60	91.20	1.30	0.60	0.30	0.80	0.30

Table 4.3 continued

Sample Mineral Location	LL99-11 K-feldspar core n		LL99-11 K-feldspar rim 3		LL99-11 plagioclase core 4		LL99-11 plagioclase rim 4		LL99-12 K-feldspar core 6		LL99-12 K-feldspar rim 5	
	average	σ	average	σ	average	σ	average	σ	average	σ	average	σ
SiO ₂	63.83	0.40	63.26	1.14	68.00	0.58	67.25	0.78	63.71	0.32	63.65	0.36
TiO ₂	0.06	0.04	0.01	0.01	0.02	0.04	0.00	0.01	0.06	0.07	0.03	0.04
Al ₂ O ₃	18.80	0.13	19.54	1.35	19.95	0.17	20.18	0.36	19.00	0.18	19.02	0.24
FeO	0.12	0.15	0.03	0.04	0.07	0.08	0.03	0.02	0.03	0.03	0.00	0.01
MnO	0.02	0.02	0.00	0.00	0.02	0.02	0.02	0.03	0.02	0.03	0.01	0.02
MgO	0.06	0.05	0.07	0.12	0.03	0.04	0.05	0.02	0.02	0.02	0.03	0.03
BaO	0.00	0.00	0.05	0.05	0.02	0.04	0.07	0.07	0.06	0.05	0.01	0.02
CaO	0.00	0.00	0.04	0.07	0.07	0.11	0.19	0.16	0.03	0.03	0.00	0.00
Na ₂ O	1.37	0.25	0.63	0.35	10.80	0.98	11.08	0.78	1.02	0.59	0.68	0.33
K ₂ O	14.96	0.64	15.48	0.36	0.13	0.05	0.17	0.12	14.99	1.06	15.63	0.20
Total	99.72	0.84	99.68	0.36	99.25	0.64	99.62	0.54	99.82	0.61	99.97	0.38
Si	11.87	0.00	11.79	0.21	11.95	0.08	11.86	0.11	11.87	0.02	11.87	0.04
Al	4.12	0.00	4.29	0.30	4.13	0.03	4.19	0.08	4.17	0.05	4.18	0.05
Ti	0.01	0.01	0.00	0.00	0.00	0.01	0.00	0.00	0.01	0.01	0.01	0.01
Fe	0.02	0.02	0.01	0.01	0.01	0.01	0.01	0.00	0.00	0.01	0.00	0.00
Mn	0.00	0.00	0.00	0.00	0.00	0.00	0.00	0.01	0.00	0.01	0.00	0.00
Mg	0.02	0.01	0.02	0.03	0.01	0.01	0.01	0.01	0.00	0.01	0.01	0.01
Ba	0.00	0.00	0.00	0.00	0.00	0.00	0.01	0.01	0.00	0.00	0.00	0.00
Ca	0.00	0.00	0.01	0.01	0.01	0.02	0.04	0.03	0.01	0.01	0.00	0.00
Na	0.49	0.09	0.23	0.13	3.68	0.34	3.79	0.27	0.37	0.21	0.25	0.12
K	3.55	0.13	3.68	0.09	0.03	0.01	0.04	0.03	3.56	0.25	3.72	0.05
Ab	12.20	2.40	5.70	3.10	98.90	0.70	98.10	1.20	9.40	5.40	6.20	2.90
An	0.00	0.00	0.20	0.30	0.40	0.50	0.90	0.70	0.10	0.20	0.00	0.00
Or	87.80	2.40	94.10	2.70	0.80	0.30	1.00	0.70	90.50	5.50	93.80	2.90

Table 4.3 continued

Sample	LL99-12		LL99-12	
Mineral	plagioclase		plagioclase	
Location	core	n	rim	n
	5		5	
	average	σ	average	σ
SiO ₂	67.20	0.83	67.50	0.35
TiO ₂	0.03	0.03	0.02	0.05
Al ₂ O ₃	20.14	0.39	19.97	0.38
FeO	0.01	0.01	0.02	0.02
MnO	0.00	0.01	0.04	0.04
MgO	0.04	0.03	0.03	0.04
BaO	0.01	0.02	0.01	0.01
CaO	0.34	0.38	0.09	0.10
Na ₂ O	10.84	0.58	10.74	0.53
K ₂ O	0.12	0.08	0.15	0.08
Total	99.31	0.69	99.19	0.70
Si	11.88	0.09	11.93	0.05
Al	4.19	0.09	4.16	0.06
Ti	0.00	0.01	0.00	0.01
Fe	0.00	0.00	0.00	0.00
Mn	0.00	0.00	0.01	0.01
Mg	0.01	0.01	0.01	0.01
Ba	0.00	0.00	0.00	0.00
Ca	0.07	0.07	0.02	0.02
Na	3.71	0.18	3.68	0.18
K	0.03	0.02	0.03	0.02
Ab	97.60	2.00	98.60	0.50
An	1.70	1.90	0.50	0.50
Or	0.70	0.50	0.90	0.40

boundaries. This mica group also includes the micas containing muscovite-phengite epitaxial overgrowths. The second is also coarse-grained, but is anhedral with ragged edges, cataastically deformed (kinked, bent, and sheared), and altered with fluorite crystallization along cleavage planes. The Lake Lewis Leucogranite feldspars are generally unaltered and are not zoned. Chemically, the K-feldspars have compositions that range from Or_{85-100} , and the plagioclases have compositions that range from An_{0-5} .

CHAPTER 5

DISCUSSION

5.1 Introduction

The objectives of this thesis are to study the textures and chemical compositions of the white micas in the Lake Lewis Leucogranite, classify the micas on the basis of their chemistry, and understand the substitution mechanisms in the micas. This thesis attempts to differentiate between the primary and/or secondary nature of the micas from a physical and chemical point of view, and to use primary mica compositions as indicators of magmatic differentiation and secondary mica compositions micas as indicators of the type of alteration. This thesis includes a brief examination of the geochemistry of feldspars in comparison to the white micas, and some comments on the usefulness of primary and secondary micas to locate mineral deposits and yield reliable $^{40}\text{Ar}/^{39}\text{Ar}$ radiometric ages.

5.2 Lithium content of white micas

Micas have highly variable chemical compositions, and an ability to exchange components with fluids or other solid phases with changing conditions (Tischendorf et al. 1997). Lithium is an essential component in both dioctahedral and trioctahedral micas of evolved granites, aplites, and pegmatites (Stone et al. 1988). A serious disadvantage of the electron microprobe is its inability to analyze for lithium, an element that may constitute an essential component for classifying and calculating the chemical formulae of the Lake Lewis Leucogranite white micas. Table 5.1 presents a summary of the

Table 5.1. Summary of methods for calculating the lithium content in the micas of the Lake Lewis Leucogranite. This table is continued on the following page.

Source	Technique/Equation	Limits/Constraints	Result of application to Lake Lewis Leucogranite white micas
Faure (1991)	<p>based on mass balance of lithium among major minerals from known whole-rock lithium content</p> <p>$[Li] * 100 = 0 \text{ qtz} + 25x \text{ K-felds} + 70x \text{ plag} + 150x \text{ musc}$</p> <p>where $x = [Li]$ concentration relative to K-feld = 1</p>	<p>only have whole rock analyses from Clarke et al. (1993) reporting average $[Li] = 382 \text{ ppm}$ for rocks similar to samples LL99-1, LL99-2, LLL2, and LLL3</p>	$[Li]_{\text{musc}} = 1560 \text{ ppm} (\sim 0.34\% \text{ Li}_2\text{O} \text{ or } 0.19 \text{ cations per formula unit based on } 22 \text{ O})$ values generated from mass balance and distribution coefficient methods below are in very good agreement with each other
Walker et al. (1989)	<p>based on Li distribution coefficient between granite and melt for muscovite and K-feldspar</p> $[Li]_{\text{musc}} = [Li]_{\text{K-feld}} \times \left(K_D^{\text{Li}}_{\text{musc/melt}} / K_D^{\text{Li}}_{\text{K-feld/melt}} \right) = [Li]_{\text{K-feld}} \times 10$	<p>only have K-feldspar analysis from neighbouring Canoe Lake by Kontak and Martin (1997) reporting $[Li]_{\text{K-feld}} = 146 \text{ ppm}$</p>	$[Li]_{\text{musc}} = 1460 \text{ ppm} (\sim 0.31\% \text{ Li}_2\text{O} \text{ or } 0.17 \text{ Li cations per formula unit based on } 22 \text{ O})$, a result nearly identical to that from the mass balance method.
Tindle and Webb (1990)	<p>based on SiO_2</p> $\text{Li}_2\text{O} = (0.287 * \text{SiO}_2) - 9.552$	<p>$\text{MgO} < 8 \text{ wt\%}$; for trioctahedral micas only</p>	

set everything to ksp so have only 1 variable. $382 \cdot \frac{1}{245} = 245$

$(25 + 70 + 150 \cdot 245 \text{ per mineral})$

every thing is ksp
all are $x \Rightarrow$ to get an
 x

$\frac{382}{245} = 1,559$
multiply by 1000 b/c
-13 in ppm,

Table 5.1 continued

Tischendorf et al. (1997)	trioctahedral mica equation based on SiO ₂ Li ₂ O = (0.289*SiO ₂) - 9.658	SiO ₂ > 34 wt% Tischendorf et al. (1999) further constrain equation validity to MgO < 3 wt%; for trioctahedral micas only	equation is nearly the same as the one from Tindle and Webb (1990), but has stricter constraints, and is the better equation of the two; most of the LLL trioctahedral micas are secondary and this equation is only used on the coexisting protolithionite phases of sample LL99-7, altered core of sample SC-20W, and zinnwaldites of sample LL99-9; this equation overestimates Li contents of dioctahedral micas.
Tischendorf et al. (1997)	dioctahedral mica equation based on F Li ₂ O = (0.3935*F ^{1.396})	F = 0.01 - 8 wt%; for dioctahedral micas only	majority of white micas in the LLL are dioctahedral and this equation is used in conjunction with the SiO ₂ equation of Tischendorf et al. (1997); figure 5.1 shows a good correlation between octahedral values calculated with and without Li; these equations give nearly identical Li values as those calculated using the mass balance and K _D methods
Ham and Kontak (1988)	Ham and Kontak (1988) report alkali feldspar Li contents determined using ICP-MS	Ham and Kontak (1988) use bulk analyses which incorporates error resulting from zoning and heterogeneities of white micas	figure 5.2 compares the values of Li ₂ O from calculated using the Tischendorf et al. (1997) dioctahedral equation and Ham and Kontak's (1988) analyses; the results in good agreement with each other; some deviation between the two methods can be accounted for by the error associated with each method

various evidence and methods used to determine the presence of lithium in the white micas.

5.2.1 Mass balance method

Clarke et al. (1993) provided whole-rock analyses for major elements, trace elements, rare earth elements, and oxygen isotopes from the Lake Lewis Leucogranite for rocks similar to those of LLL2, LLL3, LL99-1, and LL99-2. They report an average lithium content of approximately 382 ppm for five samples. By using the lithium distribution coefficients for the major minerals found in the rock (Table 5.2), one can determine the partitioning of lithium between the minerals. Muscovite has the largest distribution coefficient (Table 5.2), meaning that it will take up most of the lithium. A mass balance equation can be set up to give an estimate of the partitioning of lithium in the minerals using modal percentages for the locality. This calculation results in a concentration of Li₂O of approximately 0.34 wt% or 0.19 lithium cations per formula unit (based on 22 oxygens) in muscovite.

Table 5.2. Granitic mineral/melt lithium distribution coefficients (K_D) from Walker et al. (1989).

Mineral	K_D^{Li} mineral/melt
K-feldspar	0.05
Plagioclase	0.10
Muscovite	0.50
Quartz	0

5.2.2 Distribution coefficient method

Kontak and Martin (1997) reported trace element data for alkali feldspars, with one analysis from the neighboring North Canoe Lake. Calculation of the lithium content in muscovite can be determined using the mineral/melt distribution coefficients (Table 5.2) for K-feldspar and muscovite using the equation listed in Table 5.1. The resulting value of lithium in a coexisting muscovite is approximately 0.31 wt% or 0.17 lithium cations per formula unit (based on 22 oxygens). This value is in excellent agreement with the value from mass balance.

5.2.3 Lithium estimates from electron microprobe analyses

An indirect estimate of Li_2O concentration in micas can be based on empirical relationships of element correlations to give resultant regression equations from electron microprobe analyses. Tischendorf et al. (1997) developed a regression equation to estimate Li_2O based on F for dioctahedral micas, and Tindle and Webb (1990) and Tischendorf et al. (1997) developed regression equations based on SiO_2 for trioctahedral micas (Table 5.1). The ability to apply these equations requires the separation of the white micas into dioctahedral and trioctahedral groups, because the application of an incorrect equation will overestimate the Li_2O content of the micas. There is no generally accepted compositional boundary between dioctahedral and trioctahedral micas. Bailey (1984) suggested a value of 5.0 octahedral cations per formula unit (based on 22 oxygens) as a convenient boundary between the two groups because few homogenous micas have octahedral cation totals near this value. Tischendorf et al. (1997) suggested that it is customary to consider micas with octahedral values between 5.0 and 6.0 to be trioctahedral, and micas with octahedral values near 4.0 to be dioctahedral. As such, they

chose a value of 4.4 as the division between the two groups. Thus, the boundary is flexible and should be set by the specific problem.

A study of intermediate micas by Green (1981) concluded that there is complete solid solution between micas with octahedral values of 5.0 and trioctahedral micas, but that a marked gap exists between micas with octahedral values of 5.0 and dioctahedral micas. The Lake Lewis Leucogranite micas are not homogeneous, and by inspection of the calculated structural formulae data, a convenient break in the octahedral values occurs between 4.81 and 4.94. The complete data set is in the Mica struc form.xls file on the included disk. I chose to apply the regression equation based on F from Tischendorf et al. (1997) for octahedral values below 4.9, and the Tischendorf et al. (1997) regression equation based on SiO₂ for octahedral values above 4.9. A plot of the octahedral values calculated with Li₂O estimates and no lithium (Fig. 5.1) shows the effects of the equations. Some deviation from a straight line does occur around the dioctahedral-trioctahedral boundary with some epitaxial overgrowth analyses from sample LL99-7 and the altered core analyses from sample SC-20W. Naturally, with addition of Li₂O to the mica, the octahedral values increase.

5.2.4 Comparison of analyzed and calculated lithium

Ham and Kontak (1988) report lithium concentrations in white micas analyzed by ICP-MS. Figure 5.2 compares the analyzed lithium concentrations with those calculated using the regression equation based on F by Tischendorf et al. (1997). The two methods are in good agreement with consideration of error from both methods, especially because Ham and Kontak (1988) use bulk analyses that can have error as a result of zoning and heterogeneities in the white micas.

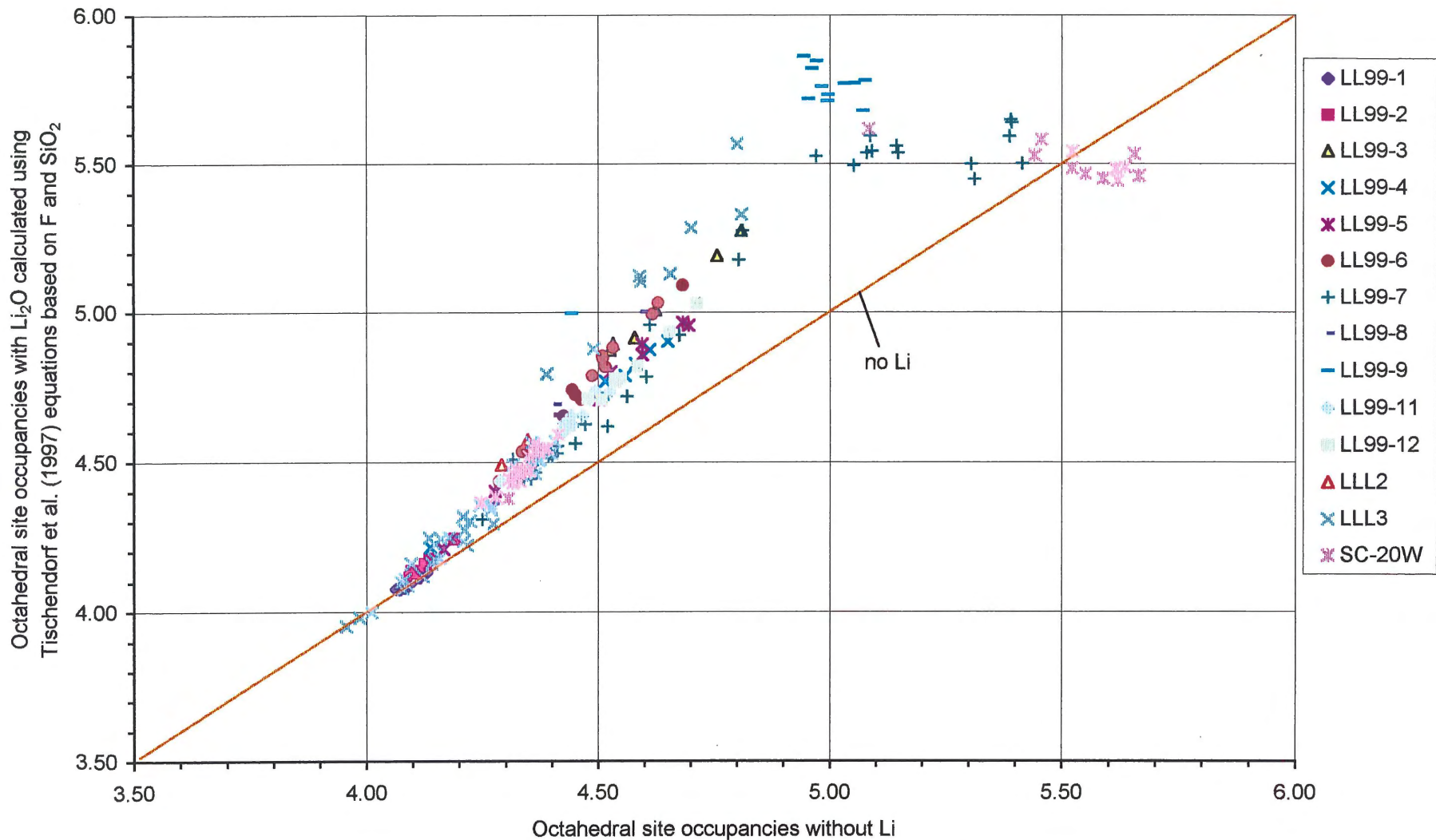


Figure 5.1. Plot of octahedral site occupancies calculated with Li_2O estimates and without lithium shows a very good correlation with some deviation from samples LL99-7 and SC-20W. The "no Li" line is drawn to show where samples without Li would fall.

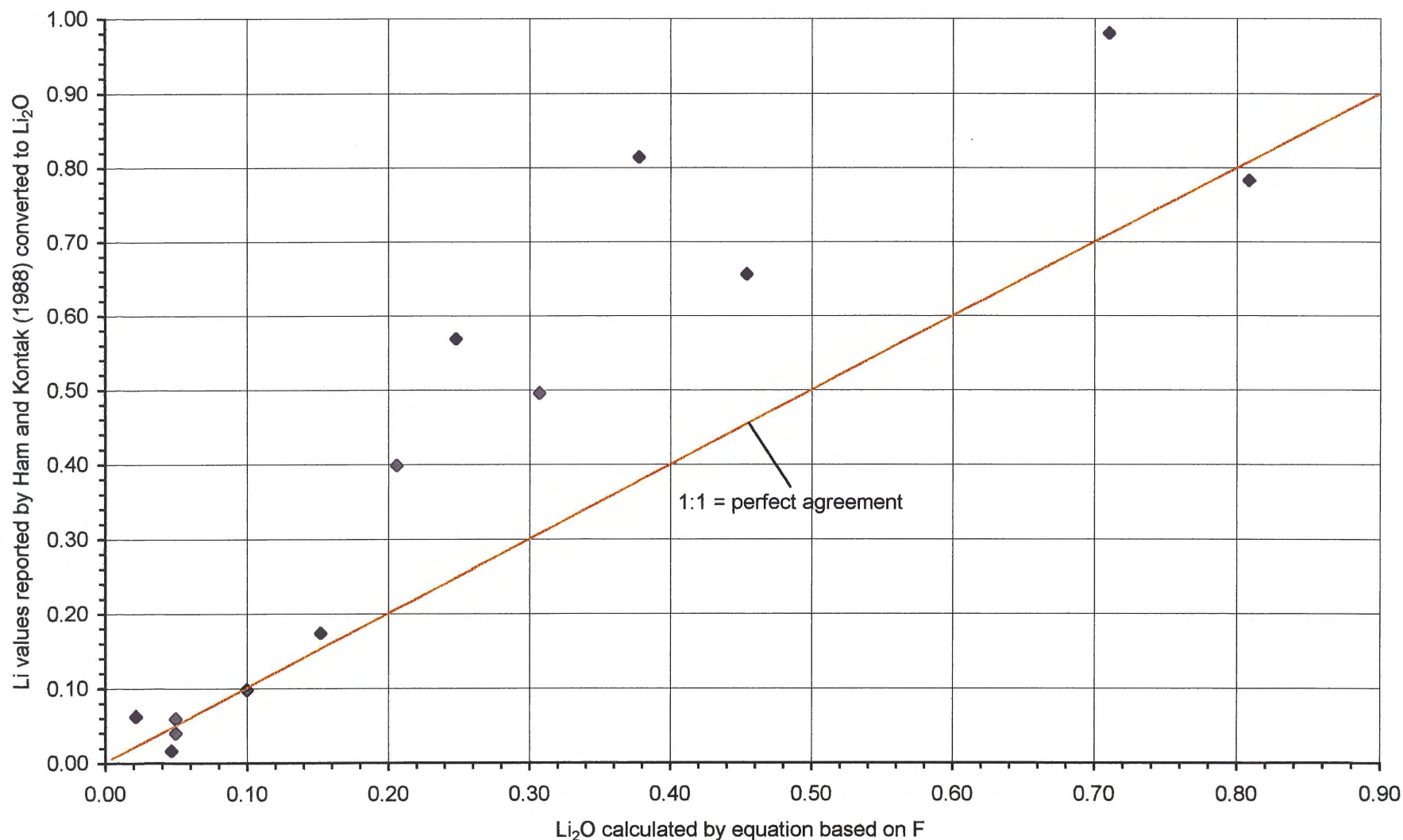


Figure 5.2. Comparison of Li calculation using Tischendorf et al. (1997) equation based on F with Ham and Kontak (1988) values of Li analyzed using ICP-MS. The perfect agreement line between the two methods would lie along the line with slope = 1.

5.2.5 Summary

The four independent methods for calculating lithium content in the white micas outlined above are in very good agreement with each other. This degree of agreement suggests that the use of the Tischendorf et al. (1997) regression equations is a satisfactory method for determining the lithium contents of micas.

5.3 Classification and nomenclature of white micas

Two different methods are available to classify the white micas of the Lake Lewis Leucogranite based on their chemical compositions. The first classification method assigns names based on cation proportions without lithium. The second method uses regression equations to calculate the lithium content of the white micas from electron microprobe analyses, and then assigns names on the basis of the Mg-Li and Fe+Mn+Ti-Al^{VI} diagram of Tischendorf et al. (1997).

Table 5.3. Mica cation proportions for end-member micas based on 24 O, OH, and F (Deer et al. 1992 and WWW-MYNCRYST (new revision) 2001).

Mica	Dioctahedral or Trioctahedral	Number of cations					
		K+Na	Fe+Mn+Mg	Al ^{VI}	Al ^{IV}	Al _{total}	Si
Muscovite	Dioctahedral	2	0	4	2	6	6
Phengite	Dioctahedral	2	1	3	1	4	7
Celadonite	Dioctahedral	2	2	2	0	2	8
Annite	Trioctahedral	2	6	0	2	2	6
Siderophyllite	Trioctahedral	2	4	2	4	6	4
Phlogopite	Trioctahedral	2	6	0	2	2	6
Eastonite	Trioctahedral	2	5	2	4	6	5
Protolithionite	Trioctahedral	2	4	1	2	3	6
Zinnwaldite	Trioctahedral	2	3-1	2	3-1	5-3	5-7

ferro - dioct. 2 4 2 0 2 6

5.3.1 Classification without lithium

Using the values calculated for the structural formulae of the micas without lithium (in the spreadsheet), each analyzed mica receives a name based on cation

proportions. Table 5.3 lists the cation occupancies for end-member micas with the cation groups used for naming. The micas fall into dioctahedral and trioctahedral groupings with the boundary set at 4.90 octahedral cations as discussed in the previous section. For cation occupancy values that fall between two end-member values, the analysis receives both names in that category. The final mica name chosen is the one that fits the most of the criteria in the seven columns of Table 5.3.

Figures 5.3 a and b show the micas plotted with axis variables Si against Al, and Fe + Mn + Mg against Al. The majority of white micas classify as dioctahedral. The white micas fall into three groups definitively termed as muscovites (dioctahedral), phengites (dioctahedral), and zinnwaldites (trioctahedral) based on cation occupancy. A distinction exists between two different phengitic groups on these classification diagrams. The protolithionite (trioctahedral) and siderophyllite (trioctahedral) groups occur where it is not possible to assign specific names through end-member cation occupancy because they fall between the end-members eastonite, siderophyllite, and protolithionite. However, on a diagram of principal biotite components showing the field in which most natural biotite plots (Fig. 5.4), the field does not extend to end-members siderophyllite and eastonite. The micas classified here as siderophyllite are not near end-member siderophyllite and are also remote from biotite (phlogopite-annite) compositions.

5.3.2 Classification with lithium

Lithium is critical for full calculation of the white mica chemical formulae and their correct classification. The regression equations of Tischendorf et al. (1997) use electron microprobe analyses to indirectly estimate the lithium content in dioctahedral and trioctahedral micas by empirical approaches based on element correlations. The

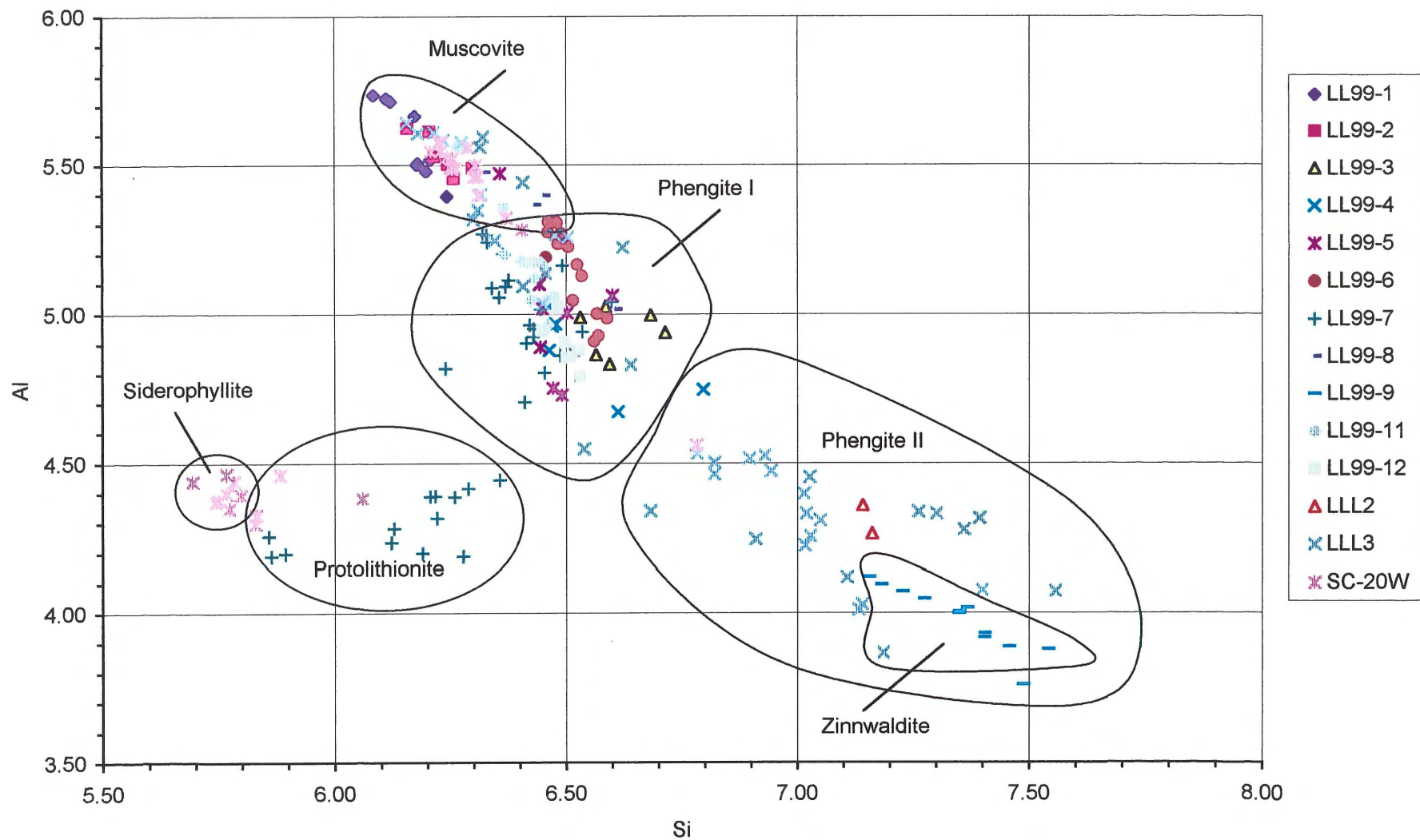


Figure 5.3a. Grouping of micas based on end-member mica cation proportion of Si against Al.

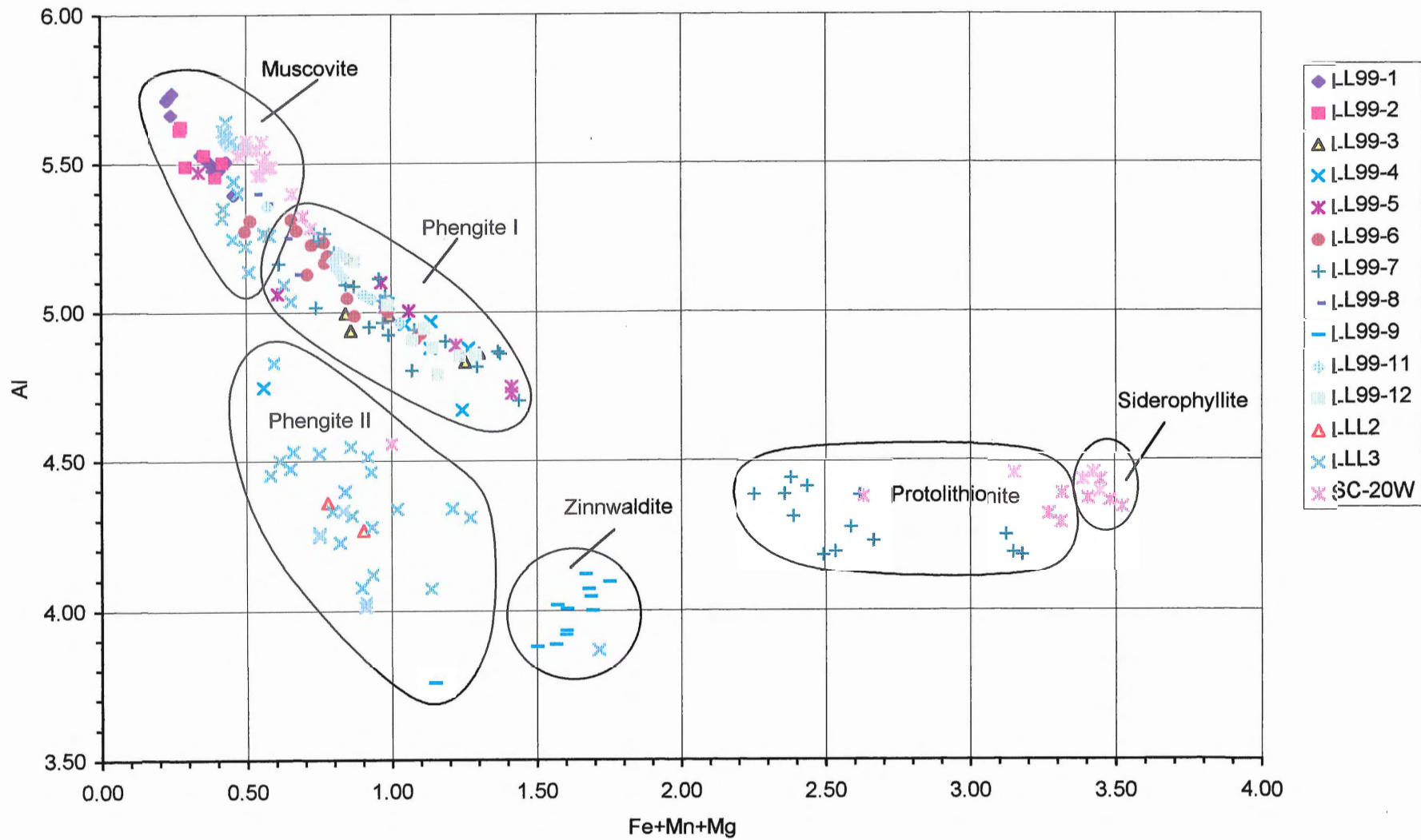


Figure 5.3b. Grouping of micas based on end-member mica cation proportions of $\text{Fe}+\text{Mn}+\text{Mg}$ and Al .

Li_2O content of the white micas can be calculated with the use of empirical relationships between Li_2O and F in dioctahedral micas, and Li_2O and SiO_2 in trioctahedral micas.

The white micas separated into dioctahedral and trioctahedral micas by the method described above using a boundary of 4.90 without lithium. The micas can be classified using a diagram with axis variables Mg-Li and Fe+Mn+Ti-Al^{VI} (Fig. 5.5). This “mgli-feal” diagram provides a simple means to classify micas in terms of composition and allows relationships between dioctahedral and trioctahedral micas, as well as compositional relationships between lithium-free and lithium-bearing mica varieties, to be displayed on a single diagram (Tischendorf et al. 1997). Figure 5.6 presents the mica analyses plotted on the mgli-feal diagram.

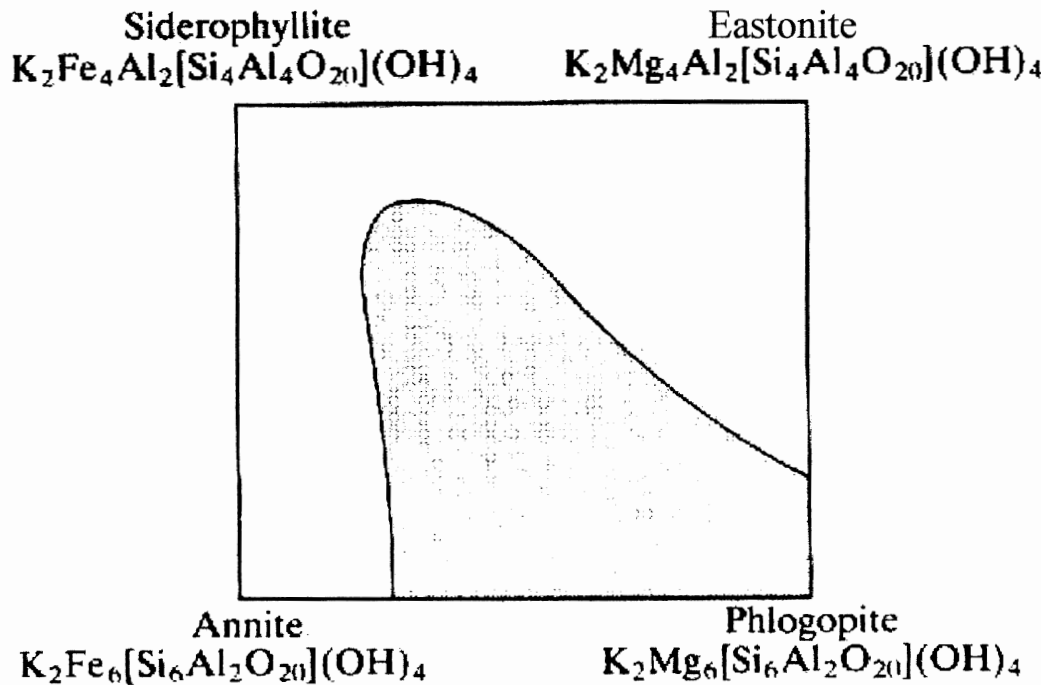


Figure 5.4. Diagram of principal components of biotite compositions, siderophyllite, eastonite, annite, and phlogopite (at four corners) and the area in which most natural biotites plot (modified from Deer et al. 1992).

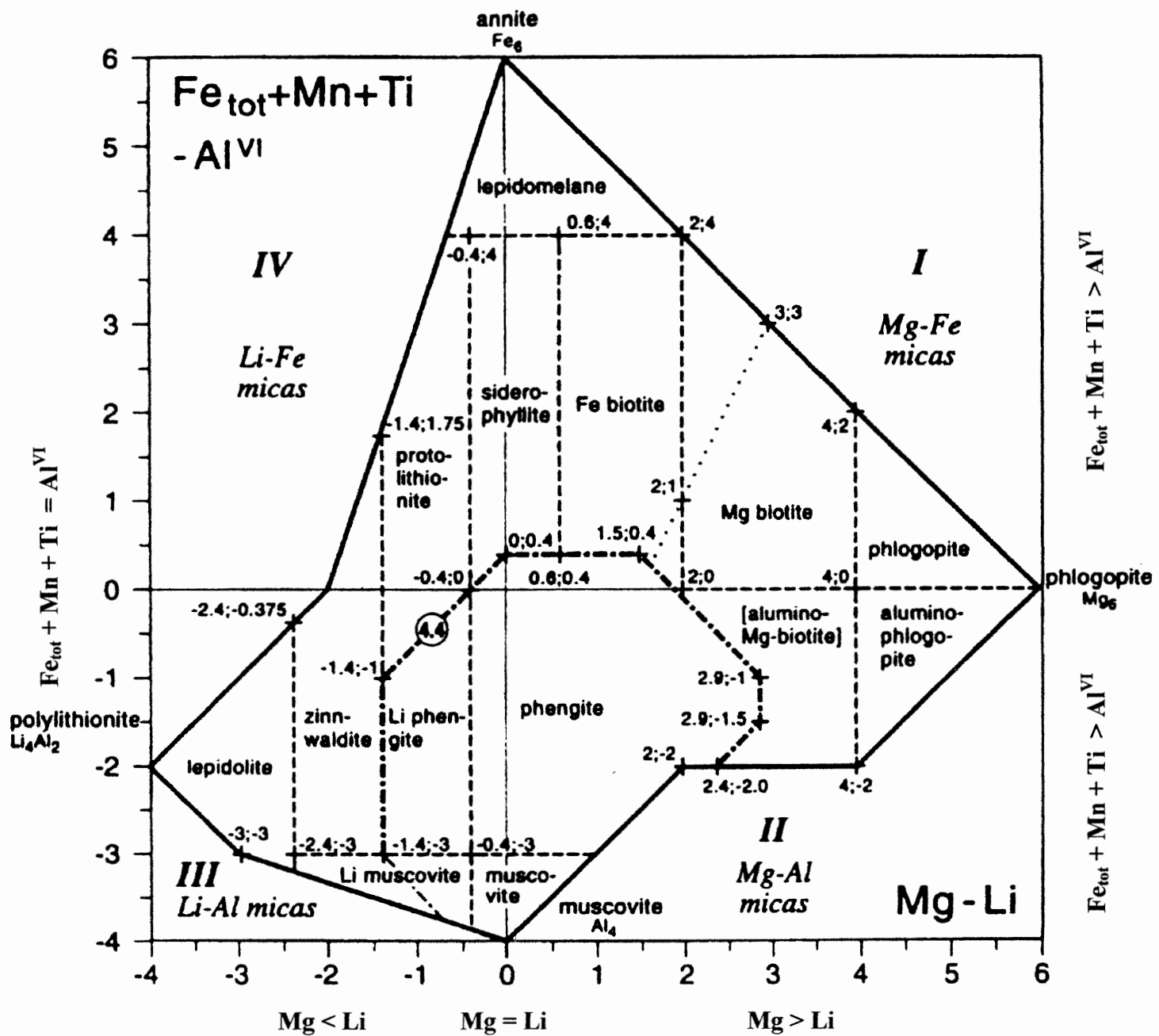


Figure 5.5. Compositional fields of natural micas on the two-dimensional diagram of $\text{Fe} + \text{Mn} + \text{Ti} - \text{Al}^{\text{VI}}$ against $\text{Mg} - \text{Li}$. This diagram is based on the octahedral cations in micas with corner variables annite, phlogopite, polylithionite, and muscovite, calculated on 22 O (modified from Tischendorf et al. 1997).

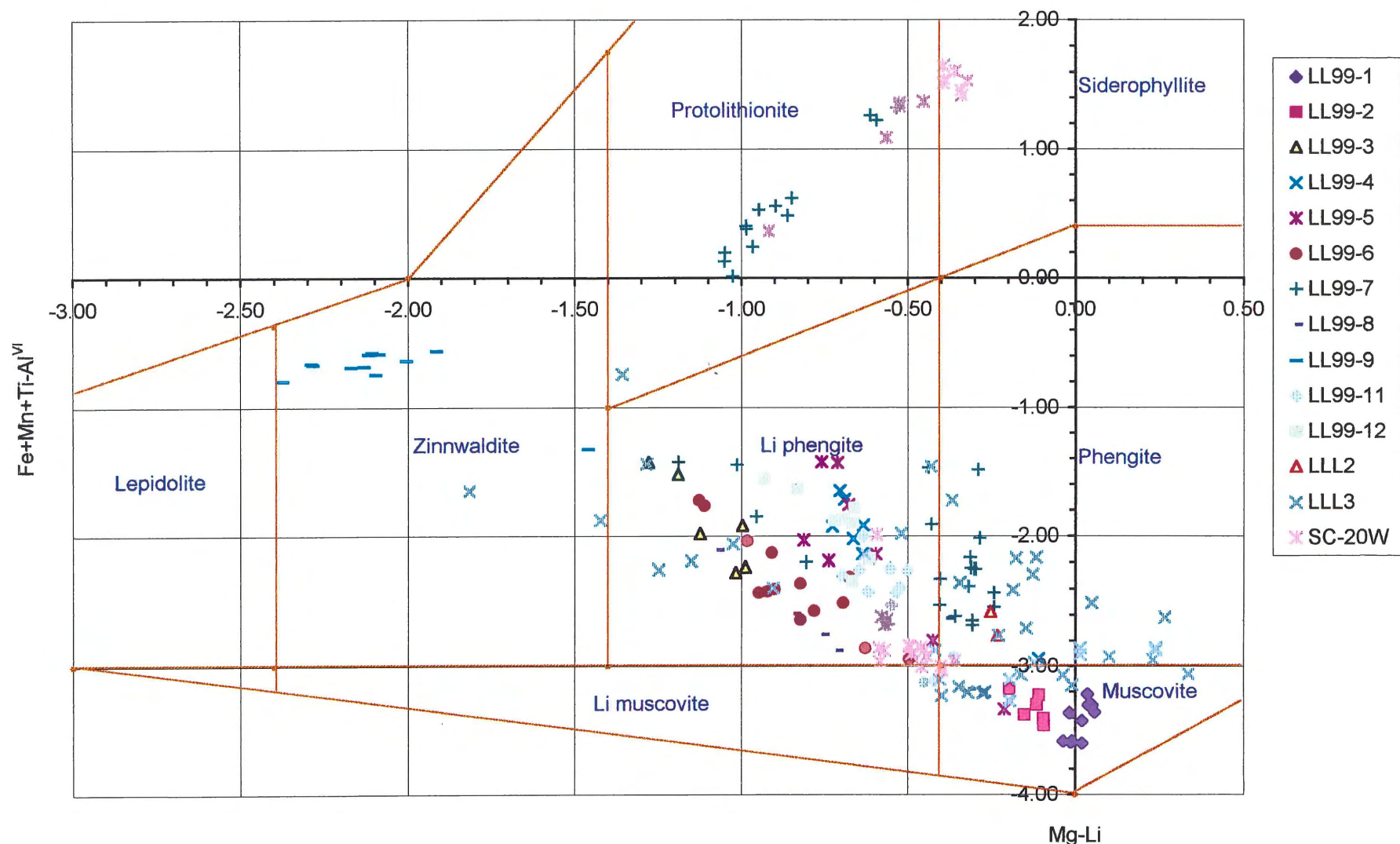


Figure 5.6. MgLi-feal diagram with Li calculated from equations based on F for dioctahedral micas and SiO_2 for trioctahedral micas.

5.3.3 Summary of mica classification

The classification of the micas using the mgli-feal diagram (Fig. 5.6) matches the classification using lithium-free cation proportions (Fig. 5.3 a and b). The two classification schemes were generated at different stages of the project, and the naming with the mgli-feal plot did not influence the naming using the cation proportion method done previously. The majority of the white micas plot as dioctahedral micas (muscovites and phengites). The muscovites named using cation occupancy also plot as muscovites on the mgli-feal plot, with some located in the lithian-phengite field. The two separate groups named Phengite I and Phengite II through the cation proportion plot as lithian-phengites and phengites on the mgli-feal diagram. The trioctahedral micas (zinnwaldites, protolithionites, and siderophyllites) retain their separate positions using either classification method.

5.4 Are the white micas primary or secondary?

Ham and Kontak (1988) examined the question of primary versus secondary white mica in the South Mountain Batholith leucogranites. They found no systematic correlation between textural varieties of white micas and white mica chemistry. Ham and Kontak (1988) reported that only a small modal percentage of the white micas appear primary on textural grounds but, chemically, a large proportion appear to have formed as an integral part of the magmatic evolution. Their use of major element discriminant diagrams proved inconclusive. Ham and Kontak (1988) concluded that textural and chemical signatures can be highly variable, even in a single granitoid unit.

The characterization of white micas as primary or secondary is determined using the guidelines set out in Table 1.2 and the following two sections.

5.4.1 Physical evidence

The white micas of the Lake Lewis Leucogranite are coarse-grained, dimensionally compatible with other minerals, and mostly euhedral to subhedral in habit with well-defined, straight grain boundaries. Euhedral to subhedral inclusions of white micas are also present in widely recognized magmatic minerals such as plagioclase, K-feldspar, and quartz, all of which point to a primary magmatic origin for the white micas.

Samples LLL2, LLL3, and SC-20W contain large white micas that have undergone deformation, and are bent, kinked, and sheared. The presence of fluorite crystals in cleavage planes suggests that penetration and alteration by a fluid phase was made possible by the deformation of these micas or vice-versa. It would appear that these micas were at one time texturally primary and grew out of the magmatic melt because they are coarse-grained dimensionally compatible with other minerals.

Twiss and Moores (1992) reported that brittle deformation is associated with high fluid pressures. They also reported that high fluid pressures reduce the stress necessary for frictional sliding. Thus, high fluid pressures may have caused these white micas to separate along cleavage planes and deform in a brittle fashion allowing fluid access to crystallize fluorite in the cleavage planes. These white micas have textural characteristics suggesting secondary, post-magmatic deformation, and alteration by a fluid phase.

5.4.2 Chemical evidence

Table 1.2 contains the guidelines presented by Miller et al. (1981) and Speer (1984). Magmatic muscovite may have TiO_2 contents > 1 wt%, but whole rock analyses from Clarke et al. (1993), and the current white mica microprobe analyses, show that the

Lake Lewis Leucogranite rocks and white micas have very low TiO_2 contents. Thus, this criterion is probably irrelevant in this situation. Primary muscovite should have an $\text{Na}/(\text{Na}+\text{K})$ ratio > 0.06 . Figure 5.7 shows that the deformed mica grains in samples LLL2 and LLL3 plot below 0.04, and analyses from the Walker deposit sample SC-20W plot in the middle of the majority of analyses. I have separated the mechanically deformed samples by a boundary on the major element discrimination diagrams. Primary muscovite may be richer in Al_2O_3 and Na_2O than secondary muscovite. Figure 5.8 shows that the deformed mica grains of samples LLL2 and LLL3 plot below the majority of analyses. The deformed mica grains in sample SC-20W have a lower Na_2O content than the majority of analyses, but no distinction occurs in Al_2O_3 content. Primary muscovite may also be poorer in SiO_2 and MgO compared with obvious secondary muscovite. Figure 5.9 shows that the analyses from deformed mica grains in samples LLL2 and LLL3 have higher SiO_2 and MgO contents than the rest of the analyses. The deformed mica grains in sample SC-20W have much lower SiO_2 contents than the rest of the analyses, and very low MgO contents. The gap between coexisting phengite and protolithionite phases in Figure 5.3b follows the miscibility gap of Monier and Robert (1986a) between muscovite and biotite (Fig. 5.10). This gap decreases as the lithium content in the micas increases. These two phases are also mutually saturated in each other.

The combination of physical and chemical evidence shows that the deformed micas are secondary, whereas the rest of the micas appear to have primary magmatic signatures. Deformation appears to have been necessary to provide an avenue for late magmatic fluids to chemically alter the micas.

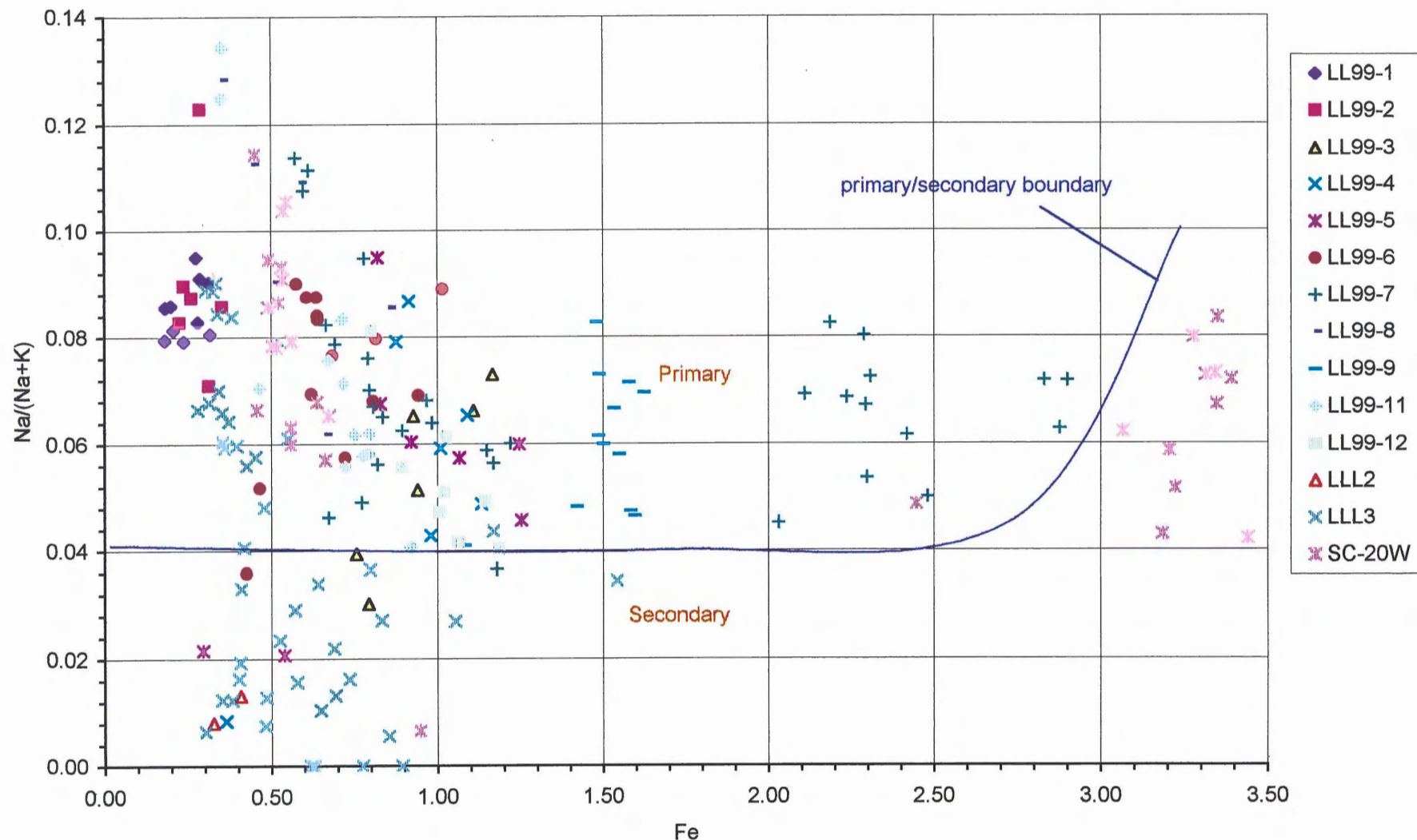


Figure 5.7. Plot of Fe against $\text{Na}/(\text{Na}+\text{K})$. Primary micas should have $\text{Na}/(\text{Na}+\text{K}) > 0.6$. The deformed micas in LLL2, LLL3, and SC-20W are separated from the undeformed micas by the primary/secondary boundary based on textural observations.

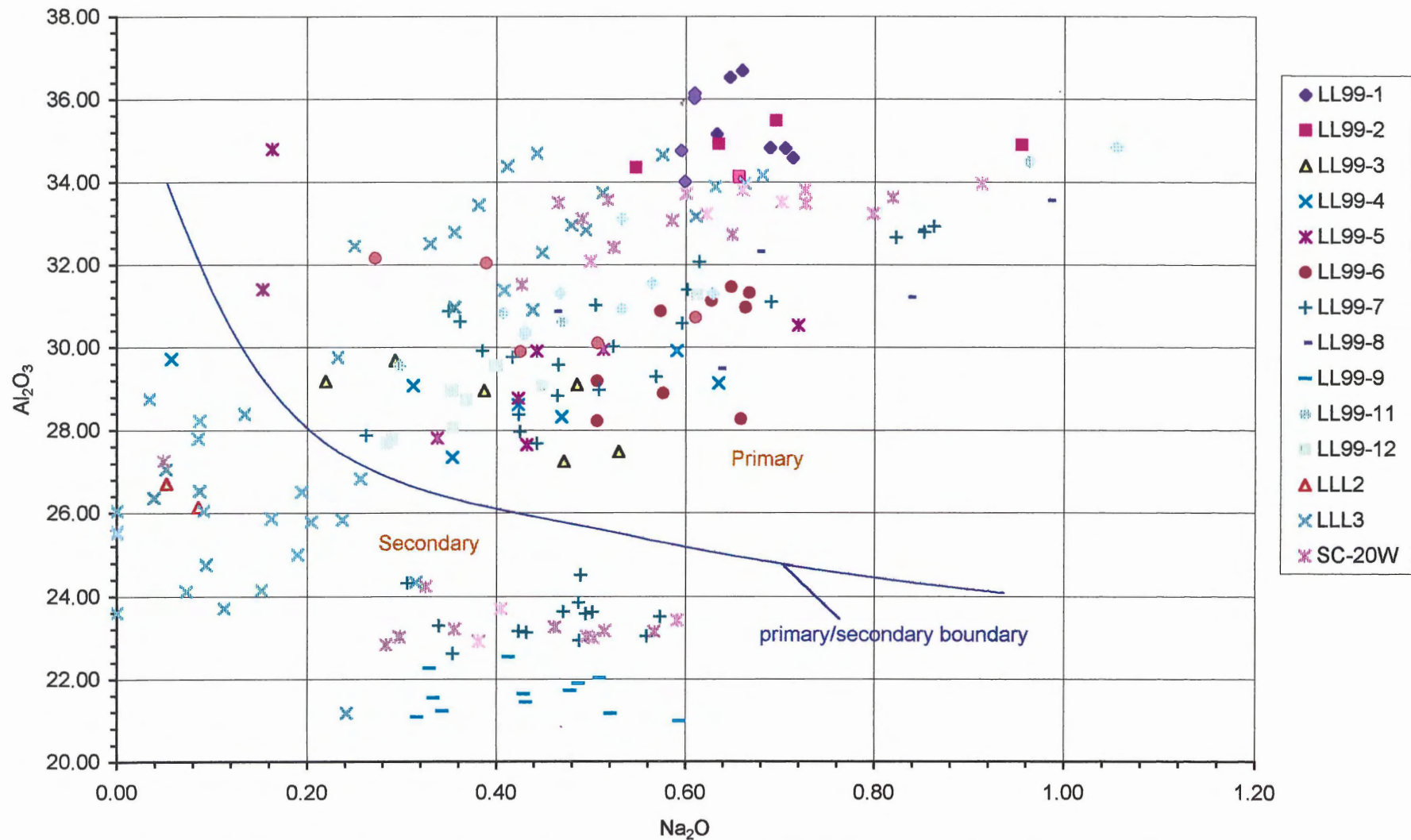


Figure 5.8. Plot of Na_2O against Al_2O_3 . Primary muscovites may be richer in Na_2O and Al_2O_3 than secondary muscovite. The deformed micas in LLL2, LLL3, and SC-20W are separated by the primary/secondary boundary based on textural observations.

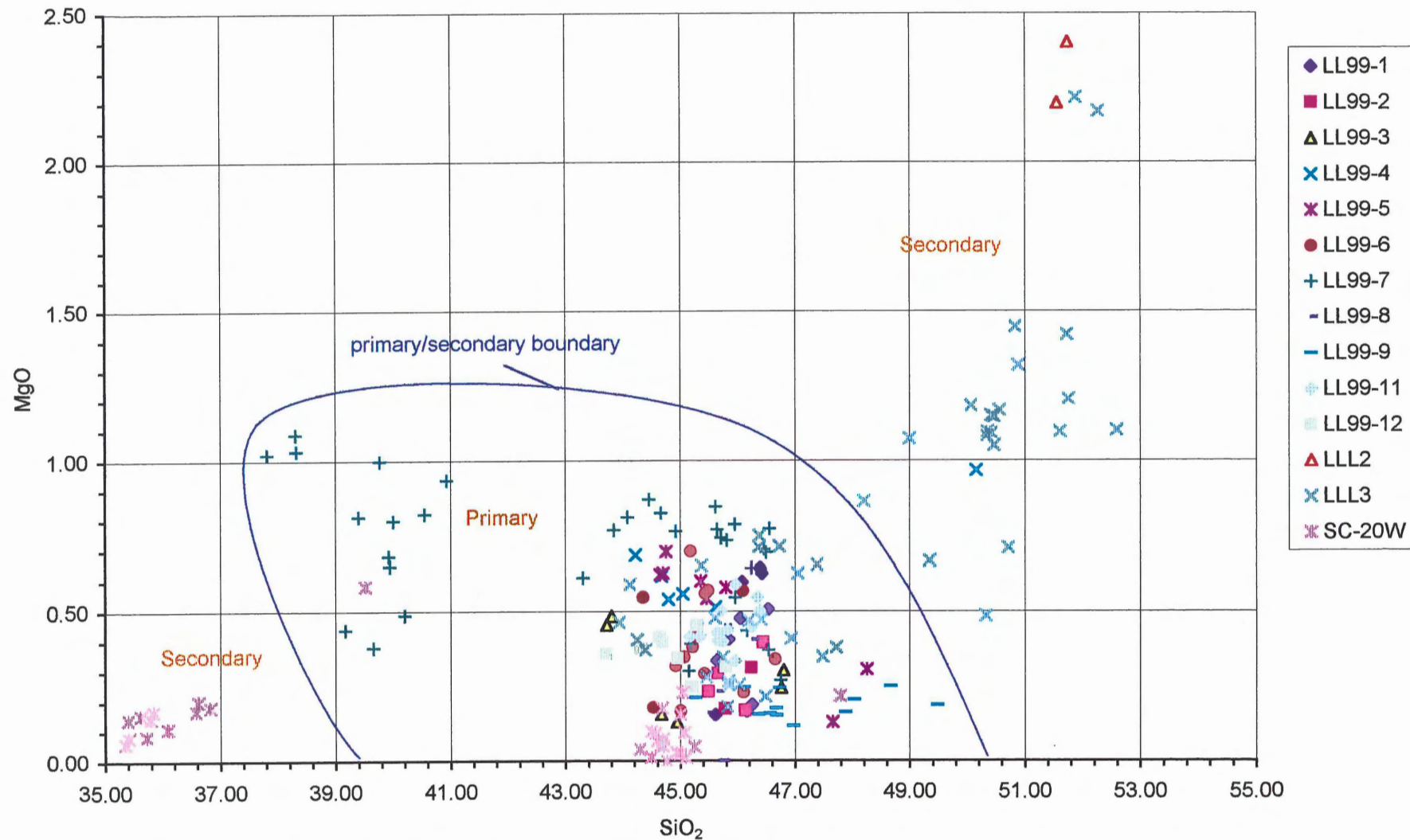


Figure 5.9. Plot of SiO_2 against MgO . Primary muscovite may be poorer in SiO_2 and MgO than secondary muscovite. The deformed micas in LLL2, LLL3, and SC-20W are separated by the primary/secondary boundary based on textural observations.

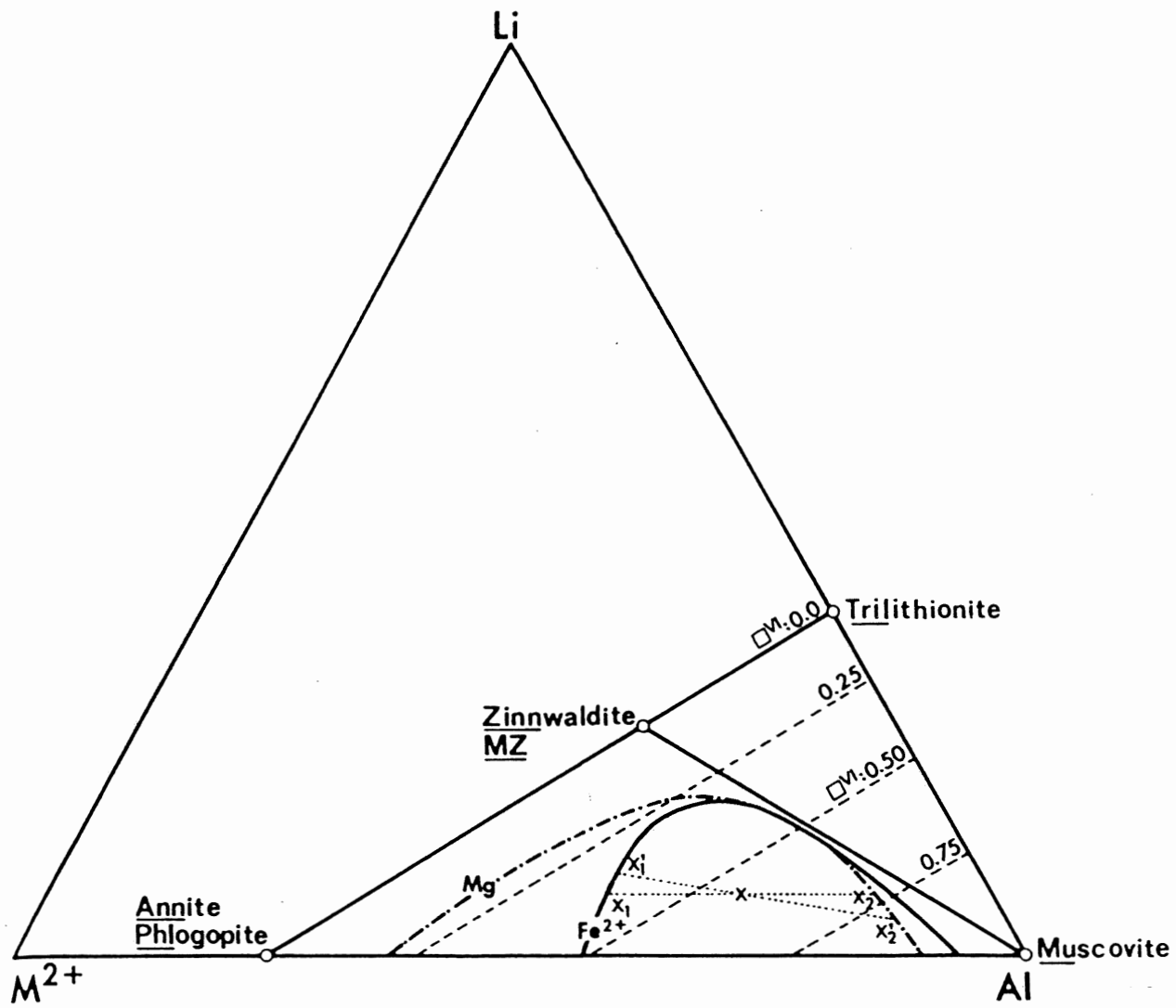


Figure 5.10. The evolution of the miscibility gap between muscovite and biotite with increasing lithium contents in the micas where \square^{VI} represents the number of octahedral vacancies per formula unit (Monier and Robert 1986a).

5.4.3 Coexisting feldspars

Logothetis (1985) stated that plagioclase feldspars in the Lake Lewis Leucogranite are secondary. He described the feldspars as minute grains, anhedral to subhedral in habit, with intergrowths and rimmed overgrowths replacing primary plagioclase, K-feldspar, and quartz. He also stated that primary K-feldspars are perthitic, and secondary K-feldspars have a high Fe content from biotite replacement. O'Reilly (1982) stated that secondary K-feldspars are compositionally zoned with K-rich cores and more sodic rims. Kontak and Martin (1997, p. 970) stated that, although "these rocks contain many minerals that crystallized directly from the relevant magmas, the alkali feldspars are not one of them." Rather, these authors suggested that the alkali feldspars are modified primary magmatic alkali feldspars that grew under conditions of Rayleigh fractional crystallization and underwent subsequent subsolidus hydrothermal alteration.

The current work shows that K-feldspars and plagioclases occur as grains that are dimensionally compatible with other minerals (medium- to coarse-grained in most samples), euhedral to subhedral in habit, and without replacement textures (feldspars are generally unaltered). The iron content in the K-feldspars and plagioclases is low, close to zero in most cases, in contrast to the high iron content described by Logothetis (1985). The K-feldspars also have low anorthite contents (Fig. 5.11). Probing of euhedral and unaltered plagioclase inclusions in one large K-feldspar grain (Fig. 5.12) also revealed that these inclusions have very low anorthite contents, similar to albites outside this perthitic K-feldspar grain.

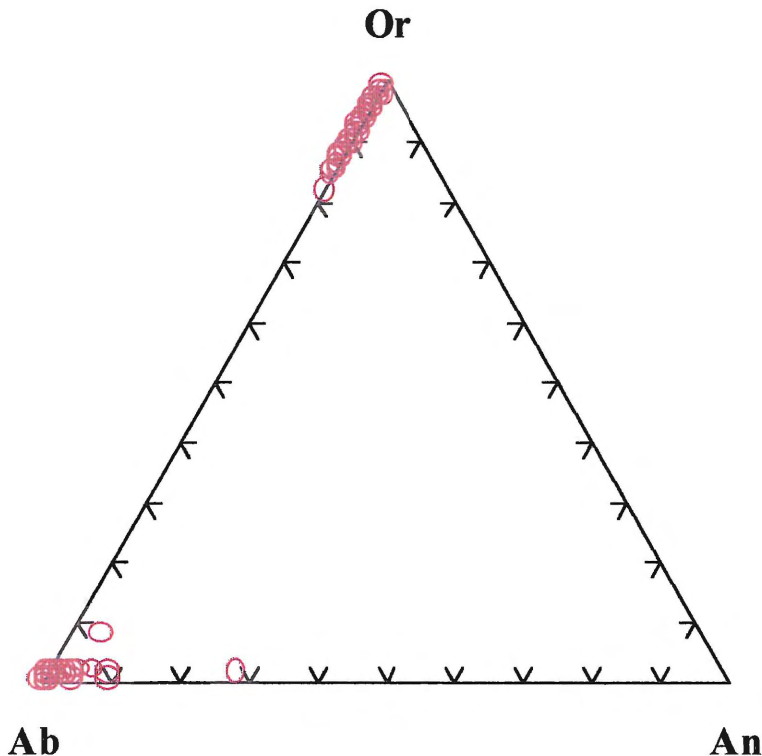
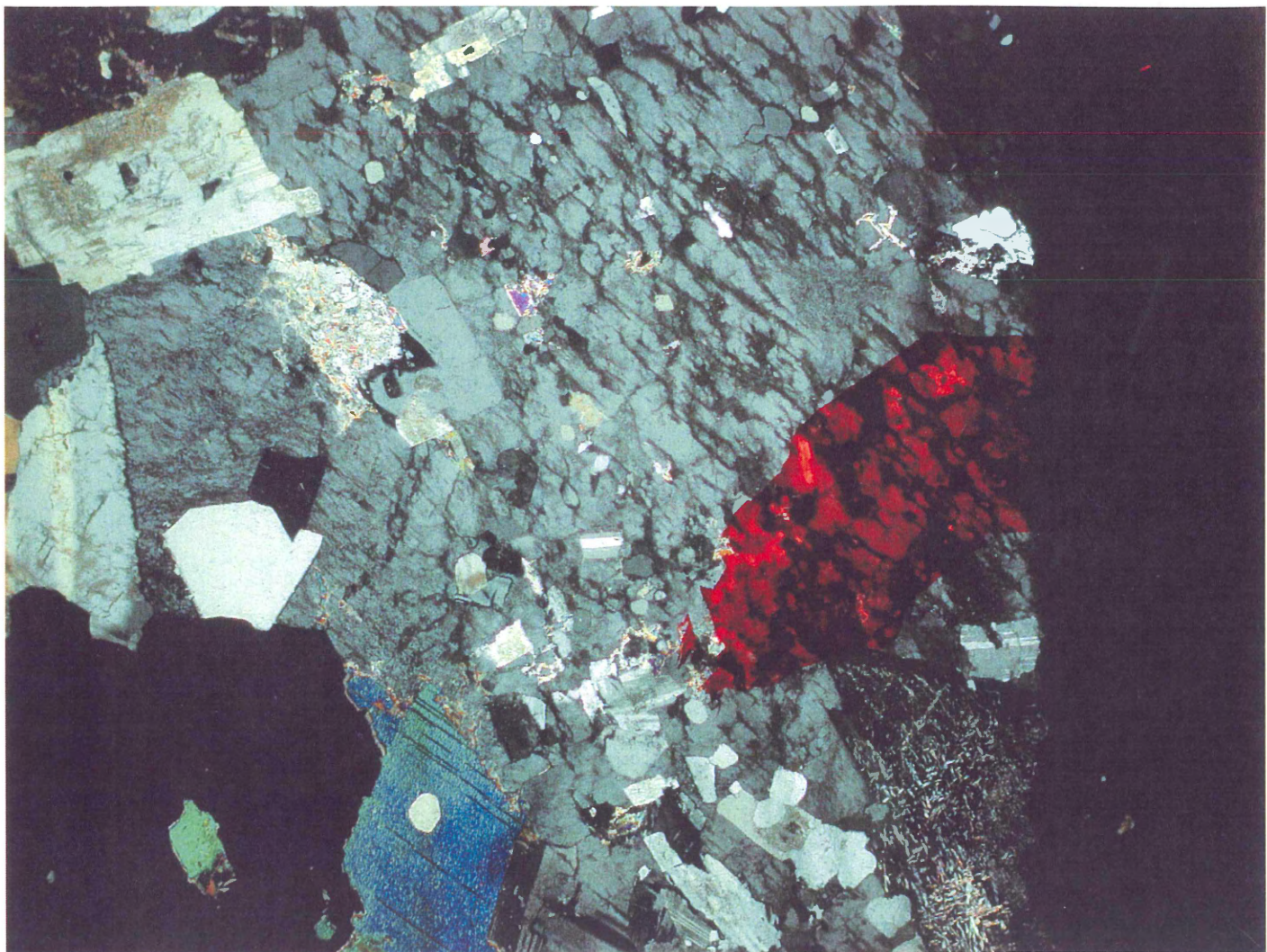


Figure 5.11. Ternary plot of Lake Lewis Leucogranite feldspar compositions. Plagioclases are pure albite, except for a single analysis, which yields An₂₈.

Weidner and Martin (1987) reported evidence for fractional crystallization of feldspars resulting in magmatic albite with An₁ in a fluorine-rich granite. The progressive buildup of fluorine in their leucogranite system caused the calcium to be stably incorporated into the structure of the melt by complexing with fluorine. The Lake Lewis Leucogranite contains primary topaz suggesting the melt was also rich in fluorine. Thus, the low anorthite content of the feldspars may be the result of fluorine complexing with calcium. With the calcium trapped in the melt, and not available for crystallization of feldspars, the melt precipitated nearly pure albite.

In summary, the textural and chemical evidence supports the plagioclases as being magmatic in origin, and as having undergone perfect fractional crystallization, rather than the product of albitization. Albitization cannot be the cause of the low anorthite contents

a XN



b XN



Figure 5.12. (a) Sample LL99-8 large perthitic K-feldspar grain with plagioclase inclusions. The K-feldspar grain acts as a protective jacket preventing further alteration of its inclusions. The plagioclase inclusions yield anorthite contents of $An_{0.5}$. (b) Plagioclase grain outside the K-feldspar grain in (a). Plagioclase grains from the Lake Lewis Leucogranite are $An_{0.5}$.

because: 1) there is no Ca sink (epidote, carbonate, or fluorite) if the Ca had been removed from the feldspars by a sodium-rich fluid; 2) the feldspars are homogeneous, meaning that the replacement would have to have been perfect so as to not produce relict high anorthite cores and low anorthite rims; and 3) plagioclase inclusions in primary K-feldspars would be expected to preserve the original anorthite content and not be affected by a fluid; if they were the product of albitization, the K-feldspar host should have also been altered.

5.4.4 Evidence from Roycroft method

Visual inspection of the white micas, using the Roycroft thick section method, revealed colorless muscovite cores with epitaxial overgrowth of a light brown phengite and alternating bands of colorless and brown mica with sharp boundaries between the two varieties of mica. The muscovite-phengite overgrowths are in optical continuity (extinguish together in crossed nicols, and the optic axial planes are parallel) and, therefore, they must be in crystallographic continuity.

The possible explanations for such muscovite-phengite epitaxial overgrowths are: 1) secondary alteration; 2) water-undersaturated magmatic processes; or 3) fluido-magmatic processes. The hypothesis of secondary alteration as the cause for the epitaxial overgrowth of phengite on muscovite cannot explain the sharp boundaries between overgrowths, or explain how selective replacement of internal bands of muscovite in a single grain could occur. The hypothesis that the epitaxial overgrowth is the result of water-undersaturated magmatic processes is problematic, because there is no apparent reason why the bulk composition of the magma would oscillate chemically between crystallizing muscovite and phengite. Velde (1980) and Green (1981) discussed the

fluido-magmatic hypothesis, and demonstrated an increase in phengitic substitution with increasing water pressure. Oscillating fluid pressure may be responsible for the oscillatory zoning in the Lake Lewis Leucogranite micas. As fluid pressure builds up in the leucogranite magma, the melt produces increasing amounts of phengite. At high fluid pressures, the wall rocks may fracture, releasing the fluid and carrying away Ca, F, and other metallic elements. At lower fluid pressure, the melt crystallizes muscovite again until sufficient fluid pressure builds up to grow phengite again.

5.4.5 Summary

Textural and compositional evidence shows that most of the white micas in the Lake Lewis Leucogranite are primary magmatic, or fluido-magmatic. Their compositions follow the well-defined magmatic trend on most chemical variation diagrams. The epitaxial muscovite-phengite overgrowths are primary fluido-magmatic features that result from alternating low and high fluid pressure, respectively. Mica compositions lying off the magmatic trend are mainly mechanically deformed and secondary hydrothermal in origin.

Textural and compositional evidence shows that plagioclase and K-feldspars in the Lake Lewis Leucogranite are primary magmatic in origin. The low anorthite contents of the plagioclase ($An_{0.5}$) are probably the result of calcium complexing with fluorine in the melt, preventing the calcium from crystallizing plagioclase with compositions greater than An_5 .

5.5 Chemical substitution processes in the white micas

In white micas, $Fe+Mg$ and Si contents are measures of solid solution toward a “celadonite-type” end member represented by $(Mg, Fe^{2+})^{VI}, Si^{IV} \leftrightarrow Al^{IV}, Al^{VI}$

substitution mechanism. In the muscovite case, this exchange is also referred to as a phengite substitution or a Tschermak substitution. Tschermak substitution is a measure of the deviation from the ideal ($\text{Al}^{\text{IV}} + \text{Al}^{\text{VI}}$) values permissible on the ideal end-member muscovite mica plane (Guidotti, 1984). Significant deviation from the ideal muscovite composition, $\text{K}_2\text{Al}_4(\text{Al}_2\text{Si}_6\text{O}_{20})(\text{OH})_4$, can occur by both biotitic substitution, $2/3 \text{ Al}^{\text{VI}}, 1/3 \square^{\text{VI}} \leftrightarrow (\text{Fe}^{2+})^{\text{VI}}$, where \square stands for a vacant octahedral site, and Tschermak substitution. The majority of natural muscovite solid solutions are combinations of the biotitic and Tschermak substitution (Monier and Robert 1986b). Ham and Kontak (1988) also concluded that the octahedral substitutions in the white micas were the result of biotitic and phengitic substitutions. Biotitic substitution involving significant lithium contents (> 1.2 cations per formula unit, based on 22 oxygens) results in a lithian-mica phase that is intermediate between trioctahedral and dioctahedral (Monier and Robert 1986a).

Figures 5.13 a and b show that Tschermak substitution seems to dominate at the beginning of the magmatic trend, but a substitution of iron for silicon and aluminum causes the magmatic trend to move away from the ideal Tschermak substitution toward a biotitic substitution. The deformed and chemically altered white micas of samples LLL2 and LLL3 show a different trend. The beginning of this trend also follows the ideal Tschermak substitution line, where the micas are undeformed. The mechanically deformed micas apparently had strong interaction with a fluid, as evidenced by fluorite crystallization along the bent cleavage planes (Fig. 4.4). The trend produced by these micas extends into the zinnwaldite mica field. The zinnwaldites are not deformed, but do come from an aplitic sample, suggesting the micas may have grown in association with a

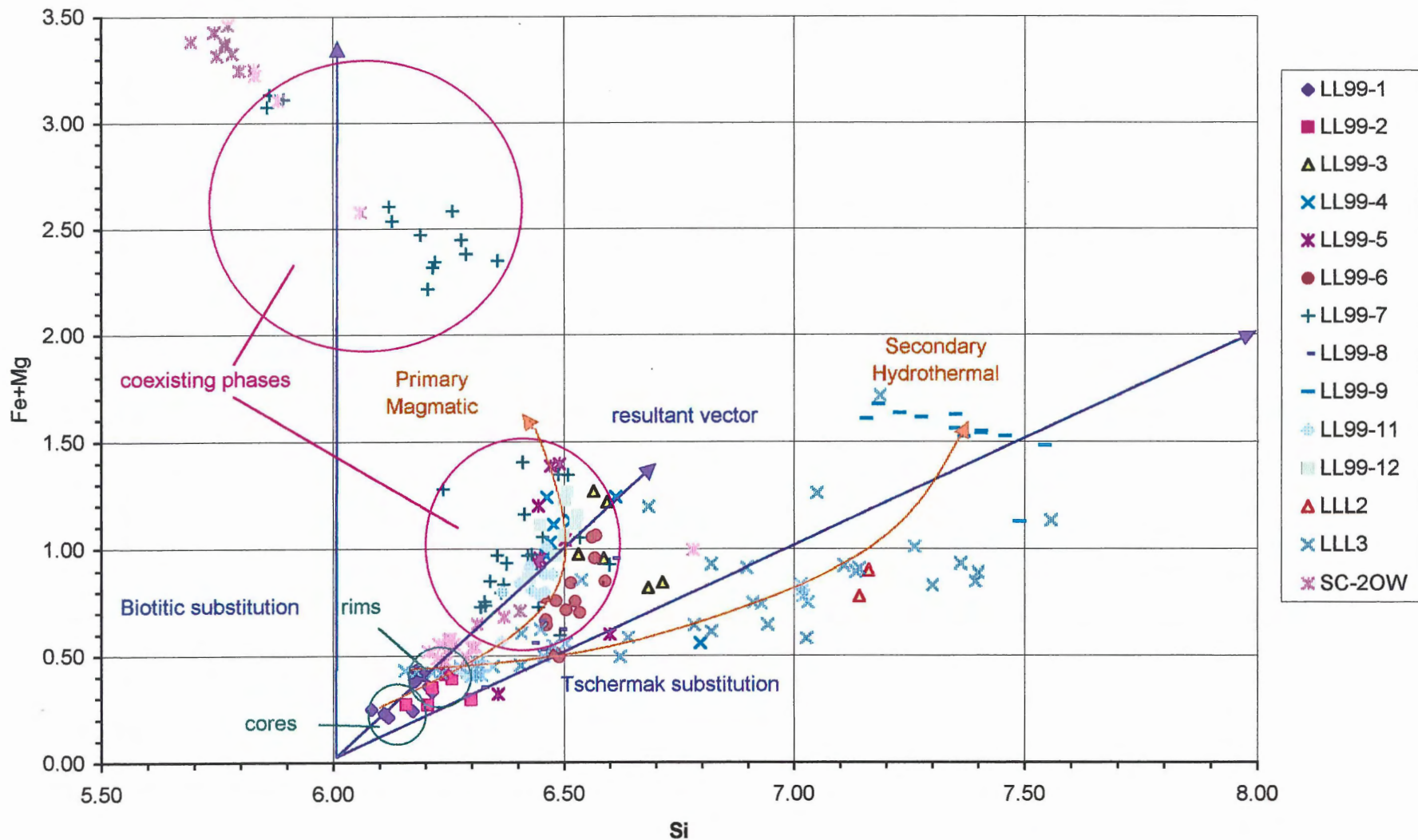


Figure 5.13a. Plot of Si against Fe+Mg showing the deformed mica trend toward the zinnwaldites, and the primary magmatic trend of muscovite-phengite overgrowths (cores and rims) and the protolithionite coexisting phase.

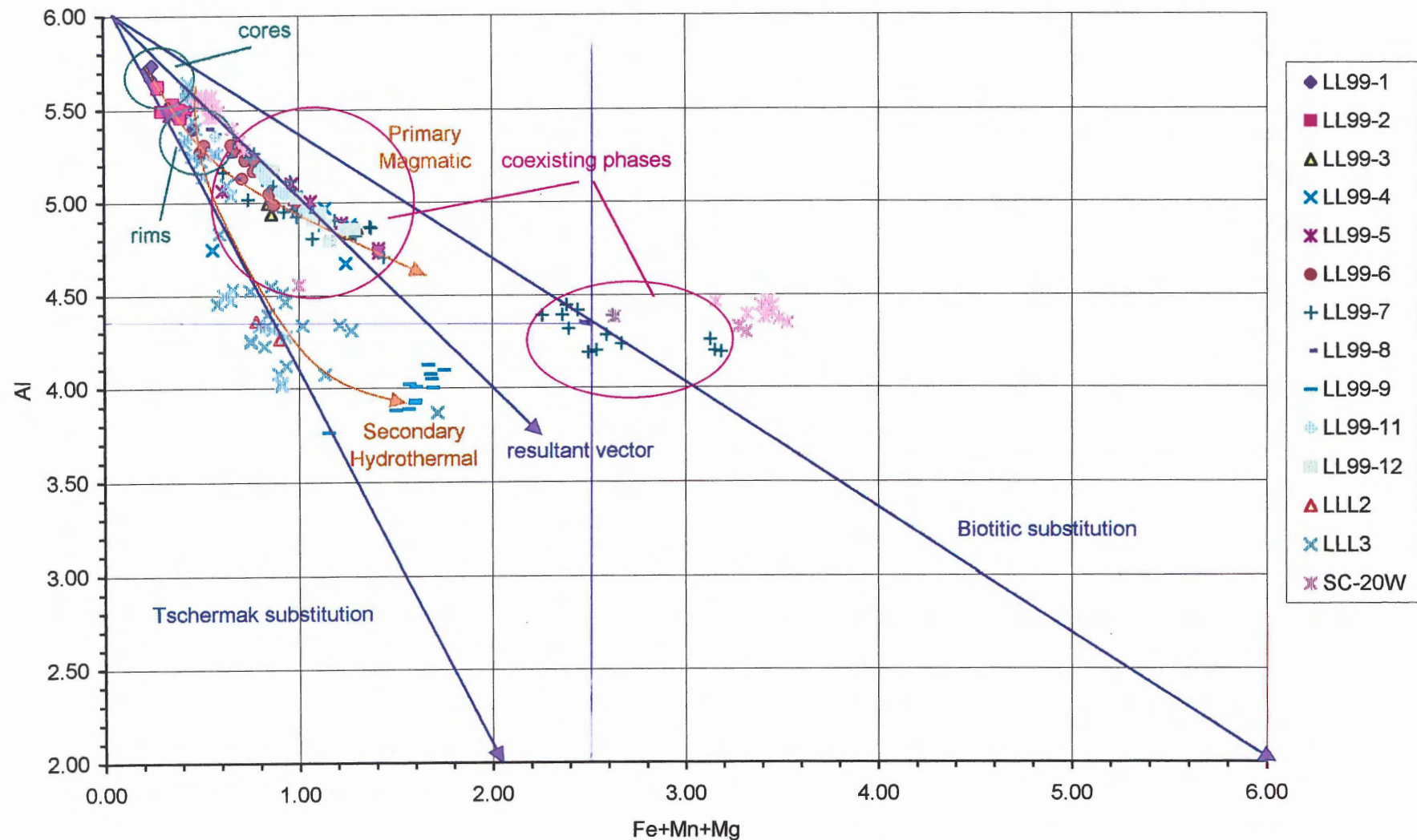


Figure 5.13b. Plot of Fe+Mn+Mg against AI showing the deformed mica trend toward the zinnwaldites, and the primary magmatic trend of muscovite-phengite overgrowths (cores and rims) and the protolithionite coexisting phase.

water-rich fluid phase. Sample LL99-12 is also aplitic, but appears to stay on the general mica trend, suggesting that it may not have grown in association with a fluid phase.

The alteration of the Lake Lewis Leucogranite muscovite to zinnwaldite appears to be the result of strong fluid interaction. The Tschermak substitution series has been related to increasing water pressure as noted by Velde (1980) and Green (1981). Monier and Robert (1986a) noted a miscibility gap between the coexisting and mutually saturated protolithionites and the lithian-phengitic micas, and determined that the gap decreases with increasing lithium content of the micas.

5.6 Systematic spatial variation of in composition of primary white micas

Within the limits of my sampling of the Lake Lewis Leucogranite, there appears to be no apparent chemical trend in the micas to link them to the mineral deposits, the nearest of which is the Walker Moly deposit more than 2 km away. The northern part of the Lake Lewis Leucogranite contains muscovites, and phengites to lithian-phengites occur to the south. The northwest half of the body has $\text{Fe}+\text{Mn}+\text{Mg} < 1.0$ and has lower lithium and fluorine contents, and the southeast half has $\text{Fe}+\text{Mn}+\text{Mg} > 1.0$ and has higher lithium and fluorine contents. As mentioned above, the released fluid may have been removing Ca, F, and metallic elements, which may subsequently have travelled to the mineralized greisen zones. The micas in the Walker Moly are also mechanically deformed and chemically altered, and were invaded by a fluorine-rich fluid transporting metallic elements, similar to the deformed samples of the Lake Lewis Leucogranite.

5.7 Implications for $^{40}\text{Ar}/^{39}\text{Ar}$ dating of white micas

Dating of muscovite bulk composites, or even of single grains, is now in question with the discovery that the Lake Lewis Leucogranite white micas contain alternating

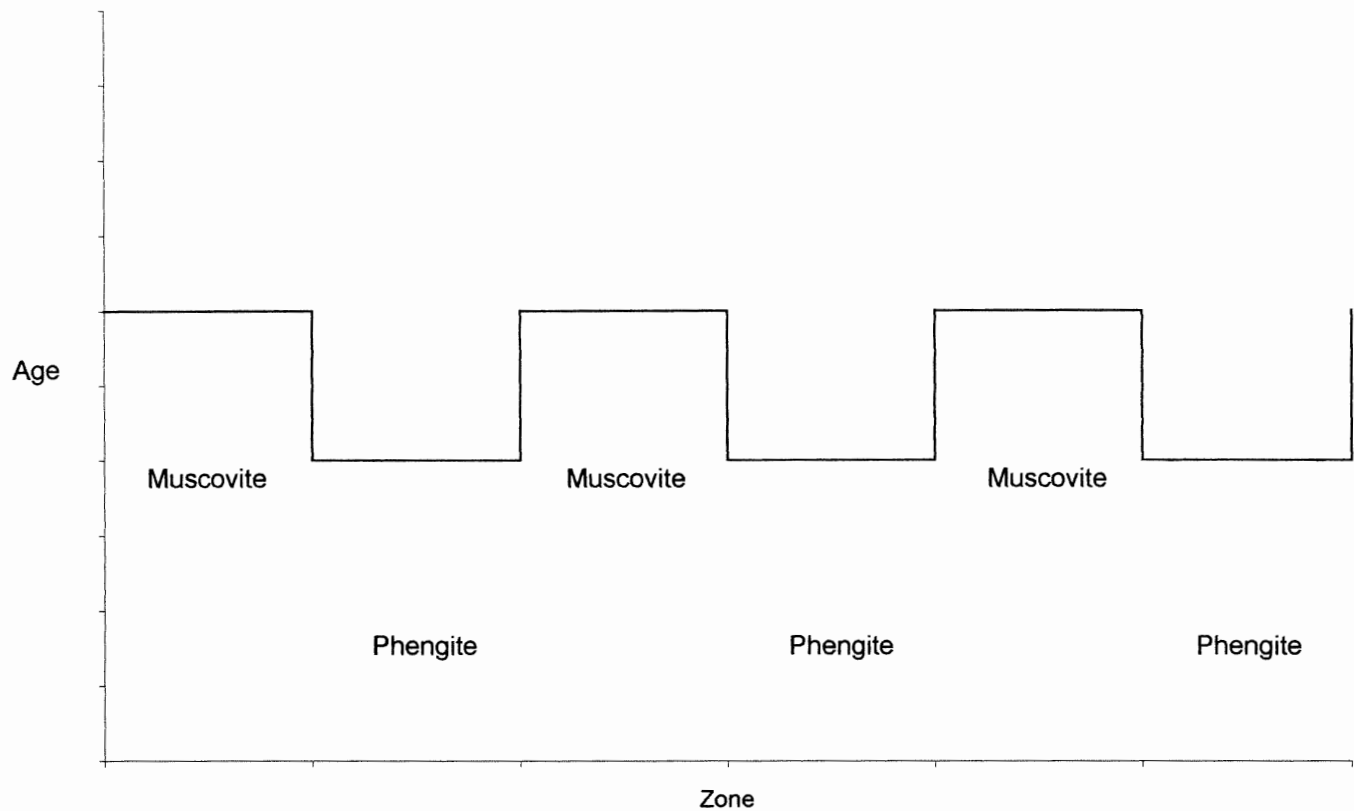


Figure 5.14a. Outcome 1 where the muscovite-phengite zones give different ages.

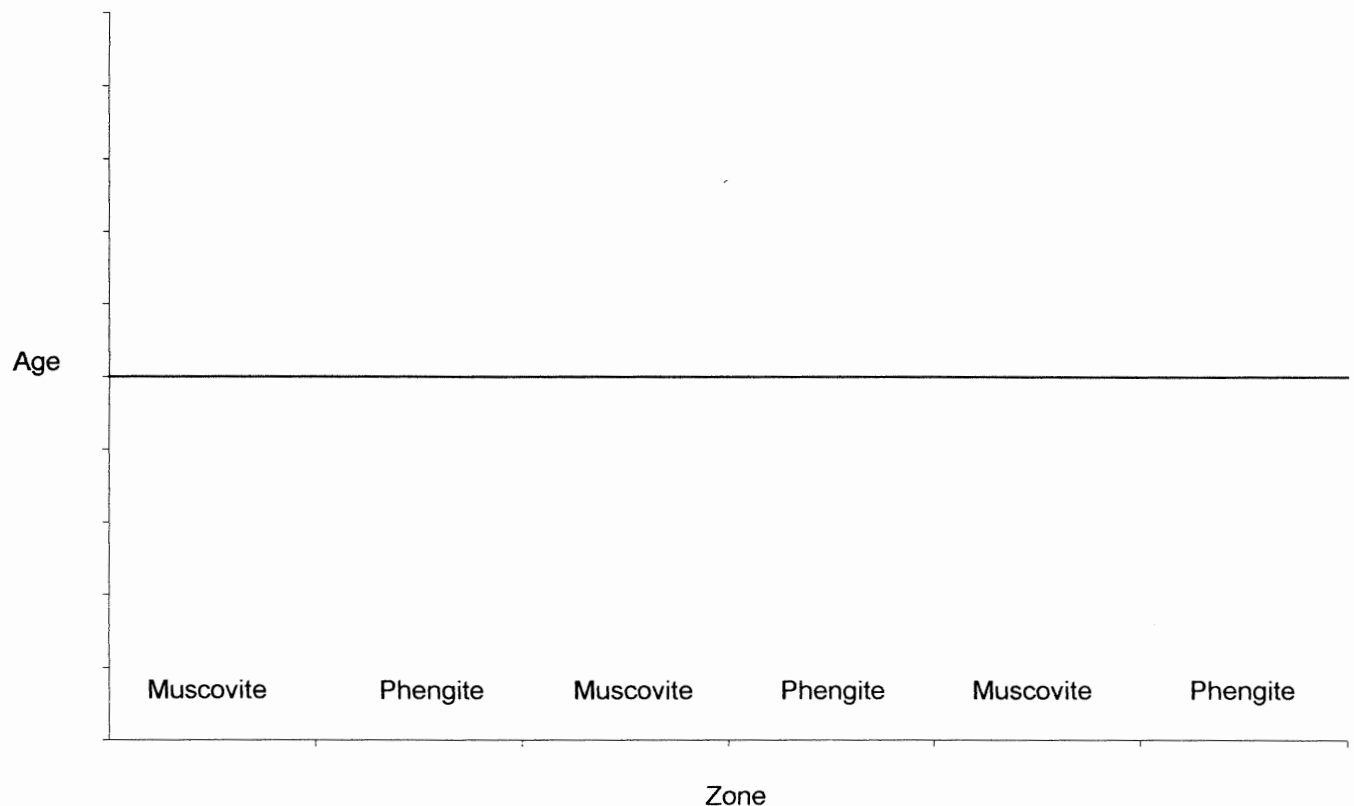


Figure 5.14b. Outcome 2 where the muscovite-phengite zones give the same age.

zones of muscovite-phengite. This compositional variation means that individual epitaxial zones must be analyzed, not because it is believed they are different ages, but because the argon retention of the phengite in the SMB is so far untested. It is precisely that the epitaxial zones must be the same age that such a test becomes useful for examining the argon retention of the phengite. Figures 5.14 a and b show two possible outcomes. I recommend that several zoned grains be dated by laser probe.

5.8 Summary

The various methods for calculating the lithium contents in the micas are in good agreement, meaning that the use of regression equations based on F and SiO₂ are valid for classification of the micas. The classifications of the micas using cation occupancy and the Mg-Li against Fe+Mn+Ti-Al^{VI} plot are in agreement. Textural and chemical evidence supports the primary nature of the Lake Lewis Leucogranite feldspars and micas, and the secondary nature of the deformed micas. The chemical substitution in the micas is a combination of biotitic and Tschermak substitution. The fluids expelled from the leucogranite may have been carrying Ca, F, and metallic elements, which may have led to local greisenization. The muscovite-phengite overgrowths require testing of argon retention in the phengites to check for the reliability of dating the white micas.

CHAPTER 6

CONCLUSIONS

6.1 Conclusions

1. Calculation of the lithium contents of the Lake Lewis Leucogranite white micas using regression equations with electron microprobe analytical data, a mass balance method, and a distribution coefficient method are in agreement. The regression equation estimates compare well with analyzed values of lithium by ICP-MS. The degree of agreement of the four independent methods for calculating lithium contents suggests that the use of regression equations is a reliable method for estimating the lithium contents of the micas.
2. The Lake Lewis Leucogranite micas were classified using two independent methods. The first method depends on cation proportions and does not take lithium into account. The second method depends on the composition and octahedral site occupancy, uses a two-dimensional diagram with axis variables Mg-Li and Fe+Mn+Ti-Al^{VI}, and requires an accurate estimation of lithium. The two classification schemes generate the same kinds of grouping of micas and yield the same names: muscovite, phengite, zinnwaldite, protolithionite, and siderophyllite.
3. The white micas that exhibit dimensional compatibility with other minerals have euhedral to subhedral grain shapes, and show well-defined straight grain boundaries, I interpreted to be primary magmatic white micas. The primary micas have higher Na/(Na+K) ratios, are richer in Al₂O₃ and Na₂O, and are poorer in SiO₂ and MgO compared with cataastically deformed and altered secondary white micas. The primary micas also have muscovite-phengite epitaxial overgrowths interpreted to

result from fluido-magmatic processes. Variable fluid pressure may be responsible for the oscillatory zoning in the Lake Lewis Leucogranite micas.

The textures and compositions of coexisting feldspars in the Lake Lewis Leucogranite are characteristic of primary magmatic origin and help demonstrate that the leucogranite body is primary magmatic. The low anorthite contents of plagioclase ($An_{0.5}$) are probably the result of calcium complexing with fluorine in the melt or fluid, preventing crystallization of plagioclase with higher anorthite contents.

4. Two separate primary magmatic substitutions occur in the primary white micas of the Lake Lewis Leucogranite. The first is the Tschermak substitution, or phengitic substitution, $(Mg, Fe^{2+})^{VI}, Si^{IV} \leftrightarrow Al^{IV}, Al^{VI}$, is proportional to fluid pressure. The second is the biotitic substitution $2/3 Al^{VI}, 1/3 \square^{VI} \leftrightarrow (Fe^{2+})^{VI}$ where \square stands for a vacant octahedral site. Biotitic substitution involving sufficient lithium contents results in a lithian-mica phase that is intermediate between dioctahedral and trioctahedral. Chemical plots show that the magmatic trend begins with a Tschermak substitution, but substitution of iron for silicon and aluminum makes the magmatic trend move toward a biotitic substitution.
5. The cataastically deformed white micas are secondary. Interaction of the deformed white micas with a fluid phase resulted in a distinct chemical signature that plots separately from undeformed micas on major element variation diagrams. These secondary micas have lower Na/(Na+K) ratios, are poorer in Al_2O_3 and Na_2O , and are richer in SiO_2 and MgO compared with primary undeformed white micas.

6. The hydrothermal alteration process results from strong fluid interaction of white micas that are cataastically deformed and chemically altered by the fluid to a zinnwaldite end-member.
7. No systematic spatial variation in the Lake Lewis Leucogranite appears to link the leucogranitic body to local greisens. There are only general chemical differences between the northwestern and southeastern portions of the leucogranite. The fluid, released when sufficient pressure built up, and responsible for the epitaxial muscovite-phengite overgrowths, may have removed Ca, F, and metallic elements from the melt, and may have subsequently produced mineralized greisen zones elsewhere. Notably, deformed fluorite-bearing white micas are common to the Walker Moly deposit and some samples of the Lake Lewis Leucogranite, but there is no simple chemical variable in the micas of the Lake Lewis Leucogranite correlates with the Walker Moly deposit.

6.2 Recommendations for future work

I recommend that laser ablation ICP-MS for minor and trace elements be done on the epitaxial mica overgrowths to look for chemical variations between the zones. I also recommend the thick section overgrowths be probed to see if the compositional miscibility gap can be diminished or completely removed, because I only probed high and low variations of the epitaxial overgrowths to get the maximum and minimum chemical limits. The dating implications of these phengitic overgrowths, and the argon retention of the phengites, also need to be tested.

REFERENCES

- Bailey, S.W. 1984. Classification and structure of the micas. *In Micas. Edited by S.W. Bailey.* Mineralogical Society of America, Reviews in Mineralogy, **12**, pp.1-12.
- Bates, R.L. and Jackson, J.A. (eds.). 1987. Glossary of geology. American Geological Institute, 3rd ed., Alexandria, Virginia.
- Clarke, D.B. and Chatterjee, A.K. 1988. Physical and chemical processes in the South Mountain Batholith. *In Recent advances in the Geology of Granite-Related Mineral Deposits.* Canadian Institute of Mining and Metallurgy, **39**, pp. 223-233.
- Clarke, D.B., MacDonald, M.A., Reynolds, P.H., and Longstaffe, F.J. 1993. Leucogranites from the eastern part of the South Mountain Batholith, Nova Scotia. *Journal of Petrology*, **34**: 653-679.
- Clarke, D.B. and Muecke, G.K. Review of the petrochemistry and origin of the South Mountain Batholith and associated plutons, Nova Scotia, Canada. *In High Heat Production (HHP) Granites, Hydrothermal Circulation and Ore Genesis.* London Institute of Mineralogy and Metallurgy, pp. 41-54.
- Deer, W.A., Howie, R.A., and Zussman, J. 1992. An introduction to the rock-forming minerals. Addison Wesley Longman Limited, 2nd ed., Harlow, England.
- Ding, Yi. 1995. AFM minerals in the Halifax pluton. M.Sc. thesis, Dalhousie University, Halifax, N.S.
- Fallon, R.P. 1998. Age and thermal history of the Port Mouton Pluton, southwest Nova Scotia: a combined U-Pb, $^{40}\text{Ar}/^{39}\text{Ar}$ age spectrum, and $^{40}\text{Ar}/^{39}\text{Ar}$ laserprobe study. M.Sc. thesis, Dalhousie University, Halifax, N.S.
- Faure, G. 1991. Principles and applications of inorganic geochemistry. MacMillan Publishing, New York.
- Friel, J.J. 1995. X-ray and image analysis in electron microscopy. Princeton Gamma-Tech Incorporated, New Jersey.
- Green, T.H. 1981. Synthetic high-pressure micas compositionally intermediate between the dioctahedral and trioctahedral mica series. *Contributions to Mineralogy and Petrology*, **78**: 542-8.
- Guidotti, C.V. 1984. Micas in metamorphic rocks. *In Micas. Edited by S.W. Bailey.* Mineralogical Society of America, Reviews in Mineralogy, **12**, pp. 357-467.

- Ham, L.J. 1991. Geological map of Windsor, Nova Scotia, NTS 21A/16 west half and part of 21H/01. Nova Scotia Department of Mines and Energy, Map 90-10, 1:50 000.
- Ham, L.J. and Kontak, D.J. 1988. A textural and chemical study of white mica in the South Mountain Batholith, Nova Scotia: primary versus secondary origin. *Maritime Sediments and Atlantic Geology*, **24**: 111-121.
- Kontak, D.J. and Martin, R.F. 1997. Alkali feldspar in the peraluminous South Mountain Batholith, Nova Scotia: trace-element data. *Canadian Mineralogist*, **35**: 959-977.
- Logothetis, J. 1985. The mineralogy and geochemistry of metasomatized granitoid rocks from occurrences in the South Mountain Batholith: New Ross area, southwestern Nova Scotia. M.Sc. thesis, Dalhousie University, Halifax, N.S.
- Miller, C.F., Stoddard, E.F., Bradfish, L.J., and Dollase, W.A. 1981. Composition of plutonic muscovite: genetic implications. *Canadian Mineralogist*, **19**: 25-34.
- Monier, G. and Robert, J.-L. 1986a. Evolution of the miscibility gap between muscovite and biotite solid solutions with increasing lithium content: an experimental study in the system $K_2O-Li_2O-MgO-FeO-Al_2O_3-SiO_2-H_2O-HF$ at $600\text{ }^{\circ}\text{C}$, 2 kbar P_{H_2O} : comparison with natural lithium micas. *Mineralogical Magazine*, **50**: 641-651.
- Monier, G. and Robert, J.-L. 1986b. Muscovite solid solutions in the system $K_2O-MgO-FeO-Al_2O_3-SiO_2-H_2O$: an experimental study at 2 kbar P_{H_2O} and comparison with natural Li-free white micas. *Mineralogical Magazine*, **50**: 257-266.
- Roycroft, P.D. 1989. Zoned muscovite from the Leinster Granite, S.E. Ireland. *Mineralogical Magazine*, **53**: 663-665.
- Roycroft, P. 1991. Magmatically zoned muscovite from the peraluminous two-mica granites of the Leinster batholith, southeast Ireland. *Geology*, **19**: 437-440.
- Speer, J.A. 1984. Micas in igneous rocks. In *Micas*. Edited by S.W. Bailey. Mineralogical Society of America, Reviews in Mineralogy, **12**, pp. 229-356.
- Stone, M., Exley, C.S., and George, M.C. 1988. Compositions of trioctahedral micas in the Cornubian batholith. *Mineralogical Magazine*, **52**: 175-192.
- Streckeisen, A. 1976. To each plutonic rock its proper name. *Earth Science Reviews*, **12**: 1-33.
- Strong, D.F. 1981. Ore Deposit Models –5. A Model for Granophile Mineral Deposits. *Geoscience Canada*, **8**: 155-161.

- Tischendorf, G., Gottesmann, B., Forster, H.-J., and Trumbull, R.B. 1997. On Li-bearing micas: estimating Li from electron microprobe analyses and an improved diagram for graphical representation. *Mineralogical Magazine*, **61**: 809-834.
- Tischendorf, G., Forster, H.-J., and Gottesmann, B. 1999. The correlation between lithium and magnesium in trioctahedral micas: Improved equations for Li₂O estimation from MgO data. *Mineralogical Magazine*, **63**: 57-74.
- Twiss, R.J. and Moores, E.M. 1992. Structural geology. W.H. Freeman and Company, New York.
- Velde, B. 1980. Cell dimensions, polymorph type, and infrared spectra of synthetic white micas: the importance of ordering. *American Mineralogist*, **65**: 1277-1282.
- Walker, R.J., Hanson, G.N., Papike, J.J. 1989. Trace element constraints on pegmatite genesis: Tin Mountain pegmatite, Black Hills, South Dakota. *Contributions to Mineralogy and Petrology*, **101**: 290-300.
- Weidner, J.R. and Martin, R.F. 1987. Phase equilibria of a fluorine-rich leucogranite from the St. Austell pluton, Cornwall. *Geochimica et Cosmochimica Acta*, **51**: 1591-1597.
- WWW-MINCRYST (new revision). 2001, Feb. 16. [online]. Institute of Experimental Mineralogy RAN. <http://database.iem.ac.ru/mincrysts/s_carta.php3?PROTOLITHIONITE> [2001, Mar. 15].
- Zen, E-an. 1988. Phase relations of peraluminous granitic rocks and their petrogenetic implications. *Annual Review of Earth and Planetary Sciences*, **16**: 21-51.

APPENDICES

Appendix A

Microprobe data for micas from the Lake Lewis Leucogranite and Walker Moly deposit

Lake Lewis Leucogranite samples:

LL99-1

LL99-2

LL99-3

LL99-4

LL99-5

LL99-6

LL99-7

LL99-8

LL99-9

LL99-9

LL99-11

LL99-12

Walker Moly sample:

SC-20W

Microprobe data for micas from the Lake Lewis Leucogranite.

Sample Analysis	LL99-1 1-1c	LL99-1 1-1r	LL99-1 1-2c	LL99-1 1-2r	LL99-1 1-3c	LL99-1 1-3r	LL99-1 1-4c	LL99-1 1-4r
Mineral	muscovite							
Location	core	rim	core	rim	core	rim	core	rim
SiO ₂	46.40	46.53	46.42	46.07	46.15	46.25	45.84	46.05
TiO ₂	0.21	0.14	0.28	0.09	0.00	0.03	0.12	0.10
Al ₂ O ₃	34.02	35.16	34.82	34.83	36.69	36.02	34.58	34.76
FeO	2.81	2.51	2.56	2.79	1.79	1.85	2.42	2.10
MnO	0.12	0.00	0.00	0.00	0.04	0.00	0.04	0.10
MgO	0.64	0.51	0.63	0.60	0.17	0.19	0.41	0.48
CaO	0.10	0.05	0.00	0.00	0.00	0.00	0.00	0.00
Na ₂ O	0.60	0.63	0.71	0.69	0.66	0.61	0.71	0.60
K ₂ O	10.40	10.65	10.71	10.56	10.68	10.46	10.33	10.52
Cr ₂ O ₃	0.04	0.05	0.00	0.00	0.00	0.00	0.00	0.00
Cl	0.00	0.00	0.00	0.00	0.00	0.00	0.00	0.02
P ₂ O ₅	0.16	0.16	0.05	0.14	0.11	0.02	0.19	0.10
BaO	0.00	0.17	0.00	0.05	0.07	0.03	0.07	0.00
F	0.53	0.30	0.45	0.48	0.32	0.32	0.56	0.46
Total	96.03	96.86	96.63	96.31	96.69	95.78	95.30	95.27
Si	6.24	6.18	6.20	6.18	6.11	6.17	6.21	6.21
Ti	0.02	0.01	0.03	0.01	0.00	0.00	0.01	0.01
Al Total	5.39	5.50	5.48	5.51	5.73	5.67	5.52	5.53
Al IV	1.76	1.82	1.80	1.82	1.89	1.83	1.79	1.79
Al VI	3.64	3.68	3.68	3.68	3.84	3.84	3.72	3.74
Fe	0.32	0.28	0.29	0.31	0.20	0.21	0.27	0.24
Mn	0.01	0.00	0.00	0.00	0.00	0.00	0.01	0.01
Mg	0.13	0.10	0.12	0.12	0.03	0.04	0.08	0.10
Ca	0.01	0.01	0.00	0.00	0.00	0.00	0.00	0.00
Na	0.16	0.16	0.18	0.18	0.17	0.16	0.19	0.16
K	1.79	1.80	1.82	1.81	1.80	1.78	1.78	1.81
Cr	0.00	0.00	0.00	0.00	0.00	0.00	0.00	0.00
Cl	0.00	0.00	0.00	0.00	0.00	0.00	0.00	0.00
P	0.02	0.02	0.01	0.02	0.01	0.00	0.02	0.01
Ba	0.00	0.01	0.00	0.00	0.00	0.00	0.00	0.00
F	0.23	0.13	0.19	0.20	0.13	0.14	0.24	0.20
OH	3.77	3.87	3.81	3.80	3.87	3.86	3.76	3.80
Tet	8.00	8.00	8.00	8.00	8.00	8.00	8.00	8.00
Oct	4.13	4.08	4.11	4.13	4.07	4.08	4.10	4.10
Dodec	1.96	2.00	2.01	2.00	1.99	1.94	2.00	1.98
Estimated Li content	0.07	0.04	0.06	0.06	0.03	0.03	0.06	0.05

Microprobe data for micas from the Lake Lewis Leucogranite.

Sample Analysis	LL99-1 1-5c	LL99-1 1-5r	LL99-2 II2-1	LL99-2 II2-2	LL99-2 II2-3	LL99-2 II2-4	LL99-2 II2-5	LL99-2 II2-6
Mineral	muscovite	muscovite	muscovite	muscovite	muscovite	muscovite	muscovite	muscovite
Location	core	rim	core	rim	core	rim	core	rim
SiO ₂	45.61	45.64	45.66	46.12	45.49	46.44	46.24	45.78
TiO ₂	0.00	0.07	0.22	0.13	0.12	0.31	0.19	0.29
Al ₂ O ₃	36.14	36.53	34.14	34.12	34.92	34.35	34.90	35.49
FeO	1.61	1.63	3.08	2.28	1.96	2.78	2.55	2.11
MnO	0.15	0.00	0.07	0.00	0.03	0.03	0.07	0.06
MgO	0.16	0.34	0.29	0.17	0.23	0.40	0.31	0.18
CaO	0.00	0.00	0.01	0.01	0.00	0.00	0.05	0.02
Na ₂ O	0.61	0.65	0.66	0.66	0.64	0.55	0.96	0.70
K ₂ O	10.73	10.52	10.64	10.43	10.69	10.89	10.37	10.74
Cr ₂ O ₃	0.03	0.00	0.00	0.00	0.09	0.03	0.00	0.04
Cl	0.00	0.00	0.00	0.00	0.00	0.00	0.00	0.03
P ₂ O ₅	0.15	0.19	0.09	0.15	0.00	0.11	0.17	0.14
BaO	0.07	0.00	0.00	0.04	0.01	0.00	0.00	0.00
F	0.42	0.32	1.15	0.90	0.73	0.91	0.88	0.69
Total	95.67	95.88	96.00	95.01	94.90	96.78	96.68	96.27
Si	6.12	6.08	6.24	6.30	6.20	6.26	6.21	6.16
Ti	0.00	0.01	0.02	0.01	0.01	0.03	0.02	0.03
Al Total	5.72	5.74	5.50	5.49	5.61	5.45	5.53	5.62
Al IV	1.88	1.92	1.76	1.70	1.80	1.74	1.79	1.84
Al VI	3.84	3.82	3.75	3.79	3.82	3.71	3.74	3.78
Fe	0.18	0.18	0.35	0.26	0.22	0.31	0.29	0.24
Mn	0.02	0.00	0.01	0.00	0.00	0.00	0.01	0.01
Mg	0.03	0.07	0.06	0.03	0.05	0.08	0.06	0.04
Ca	0.00	0.00	0.00	0.00	0.00	0.00	0.01	0.00
Na	0.16	0.17	0.17	0.17	0.17	0.14	0.25	0.18
K	1.84	1.79	1.86	1.82	1.86	1.87	1.78	1.84
Cr	0.00	0.00	0.00	0.00	0.01	0.00	0.00	0.00
Cl	0.00	0.00	0.00	0.00	0.00	0.00	0.00	0.01
P	0.02	0.02	0.01	0.02	0.00	0.01	0.02	0.02
Ba	0.00	0.00	0.00	0.00	0.00	0.00	0.00	0.00
F	0.18	0.13	0.50	0.39	0.31	0.39	0.37	0.29
OH	3.82	3.87	3.50	3.61	3.69	3.61	3.63	3.70
Tet	8.00	8.00	8.00	8.00	8.00	8.00	8.00	8.00
Oct	4.06	4.08	4.19	4.10	4.11	4.14	4.13	4.09
Dodec	2.02	1.98	2.04	2.01	2.04	2.03	2.05	2.04
Estimated Li content	0.03	0.02	0.10	0.07	0.12	0.11	0.07	1.16

Microprobe data for micas from the Lake Lewis Leucogranite.

Sample Analysis	LL99-3 II3-5	LL99-3 II3-6	LL99-3 II3-9	LL99-3 II3-10	LL99-3 II3-11	LL99-3 II3-12	LL99-4 4-1c	LL99-4 4-1r
Mineral	Li phengite	Li phengite	Li phengite	Li phengite	Li phengite	Li phengite	Li phengite	Li phengite
Location	core	rim	core	rim	core	rim	core	rim
SiO ₂	46.80	46.76	44.94	44.67	43.72	43.80	44.68	45.04
TiO ₂	0.05	0.13	0.26	0.59	0.71	0.65	0.26	0.29
Al ₂ O ₃	29.69	29.18	29.10	28.96	27.48	27.24	29.08	28.62
FeO	6.33	6.61	7.57	7.70	9.29	8.81	8.08	8.35
MnO	0.18	0.11	0.23	0.14	0.27	0.28	0.19	0.02
MgO	0.30	0.25	0.13	0.16	0.46	0.48	0.62	0.56
CaO	0.04	0.00	0.00	0.01	0.00	0.02	0.00	0.00
Na ₂ O	0.29	0.22	0.48	0.39	0.53	0.47	0.31	0.42
K ₂ O	10.86	10.70	10.55	10.85	10.22	10.10	10.60	10.21
Cr ₂ O ₃	0.09	0.05	0.00	0.01	0.02	0.01	0.04	0.07
Cl	0.00	0.00	0.00	0.00	0.00	0.03	0.02	0.03
P ₂ O ₅	0.01	0.01	0.01	0.02	0.00	0.06	0.02	0.05
BaO	0.04	0.05	0.08	0.00	0.00	0.00	0.10	0.14
F	3.40	3.28	3.51	3.22	3.97	3.77	2.79	2.52
Total	98.07	97.34	96.86	96.71	96.66	95.74	96.78	96.33
Si	6.68	6.71	6.59	6.53	6.56	6.59	6.48	6.52
Ti	0.00	0.01	0.03	0.06	0.08	0.07	0.03	0.03
Al Total	5.00	4.94	5.03	4.99	4.86	4.83	4.97	4.88
Al IV	1.32	1.29	1.41	1.47	1.44	1.41	1.52	1.48
Al VI	3.68	3.65	3.61	3.52	3.43	3.43	3.45	3.39
Fe	0.76	0.79	0.93	0.94	1.17	1.11	0.98	1.01
Mn	0.02	0.01	0.03	0.02	0.03	0.04	0.02	0.00
Mg	0.06	0.05	0.03	0.03	0.10	0.11	0.13	0.12
Ca	0.01	0.00	0.00	0.00	0.00	0.00	0.00	0.00
Na	0.08	0.06	0.14	0.11	0.15	0.14	0.09	0.12
K	1.98	1.96	1.97	2.02	1.96	1.94	1.96	1.88
Cr	0.01	0.01	0.00	0.00	0.00	0.00	0.00	0.01
Cl	0.00	0.00	0.00	0.00	0.00	0.01	0.00	0.01
P	0.00	0.00	0.00	0.00	0.00	0.01	0.00	0.01
Ba	0.00	0.00	0.00	0.00	0.00	0.00	0.01	0.01
F	1.53	1.49	1.63	1.49	1.89	1.80	1.28	1.15
OH	2.47	2.51	2.37	2.51	2.11	2.20	2.72	2.84
Tet	8.00	8.00	8.00	8.00	8.00	8.00	8.00	8.00
Oct	4.53	4.53	4.62	4.58	4.81	4.76	4.61	4.56
Dodec	2.07	2.03	2.12	2.14	2.11	2.09	2.06	2.02
Estimated Li content	1.52	1.40	2.21	2.00	1.25	1.16	1.07	0.99

Microprobe data for micas from the Lake Lewis Leucogranite.

Sample	LL99-4	LL99-4	LL99-4	LL99-4	LL99-4	LL99-5	LL99-5	LL99-5
Analysis	4-2c	4-2r	4-3c	4-5c	4-5r2	5-1r	5-1c	5-2c
Mineral	Li phengite	Li phengite	Li phengite	muscovite	Li phengite	Li phengite	Li phengite	Li phengite
Location	core	rim	core	core	rim	rim	core	core
SiO ₂	44.22	44.80	45.29	50.15	45.61	44.75	45.45	45.36
TiO ₂	0.40	0.37	0.28	0.34	0.49	0.58	0.20	0.48
Al ₂ O ₃	28.33	29.14	29.92	29.72	27.35	27.66	30.53	29.95
FeO	8.92	7.58	7.34	3.21	9.34	10.28	6.93	6.97
MnO	0.21	0.11	0.15	0.00	0.00	0.14	0.24	0.19
MgO	0.68	0.54	0.44	0.97	0.51	0.70	0.54	0.60
CaO	0.00	0.00	0.00	0.00	0.00	0.00	0.00	0.03
Na ₂ O	0.47	0.64	0.59	0.06	0.35	0.43	0.72	0.51
K ₂ O	10.19	10.17	10.46	10.24	10.46	10.30	10.42	10.76
Cr ₂ O ₃	0.00	0.10	0.01	0.05	0.00	0.00	0.00	0.00
Cl	0.00	0.00	0.00	0.01	0.01	0.00	0.00	0.00
P ₂ O ₅	0.05	0.14	0.03	0.12	0.04	0.05	0.14	0.00
BaO	0.00	0.01	0.03	0.10	0.04	0.00	0.17	0.00
F	2.72	2.59	2.49	1.31	2.68	2.80	2.82	2.48
Total	96.19	96.19	97.03	96.27	96.89	97.66	98.17	97.33
Si	6.46	6.47	6.46	6.80	6.61	6.49	6.44	6.45
Ti	0.04	0.04	0.03	0.03	0.05	0.06	0.02	0.05
Al Total	4.88	4.96	5.03	4.75	4.67	4.73	5.10	5.02
Al IV	1.54	1.53	1.54	1.20	1.39	1.51	1.56	1.55
Al VI	3.34	3.43	3.49	3.54	3.28	3.22	3.54	3.47
Fe	1.09	0.91	0.88	0.36	1.13	1.25	0.82	0.83
Mn	0.03	0.01	0.02	0.00	0.00	0.02	0.03	0.02
Mg	0.15	0.12	0.09	0.20	0.11	0.15	0.11	0.13
Ca	0.00	0.00	0.00	0.00	0.00	0.00	0.00	0.00
Na	0.13	0.18	0.16	0.02	0.10	0.12	0.20	0.14
K	1.90	1.87	1.90	1.77	1.93	1.91	1.88	1.95
Cr	0.00	0.01	0.00	0.00	0.00	0.00	0.00	0.00
Cl	0.00	0.00	0.00	0.00	0.00	0.00	0.00	0.00
P	0.01	0.02	0.00	0.01	0.01	0.01	0.02	0.00
Ba	0.00	0.00	0.00	0.01	0.00	0.00	0.01	0.00
F	1.26	1.18	1.12	0.56	1.23	1.28	1.26	1.11
OH	2.74	2.82	2.88	3.44	2.77	2.72	2.74	2.89
Tet	8.00	8.00	8.00	8.00	8.00	8.00	8.00	8.00
Oct	4.65	4.52	4.51	4.14	4.58	4.70	4.53	4.50
Dodec	2.04	2.08	2.07	1.81	2.04	2.03	2.11	2.09
Estimated Li content	0.20	1.39	1.60	1.03	0.92	1.25	1.31	0.44

Microprobe data for micas from the Lake Lewis Leucogranite.

Sample Analysis	LL99-5 5-2r	LL99-5 5-3c	LL99-5 5-3r	LL99-5 5-4c	LL99-5 5-4r	LL99-6 II6-1	LL99-6 II6-2	LL99-6 II6-3
Mineral	Li phengite	Li phengite	Li phengite	Li phengite	muscovite	Li phengite	Li phengite	Li phengite
Location	rim	core	rim	core	rim	core	rim	core
SiO ₂	44.65	45.79	44.70	48.26	47.66	46.09	45.48	45.44
TiO ₂	0.43	0.18	0.37	0.00	0.00	0.45	0.48	0.44
Al ₂ O ₃	27.81	29.91	28.78	31.40	34.80	30.97	29.89	31.13
FeO	10.34	7.76	8.85	4.72	2.65	5.38	6.03	5.36
MnO	0.23	0.14	0.17	0.05	0.15	0.12	0.04	0.09
MgO	0.62	0.58	0.63	0.31	0.13	0.57	0.57	0.56
CaO	0.00	0.07	0.00	0.05	0.00	0.02	0.01	0.00
Na ₂ O	0.34	0.44	0.42	0.15	0.16	0.66	0.43	0.63
K ₂ O	10.70	10.47	10.56	11.01	11.22	10.52	10.61	10.39
Cr ₂ O ₃	0.00	0.00	0.08	0.00	0.00	0.00	0.06	0.00
Cl	0.00	0.00	0.00	0.00	0.01	0.00	0.00	0.00
P ₂ O ₅	0.15	0.17	0.13	0.06	0.00	0.07	0.01	0.10
BaO	0.00	0.03	0.04	0.05	0.00	0.07	0.13	0.00
F	2.88	3.03	2.68	1.88	1.10	3.26	2.66	3.29
Total	98.13	98.56	97.41	97.95	97.88	98.17	96.40	97.42
Si	6.47	6.50	6.44	6.60	6.36	6.52	6.51	6.48
Ti	0.05	0.02	0.04	0.00	0.00	0.05	0.05	0.05
Al Total	4.75	5.00	4.89	5.06	5.47	5.17	5.05	5.23
Al IV	1.53	1.50	1.56	1.40	1.64	1.48	1.49	1.52
Al VI	3.22	3.51	3.33	3.66	3.83	3.69	3.56	3.72
Fe	1.25	0.92	1.07	0.54	0.30	0.64	0.72	0.64
Mn	0.03	0.02	0.02	0.01	0.02	0.01	0.00	0.01
Mg	0.13	0.12	0.13	0.06	0.03	0.12	0.12	0.12
Ca	0.00	0.01	0.00	0.01	0.00	0.00	0.00	0.00
Na	0.09	0.12	0.12	0.04	0.04	0.18	0.12	0.17
K	1.98	1.90	1.94	1.92	1.91	1.90	1.94	1.89
Cr	0.00	0.00	0.01	0.00	0.00	0.00	0.01	0.00
Cl	0.00	0.00	0.00	0.00	0.00	0.00	0.00	0.00
P	0.02	0.02	0.02	0.01	0.00	0.01	0.00	0.01
Ba	0.00	0.00	0.00	0.00	0.00	0.00	0.01	0.00
F	1.32	1.36	1.22	0.81	0.47	1.46	1.20	1.48
OH	2.68	2.64	2.78	3.19	3.53	2.54	2.80	2.52
Tet	8.00	8.00	8.00	8.00	8.00	8.00	8.00	8.00
Oct	4.68	4.60	4.60	4.28	4.17	4.51	4.46	4.53
Dodec	2.09	2.04	2.09	1.97	1.95	2.09	2.07	2.08
Estimated Li content	0.14	0.93	0.86	0.95	1.29	1.61	0.50	1.67

Microprobe data for micas from the Lake Lewis Leucogranite.

Sample Analysis	LL99-6 II6-4	LL99-6 II6-5	LL99-6 II6-6	LL99-6 II6-7	LL99-6 II6-9	LL99-6 II6-10	LL99-6 II6-8	LL99-6 II6-11	
Mineral Location	Li phengite rim	Li phengite core	Li phengite rim	Li phengite core	muscovite core	Li phengite rim	Li phengite core	muscovite rim	Li phengite core
SiO ₂	45.18	45.26	44.35	46.10	44.53	45.01	46.66	44.92	
TiO ₂	0.55	0.57	0.76	0.30	0.69	0.59	0.20	0.15	
Al ₂ O ₃	29.20	30.87	28.23	32.04	28.28	28.90	32.16	31.33	
FeO	6.64	5.73	7.61	3.96	8.24	6.67	3.66	4.79	
MnO	0.25	0.06	0.30	0.01	0.23	0.17	0.00	0.09	
MgO	0.70	0.42	0.55	0.23	0.18	0.17	0.34	0.32	
CaO	0.00	0.00	0.00	0.01	0.00	0.01	0.06	0.00	
Na ₂ O	0.51	0.57	0.51	0.39	0.66	0.58	0.27	0.67	
K ₂ O	10.54	10.53	10.37	10.82	10.25	10.12	11.07	10.26	
Cr ₂ O ₃	0.02	0.06	0.00	0.00	0.05	0.02	0.00	0.04	
Cl	0.00	0.05	0.02	0.00	0.01	0.00	0.00	0.00	
P ₂ O ₅	0.00	0.10	0.02	0.02	0.11	0.00	0.03	0.13	
BaO	0.00	0.00	0.00	0.00	0.00	0.02	0.05	0.00	
F	3.47	2.97	3.66	2.38	3.53	3.00	2.09	2.89	
Total	97.04	97.19	96.37	96.26	96.75	95.24	96.57	95.59	
Si	6.57	6.46	6.57	6.48	6.56	6.59	6.49	6.46	
Ti	0.06	0.06	0.08	0.03	0.08	0.06	0.02	0.02	
Al Total	5.00	5.19	4.93	5.31	4.91	4.99	5.27	5.31	
Al IV	1.43	1.54	1.43	1.52	1.44	1.41	1.51	1.54	
Al VI	3.57	3.64	3.50	3.79	3.47	3.58	3.76	3.77	
Fe	0.81	0.68	0.94	0.47	1.02	0.82	0.43	0.58	
Mn	0.03	0.01	0.04	0.00	0.03	0.02	0.00	0.01	
Mg	0.15	0.09	0.12	0.05	0.04	0.04	0.07	0.07	
Ca	0.00	0.00	0.00	0.00	0.00	0.00	0.01	0.00	
Na	0.14	0.16	0.15	0.11	0.19	0.16	0.07	0.19	
K	1.95	1.92	1.96	1.94	1.93	1.89	1.96	1.88	
Cr	0.00	0.01	0.00	0.00	0.01	0.00	0.00	0.00	
Cl	0.00	0.01	0.00	0.00	0.00	0.00	0.00	0.00	
P	0.00	0.01	0.00	0.00	0.01	0.00	0.00	0.02	
Ba	0.00	0.00	0.00	0.00	0.00	0.00	0.00	0.00	
F	1.59	1.34	1.71	1.06	1.64	1.39	0.92	1.32	
OH	2.41	2.65	2.28	2.94	2.36	2.61	3.08	2.68	
Tet	8.00	8.00	8.00	8.00	8.00	8.00	8.00	8.00	
Oct	4.62	4.49	4.68	4.34	4.63	4.52	4.29	4.44	
Dodec	2.10	2.09	2.11	2.05	2.13	2.06	2.04	2.09	
Estimated Li content	1.14	0.40	0.77	0.77	0.94	0.73	0.52	1.10	

Microprobe data for micas from the Lake Lewis Leucogranite.

Sample	LL99-6	LL99-6	LL99-6	LL99-7	LL99-7	LL99-7	LL99-7
Analysis	II6-12	II6-13	II6-14	II7-1	II7-2	II7-3	II7-4
Mineral	Li phengite	protolithionite	Li phengite				
Location	rim	core	rim	core	rim	core	core
SiO ₂	45.42	45.07	45.22	46.54	46.16	40.20	45.18
TiO ₂	0.38	0.49	0.48	0.47	0.45	1.01	0.52
Al ₂ O ₃	31.47	30.72	30.10	31.40	29.92	23.85	28.98
FeO	5.11	5.30	5.14	4.43	6.99	16.91	8.00
MnO	0.04	0.09	0.05	0.15	0.29	0.26	0.22
MgO	0.29	0.35	0.38	0.37	0.44	0.49	0.39
CaO	0.00	0.00	0.01	0.00	0.17	0.00	0.00
Na ₂ O	0.65	0.61	0.51	0.60	0.39	0.49	0.51
K ₂ O	10.28	10.21	10.33	10.75	8.40	10.03	10.55
Cr ₂ O ₃	0.12	0.04	0.00	0.06	0.00	0.00	0.09
Cl	0.00	0.00	0.04	0.00	0.03	0.00	0.03
P ₂ O ₅	0.00	0.08	0.00	0.04	0.00	0.00	0.05
BaO	0.00	0.00	0.00	0.08	0.04	0.03	0.00
F	2.80	3.22	2.59	2.28	2.93	4.36	3.26
Total	96.55	96.17	94.85	97.17	96.19	97.62	97.79
Si	6.46	6.50	6.53	6.49	6.60	6.36	6.53
Ti	0.04	0.05	0.05	0.05	0.05	0.12	0.06
Al Total	5.27	5.23	5.13	5.16	5.04	4.44	4.94
Al IV	1.54	1.50	1.47	1.51	1.40	1.64	1.47
Al VI	3.74	3.73	3.66	3.65	3.64	2.80	3.47
Fe	0.61	0.64	0.62	0.52	0.83	2.24	0.97
Mn	0.00	0.01	0.01	0.02	0.04	0.03	0.03
Mg	0.06	0.08	0.08	0.08	0.09	0.11	0.08
Ca	0.00	0.00	0.00	0.00	0.03	0.00	0.00
Na	0.18	0.17	0.14	0.16	0.11	0.15	0.14
K	1.87	1.88	1.90	1.91	1.53	2.02	1.95
Cr	0.01	0.00	0.00	0.01	0.00	0.00	0.01
Cl	0.00	0.00	0.01	0.00	0.01	0.00	0.01
P	0.00	0.01	0.00	0.00	0.00	0.00	0.01
Ba	0.00	0.00	0.00	0.00	0.00	0.00	0.00
F	1.26	1.47	1.18	1.00	1.32	2.18	1.49
OH	2.74	2.53	2.81	3.00	2.67	1.82	2.50
Tet	8.00	8.00	8.00	8.00	8.00	8.00	8.00
Oct	4.45	4.51	4.42	4.32	4.68	5.30	4.61
Dodec	2.06	2.06	2.05	2.09	1.64	2.17	2.11
Estimated Li content	4.88	1.45	5.06	2.18	1.95	2.81	2.80

Microprobe data for micas from the Lake Lewis Leucogranite.

Sample	LL99-7	LL99-7	LL99-7	LL99-7	LL99-7	LL99-7
Analysis	II7-5	II7-6	II7-7	II7-8	7-1r	7-1c
Mineral	protolithionite	protolithionite	Li phengite	Li phengite	protolithionite	protolithionite
Location	rim	rim	core	rim	rim	core
SiO ₂	39.65	39.17	44.08	43.85	40.92	39.76
TiO ₂	1.36	1.23	0.52	0.66	0.98	1.19
Al ₂ O ₃	23.63	23.30	27.97	27.88	24.53	23.57
FeO	17.29	18.56	9.46	9.53	16.60	17.91
MnO	0.43	0.27	0.16	0.21	0.33	0.41
MgO	0.38	0.44	0.81	0.77	0.93	1.00
CaO	0.03	0.00	0.07	0.04	0.03	0.04
Na ₂ O	0.47	0.34	0.42	0.26	0.49	0.49
K ₂ O	9.92	9.79	10.80	10.49	10.00	9.62
Cr ₂ O ₃	0.03	0.02	0.09	0.00	0.05	0.00
Cl	0.01	0.02	0.00	0.00	0.00	0.03
P ₂ O ₅	0.16	0.00	0.07	0.01	0.02	0.12
BaO	0.03	0.00	0.00	0.02	0.00	0.00
F	4.41	4.22	3.98	3.54	2.78	2.49
Total	97.80	97.34	98.44	97.25	97.66	96.64
Si	6.29	6.26	6.51	6.49	6.22	6.13
Ti	0.16	0.15	0.06	0.07	0.11	0.14
Al Total	4.42	4.39	4.87	4.86	4.39	4.28
Al IV	1.71	1.74	1.49	1.51	1.78	1.87
Al VI	2.70	2.65	3.38	3.35	2.61	2.41
Fe	2.29	2.48	1.17	1.18	2.11	2.31
Mn	0.06	0.04	0.02	0.03	0.04	0.05
Mg	0.09	0.10	0.18	0.17	0.21	0.23
Ca	0.01	0.00	0.01	0.01	0.01	0.01
Na	0.14	0.11	0.12	0.08	0.14	0.15
K	2.01	1.99	2.03	1.98	1.94	1.89
Cr	0.00	0.00	0.01	0.00	0.01	0.00
Cl	0.00	0.01	0.00	0.00	0.00	0.01
P	0.02	0.00	0.01	0.00	0.00	0.02
Ba	0.00	0.00	0.00	0.00	0.00	0.00
F	2.21	2.13	1.86	1.65	1.33	1.21
OH	1.79	1.86	2.14	2.35	2.67	2.78
Tet	8.00	8.00	8.00	8.00	8.00	8.00
Oct	5.31	5.41	4.81	4.80	5.09	5.14
Dodec	2.18	2.10	2.17	2.06	2.09	2.05
Estimated Li content	2.77	2.83	0.85	1.21	0.63	0.48

Microprobe data for micas from the Lake Lewis Leucogranite.

Sample Analysis	LL99-7 7-2c	LL99-7 7-2r	LL99-7 7-2rb	LL99-7 7-3c	LL99-7 7-3r	LL99-7 7-3r	LL99-7 7-2rc
Mineral	protolithionite	protolithionite	Li phengite	Li phengite	Li phengite	Li phengite	protolithionite
Location	core	rim	rim	core	rim	rim	rim
SiO ₂	40.00	39.39	43.30	44.46	44.66	44.92	39.92
TiO ₂	1.41	1.04	1.50	0.47	0.41	0.35	1.03
Al ₂ O ₃	23.03	23.13	28.38	27.68	29.29	30.58	23.51
FeO	17.69	18.60	9.53	10.12	6.58	5.86	16.78
MnO	0.49	0.47	0.13	0.27	0.03	0.15	0.38
MgO	0.80	0.81	0.61	0.87	0.82	0.76	0.68
CaO	0.00	0.01	0.05	0.00	0.00	0.03	0.00
Na ₂ O	0.56	0.43	0.42	0.44	0.57	0.60	0.57
K ₂ O	9.74	9.99	10.30	10.52	10.50	10.61	9.68
Cr ₂ O ₃	0.00	0.00	0.03	0.00	0.02	0.00	0.00
Cl	0.00	0.04	0.02	0.00	0.00	0.02	0.00
P ₂ O ₅	0.04	0.07	0.09	0.13	0.02	0.18	0.05
BaO	0.00	0.06	0.00	0.17	0.05	0.07	0.05
F	2.47	2.38	1.61	2.18	1.76	1.58	2.51
Total	96.22	96.43	95.97	97.31	94.71	95.72	95.15
Si	6.19	6.12	6.24	6.41	6.42	6.34	6.22
Ti	0.16	0.12	0.16	0.05	0.04	0.04	0.12
Al Total	4.20	4.24	4.82	4.70	4.96	5.09	4.32
Al IV	1.81	1.88	1.76	1.59	1.58	1.66	1.78
Al VI	2.39	2.36	3.06	3.11	3.38	3.43	2.54
Fe	2.29	2.42	1.15	1.22	0.79	0.69	2.19
Mn	0.06	0.06	0.02	0.03	0.00	0.02	0.05
Mg	0.18	0.19	0.13	0.19	0.18	0.16	0.16
Ca	0.00	0.00	0.01	0.00	0.00	0.00	0.00
Na	0.17	0.13	0.12	0.12	0.16	0.16	0.17
K	1.92	1.98	1.89	1.94	1.93	1.91	1.92
Cr	0.00	0.00	0.00	0.00	0.00	0.00	0.00
Cl	0.00	0.01	0.00	0.00	0.00	0.00	0.00
P	0.01	0.01	0.01	0.02	0.00	0.02	0.01
Ba	0.00	0.00	0.00	0.01	0.00	0.00	0.00
F	1.21	1.17	0.74	0.99	0.80	0.70	1.24
OH	2.79	2.82	3.26	3.01	3.20	3.29	2.76
Tet	8.00	8.00	8.00	8.00	8.00	8.00	8.00
Oct	5.09	5.15	4.52	4.60	4.40	4.34	5.05
Dodec	2.10	2.12	2.03	2.09	2.09	2.10	2.11
Estimated Li content	2.72	0.68	0.52	2.21	2.81	0.58	0.65

Microprobe data for micas from the Lake Lewis Leucogranite.

Sample	LL99-7	LL99-7	LL99-7	LL99-7	LL99-7	LL99-7	LL99-7	LL99-7
Analysis	7-4r	7-4c	7-4rb	7-2rc	7-5c	7-5r	7-6c	
Mineral	Li phengite	Li phengite	protolithionite	protolithionite	Li phengite	Li phengite	Li phengite	
Location	rim	core	rim	rim	core	rim	core	
SiO ₂	45.64	45.14	40.54	39.94	45.96	45.81	46.75	
TiO ₂	0.59	0.48	1.02	0.96	0.57	0.62	0.36	
Al ₂ O ₃	28.83	30.62	24.33	22.62	30.02	29.76	30.88	
FeO	7.56	6.55	15.86	17.48	6.81	6.99	5.84	
MnO	0.12	0.05	0.31	0.35	0.12	0.13	0.11	
MgO	0.77	0.30	0.82	0.65	0.54	0.73	0.27	
CaO	0.00	0.00	0.00	0.02	0.00	0.02	0.08	
Na ₂ O	0.46	0.36	0.31	0.35	0.52	0.42	0.35	
K ₂ O	10.58	10.63	9.81	9.49	10.54	10.65	10.95	
Cr ₂ O ₃	0.12	0.02	0.00	0.04	0.00	0.06	0.03	
Cl	0.04	0.01	0.05	0.02	0.01	0.05	0.00	
P ₂ O ₅	0.11	0.03	0.16	0.08	0.05	0.05	0.09	
BaO	0.07	0.05	0.12	0.15	0.09	0.00	0.00	
F	1.71	1.52	2.25	2.46	1.63	1.78	1.28	
Total	96.62	95.78	95.57	94.61	96.87	97.05	96.98	
Si	6.45	6.37	6.21	6.28	6.43	6.43	6.44	
Ti	0.06	0.05	0.12	0.11	0.06	0.07	0.04	
Al Total	4.80	5.09	4.39	4.19	4.95	4.92	5.02	
Al IV	1.55	1.63	1.79	1.72	1.57	1.57	1.56	
Al VI	3.26	3.46	2.59	2.47	3.38	3.35	3.46	
Fe	0.89	0.77	2.03	2.30	0.80	0.82	0.67	
Mn	0.01	0.01	0.04	0.05	0.01	0.02	0.01	
Mg	0.16	0.06	0.19	0.15	0.11	0.15	0.06	
Ca	0.00	0.00	0.00	0.00	0.00	0.00	0.01	
Na	0.13	0.10	0.09	0.11	0.14	0.11	0.09	
K	1.91	1.91	1.91	1.90	1.88	1.91	1.93	
Cr	0.01	0.00	0.00	0.00	0.00	0.01	0.00	
Cl	0.01	0.00	0.01	0.00	0.00	0.01	0.00	
P	0.01	0.00	0.02	0.01	0.01	0.01	0.01	
Ba	0.00	0.00	0.01	0.01	0.00	0.00	0.00	
F	0.76	0.68	1.09	1.22	0.72	0.79	0.56	
OH	3.23	3.32	2.90	2.78	3.28	3.20	3.44	
Tet	8.00	8.00	8.00	8.00	8.00	8.00	8.00	
Oct	4.39	4.35	4.97	5.08	4.36	4.41	4.25	
Dodec	2.07	2.02	2.03	2.04	2.03	2.03	2.03	
Estimated Li content	0.38	3.28	3.14	3.25	0.64	0.58	0.70	

Microprobe data for micas from the Lake Lewis Leucogranite.

Sample	LL99-7	LL99-7	LL99-7	LL99-7	LL99-7	LL99-7	LL99-7
Analysis	7b-c	7b-1c	7b-1r	7un-1	7un-2	7un-3	7un-4
Mineral	protolithionite	protolithionite	protolithionite	Li phengite	Li phengite	Li phengite	Li phengite
Location	core	core	rim	rim	core	core	core
SiO ₂	37.81	38.32	38.30	45.95	46.24	45.71	46.46
TiO ₂	1.22	1.19	1.29	0.56	0.33	0.23	0.33
Al ₂ O ₃	22.93	23.16	23.62	31.02	32.07	31.10	32.80
FeO	22.37	22.37	22.14	6.98	5.77	6.68	5.37
MnO	0.37	0.31	0.39	0.09	0.06	0.20	0.14
MgO	1.02	1.03	1.09	0.79	0.64	0.74	0.70
CaO	0.03	0.04	0.00	0.02	0.07	0.01	0.00
Na ₂ O	0.49	0.42	0.50	0.50	0.61	0.69	0.85
K ₂ O	9.58	9.59	9.85	10.68	10.41	10.03	10.33
Cr ₂ O ₃	0.00	0.00	0.04	0.00	0.05	0.00	0.00
Cl	0.03	0.05	0.00	0.03	0.01	0.01	0.00
P ₂ O ₅	0.14	0.05	0.00	0.00	0.05	0.11	0.03
BaO	0.23	0.24	0.12	0.00	0.21	0.12	0.09
F	2.30	2.25	2.38	1.82	2.01	2.05	1.92
Total	98.53	99.03	99.72	98.43	98.53	97.70	99.04
Si	5.86	5.89	5.86	6.35	6.36	6.38	6.33
Ti	0.14	0.14	0.15	0.06	0.03	0.02	0.03
Al Total	4.19	4.20	4.26	5.06	5.20	5.11	5.26
Al IV	2.14	2.11	2.14	1.65	1.64	1.62	1.67
Al VI	2.05	2.09	2.11	3.41	3.56	3.49	3.59
Fe	2.90	2.88	2.83	0.81	0.66	0.78	0.61
Mn	0.05	0.04	0.05	0.01	0.01	0.02	0.02
Mg	0.24	0.24	0.25	0.16	0.13	0.15	0.14
Ca	0.01	0.01	0.00	0.00	0.01	0.00	0.00
Na	0.15	0.13	0.15	0.14	0.16	0.19	0.22
K	1.90	1.88	1.92	1.88	1.83	1.78	1.79
Cr	0.00	0.00	0.00	0.00	0.01	0.00	0.00
Cl	0.01	0.01	0.00	0.01	0.00	0.00	0.00
P	0.02	0.01	0.00	0.00	0.01	0.01	0.00
Ba	0.01	0.01	0.01	0.00	0.01	0.01	0.00
F	1.13	1.09	1.15	0.79	0.88	0.90	0.83
OH	2.86	2.89	2.85	3.20	3.12	3.09	3.17
Tet	8.00	8.00	8.00	8.00	8.00	8.00	8.00
Oct	5.39	5.39	5.39	4.45	4.41	4.47	4.40
Dodec	2.07	2.03	2.08	2.02	2.01	1.99	2.03
Estimated Li content	0.51	0.46	0.95	0.44	0.54	1.40	0.21

Microprobe data for micas from the Lake Lewis Leucogranite.

Sample Analysis	LL99-7 7un-5	LL99-7 7un-6	LL99-7 7un-7	LL99-8 II8-1	LL99-8 II8-2	LL99-8 II8-3	LL99-8 II8-4	LL99-8 II8-5
Mineral	Li phengite	muscovite	Li phengite	Li phengite				
Location	rim	rim	core	core	rim	core	rim	core
SiO ₂	46.50	45.61	46.55	46.26	45.78	45.69	45.75	45.65
TiO ₂	0.33	0.42	0.36	0.21	0.08	0.19	0.19	0.28
Al ₂ O ₃	32.66	29.58	32.93	32.84	29.49	33.57	30.87	32.31
FeO	5.24	8.37	5.05	3.82	7.11	3.05	5.63	4.33
MnO	0.11	0.21	0.04	0.04	0.04	0.11	0.07	0.10
MgO	0.69	0.85	0.77	0.41	0.45	0.00	0.00	0.23
CaO	0.00	0.11	0.00	0.00	0.01	0.03	0.03	0.05
Na ₂ O	0.82	0.47	0.86	0.85	0.64	0.98	0.46	0.68
K ₂ O	10.36	10.34	10.22	10.15	10.34	10.15	10.65	10.35
Cr ₂ O ₃	0.00	0.04	0.06	0.02	0.04	0.00	0.00	0.00
Cl	0.00	0.00	0.00	0.00	0.00	0.03	0.01	0.01
P ₂ O ₅	0.13	0.05	0.11	0.00	0.16	0.00	0.06	0.10
BaO	0.00	0.00	0.05	0.00	0.01	0.00	0.00	0.00
F	1.76	2.17	1.81	2.72	3.58	1.34	1.53	2.72
Total	98.60	98.20	98.82	97.31	97.73	95.15	95.26	96.82
Si	6.33	6.41	6.32	6.45	6.61	6.32	6.45	6.43
Ti	0.03	0.04	0.04	0.02	0.01	0.02	0.02	0.03
Al Total	5.24	4.90	5.27	5.40	5.02	5.48	5.13	5.37
Al IV	1.67	1.59	1.68	1.55	1.39	1.68	1.55	1.57
Al VI	3.57	3.32	3.59	3.85	3.62	3.80	3.58	3.80
Fe	0.60	0.98	0.57	0.45	0.86	0.35	0.66	0.51
Mn	0.01	0.02	0.01	0.00	0.00	0.01	0.01	0.01
Mg	0.14	0.18	0.16	0.08	0.10	0.00	0.00	0.05
Ca	0.00	0.02	0.00	0.00	0.00	0.00	0.00	0.01
Na	0.22	0.13	0.23	0.23	0.18	0.26	0.13	0.18
K	1.80	1.85	1.77	1.81	1.90	1.79	1.91	1.86
Cr	0.00	0.00	0.01	0.00	0.00	0.00	0.00	0.00
Cl	0.00	0.00	0.00	0.00	0.00	0.01	0.00	0.00
P	0.01	0.01	0.01	0.00	0.02	0.00	0.01	0.01
Ba	0.00	0.00	0.00	0.00	0.00	0.00	0.00	0.00
F	0.76	0.97	0.78	1.20	1.63	0.59	0.68	1.21
OH	3.24	3.03	3.22	2.80	2.37	3.41	3.31	2.79
Tet	8.00	8.00	8.00	8.00	8.00	8.00	8.00	8.00
Oct	4.35	4.56	4.36	4.41	4.59	4.19	4.27	4.41
Dodec	2.03	1.99	2.02	2.04	2.11	2.06	2.05	2.06
Estimated Li content	0.45	0.62	0.77	4.43	4.58	2.19	4.76	4.51

Microprobe data for micas from the Lake Lewis Leucogranite.

Sample	LL99-8	LL99-9	LL99-9	LL99-9	LL99-9	LL99-9	LL99-9	LL99-9
Analysis	II8-6	9-1c	9-1r	9-2c	9-2r	9-3c	9-3r	9-4c
Mineral	Li phengite	zinnwaldite	zinnwaldite	zinnwaldite	phengite	zinnwaldite	zinnwaldite	zinnwaldite
Location	rim	core	rim	core	rim	core	rim	core
SiO ₂	45.49	46.73	47.88	46.56	49.49	46.68	46.97	48.03
TiO ₂	0.24	0.25	0.43	0.44	0.34	0.36	0.18	0.17
Al ₂ O ₃	31.21	20.98	21.17	22.26	21.09	22.03	21.72	21.64
FeO	4.93	11.17	11.43	12.30	8.56	12.11	11.71	11.65
MnO	0.11	0.47	0.31	0.35	0.23	0.56	0.33	0.42
MgO	0.16	0.24	0.16	0.16	0.19	0.15	0.12	0.21
CaO	0.02	0.00	0.00	0.00	0.00	0.00	0.00	0.05
Na ₂ O	0.84	0.59	0.52	0.33	0.32	0.51	0.48	0.43
K ₂ O	10.38	10.01	10.05	10.27	11.25	10.05	10.18	10.22
Cr ₂ O ₃	0.00	0.00	0.00	0.00	0.04	0.04	0.00	0.04
Cl	0.00	0.00	0.01	0.00	0.06	0.02	0.00	0.00
P ₂ O ₅	0.13	0.16	0.00	0.06	0.10	0.10	0.07	0.09
BaO	0.00	0.00	0.00	0.00	0.00	0.00	0.11	0.03
F	2.87	6.01	6.04	5.83	4.24	6.12	5.95	6.03
Total	96.39	96.63	98.00	98.55	95.89	98.72	97.83	99.02
Si	6.49	7.40	7.46	7.23	7.49	7.28	7.35	7.41
Ti	0.03	0.03	0.05	0.05	0.04	0.04	0.02	0.02
Al Total	5.25	3.92	3.89	4.07	3.76	4.05	4.01	3.93
Al IV	1.51	0.60	0.54	0.77	0.51	0.72	0.65	0.59
Al VI	3.74	3.32	3.34	3.30	3.25	3.32	3.36	3.34
Fe	0.59	1.48	1.49	1.60	1.08	1.58	1.53	1.50
Mn	0.01	0.06	0.04	0.05	0.03	0.07	0.04	0.06
Mg	0.03	0.06	0.04	0.04	0.04	0.04	0.03	0.05
Ca	0.00	0.00	0.00	0.00	0.00	0.00	0.00	0.01
Na	0.23	0.18	0.16	0.10	0.09	0.15	0.14	0.13
K	1.89	2.02	2.00	2.03	2.17	2.00	2.03	2.01
Cr	0.00	0.00	0.00	0.00	0.01	0.00	0.00	0.00
Cl	0.00	0.00	0.00	0.00	0.02	0.01	0.00	0.00
P	0.02	0.02	0.00	0.01	0.01	0.01	0.01	0.01
Ba	0.00	0.00	0.00	0.00	0.00	0.00	0.01	0.00
F	1.30	3.01	2.97	2.86	2.03	3.01	2.95	2.94
OH	2.70	0.99	1.02	1.14	1.96	0.98	1.05	1.06
Tet	8.00	8.00	8.00	8.00	8.00	8.00	8.00	8.00
Oct	4.41	4.95	4.96	5.03	4.44	5.05	4.98	4.97
Dodec	2.14	2.23	2.15	2.14	2.28	2.17	2.19	2.16
Estimated Li content	4.41	4.67	4.47	4.85	4.39	0.90	0.79	0.29

Microprobe data for micas from the Lake Lewis Leucogranite.

Sample	LL99-9	LL99-9	LL99-9	LL99-9	LL99-9	LL99-11	LL99-11
Analysis	9-4r	9-5c	9-5r	9-6c	9-6r	11-1c	11-1r
Mineral	zinnwaldite	zinnwaldite	zinnwaldite	zinnwaldite	zinnwaldite	Li phengite	Li phengite
Location	rim	core	rim	core	rim	core	rim
SiO ₂	46.11	45.27	46.36	46.67	48.66	45.71	45.96
TiO ₂	0.42	0.26	0.30	0.29	0.13	0.40	0.34
Al ₂ O ₃	22.54	21.90	21.45	21.55	21.23	30.31	30.63
FeO	11.94	12.24	11.19	12.03	10.98	6.57	6.81
MnO	0.48	0.57	0.36	0.51	0.17	0.16	0.11
MgO	0.25	0.21	0.16	0.18	0.25	0.50	0.59
CaO	0.00	0.06	0.01	0.00	0.04	0.00	0.04
Na ₂ O	0.41	0.49	0.43	0.33	0.34	0.43	0.47
K ₂ O	10.18	9.90	9.99	10.17	10.28	10.63	10.80
Cr ₂ O ₃	0.03	0.03	0.06	0.00	0.07	0.00	0.00
Cl	0.01	0.01	0.00	0.01	0.00	0.01	0.00
P ₂ O ₅	0.04	0.06	0.00	0.00	0.06	0.09	0.13
BaO	0.03	0.08	0.00	0.05	0.06	0.05	0.00
F	5.51	5.73	5.96	6.16	6.30	2.56	2.23
Total	97.95	96.82	96.26	97.94	98.57	97.41	98.12
Si	7.16	7.18	7.37	7.35	7.54	6.47	6.42
Ti	0.05	0.03	0.04	0.03	0.01	0.04	0.04
Al Total	4.12	4.10	4.02	4.00	3.88	5.06	5.05
Al IV	0.84	0.82	0.63	0.65	0.46	1.53	1.58
Al VI	3.28	3.28	3.39	3.35	3.42	3.53	3.47
Fe	1.55	1.62	1.49	1.58	1.42	0.78	0.80
Mn	0.06	0.08	0.05	0.07	0.02	0.02	0.01
Mg	0.06	0.05	0.04	0.04	0.06	0.11	0.12
Ca	0.00	0.01	0.00	0.00	0.01	0.00	0.01
Na	0.12	0.15	0.13	0.10	0.10	0.12	0.13
K	2.02	2.00	2.03	2.04	2.03	1.92	1.92
Cr	0.00	0.00	0.01	0.00	0.01	0.00	0.00
Cl	0.00	0.00	0.00	0.00	0.00	0.00	0.00
P	0.01	0.01	0.00	0.00	0.01	0.01	0.02
Ba	0.00	0.01	0.00	0.00	0.00	0.00	0.00
F	2.70	2.88	3.00	3.07	3.09	1.15	0.99
OH	1.29	1.12	1.00	0.93	0.91	2.85	3.01
Tet	8.00	8.00	8.00	8.00	8.00	8.00	8.00
Oct	5.00	5.07	4.99	5.08	4.94	4.48	4.44
Dodec	2.15	2.17	2.17	2.15	2.16	2.05	2.07
Estimated Li content	0.81	0.30	0.36	0.69	0.78	1.03	0.71

Microprobe data for micas from the Lake Lewis Leucogranite.

Sample Analysis	LL99-11 11-2c	LL99-11 11-2r	LL99-11 11-3c	LL99-11 11-3r	LL99-11 11-4c	LL99-11 11-4r	LL99-11 11-5c	LL99-11 11-5r
Mineral	muscovite	Li phengite	muscovite	muscovite	Li phengite	Li phengite	Li phengite	Li phengite
Location	core	rim	core	rim	core	rim	core	rim
SiO ₂	46.25	45.82	45.96	46.39	46.35	45.74	45.65	45.34
TiO ₂	0.13	0.36	0.08	0.17	0.09	0.21	0.57	0.61
Al ₂ O ₃	34.85	30.40	34.51	33.13	31.56	30.94	31.31	29.56
FeO	3.11	6.74	3.06	4.05	5.79	6.08	6.41	7.73
MnO	0.07	0.31	0.15	0.04	0.11	0.10	0.08	0.16
MgO	0.45	0.44	0.33	0.50	0.55	0.40	0.43	0.42
CaO	0.00	0.00	0.00	0.06	0.00	0.00	0.00	0.03
Na ₂ O	1.06	0.43	0.96	0.53	0.56	0.53	0.47	0.30
K ₂ O	10.34	10.58	10.26	10.68	10.48	10.54	10.79	10.67
Cr ₂ O ₃	0.00	0.05	0.01	0.00	0.02	0.06	0.03	0.00
Cl	0.00	0.00	0.04	0.04	0.01	0.00	0.01	0.01
P ₂ O ₅	0.09	0.00	0.13	0.05	0.13	0.02	0.05	0.05
BaO	0.21	0.06	0.21	0.00	0.08	0.24	0.01	0.00
F	1.97	2.28	1.98	1.81	2.35	2.44	2.68	2.48
Total	98.53	97.48	97.68	97.45	98.08	97.30	98.48	97.35
Si	6.26	6.46	6.28	6.36	6.45	6.46	6.40	6.46
Ti	0.01	0.04	0.01	0.02	0.01	0.02	0.06	0.06
Al Total	5.56	5.05	5.56	5.36	5.17	5.15	5.18	4.96
Al IV	1.74	1.54	1.72	1.64	1.55	1.54	1.60	1.54
Al VI	3.83	3.50	3.84	3.72	3.62	3.60	3.58	3.43
Fe	0.35	0.79	0.35	0.46	0.67	0.72	0.75	0.92
Mn	0.01	0.04	0.02	0.00	0.01	0.01	0.01	0.02
Mg	0.09	0.09	0.07	0.10	0.11	0.08	0.09	0.09
Ca	0.00	0.00	0.00	0.01	0.00	0.00	0.00	0.01
Na	0.28	0.12	0.26	0.14	0.15	0.15	0.13	0.08
K	1.79	1.90	1.79	1.87	1.86	1.90	1.93	1.94
Cr	0.00	0.01	0.00	0.00	0.00	0.01	0.00	0.00
Cl	0.00	0.00	0.01	0.01	0.00	0.00	0.00	0.00
P	0.01	0.00	0.02	0.01	0.02	0.00	0.01	0.01
Ba	0.01	0.00	0.01	0.00	0.00	0.01	0.00	0.00
F	0.84	1.02	0.86	0.78	1.03	1.09	1.19	1.12
OH	3.16	2.98	3.14	3.20	2.96	2.91	2.81	2.88
Tet	8.00	8.00	8.00	8.00	8.00	8.00	8.00	8.00
Oct	4.29	4.47	4.29	4.32	4.43	4.44	4.49	4.53
Dodec	2.09	2.03	2.07	2.02	2.03	2.07	2.07	2.03
Estimated Li content	0.70	1.19	1.22	1.75	1.54	0.90	1.22	0.96

Microprobe data for micas from the Lake Lewis Leucogranite.

Sample	LL99-11	LL99-11	LL99-12	LL99-12	LL99-12	LL99-12	LL99-12
Analysis	11-6c	11-6r	12-1c	12-1r	12-2c	12-2r	12-3c
Mineral	Li phengite						
Location	core	rim	core	rim	core	rim	core
SiO ₂	45.17	45.66	45.20	44.64	43.72	44.32	45.79
TiO ₂	0.33	0.43	0.55	0.46	0.49	0.58	0.11
Al ₂ O ₃	31.31	30.83	28.96	27.79	27.69	28.08	31.27
FeO	6.07	6.14	8.38	8.70	9.53	9.33	6.83
MnO	0.15	0.21	0.10	0.06	0.19	0.08	0.02
MgO	0.42	0.40	0.25	0.41	0.36	0.37	0.32
CaO	0.00	0.00	0.00	0.02	0.02	0.00	0.00
Na ₂ O	0.63	0.41	0.35	0.29	0.28	0.35	0.61
K ₂ O	10.50	10.48	10.82	10.14	10.25	10.36	10.55
Cr ₂ O ₃	0.00	0.00	0.00	0.12	0.00	0.00	0.13
Cl	0.00	0.00	0.00	0.01	0.00	0.02	0.00
P ₂ O ₅	0.14	0.09	0.00	0.16	0.05	0.02	0.04
BaO	0.00	0.00	0.02	0.15	0.01	0.09	0.06
F	2.22	2.18	2.60	2.50	3.12	2.90	2.54
Total	96.93	96.84	97.24	95.44	95.72	96.50	98.27
Si	6.37	6.43	6.50	6.53	6.51	6.50	6.42
Ti	0.03	0.05	0.06	0.05	0.05	0.06	0.01
Al Total	5.20	5.12	4.91	4.79	4.86	4.85	5.17
Al IV	1.63	1.57	1.50	1.47	1.49	1.50	1.58
Al VI	3.57	3.55	3.40	3.32	3.36	3.35	3.59
Fe	0.72	0.72	1.01	1.06	1.19	1.14	0.80
Mn	0.02	0.03	0.01	0.01	0.02	0.01	0.00
Mg	0.09	0.08	0.05	0.09	0.08	0.08	0.07
Ca	0.00	0.00	0.00	0.00	0.00	0.00	0.00
Na	0.17	0.11	0.10	0.08	0.08	0.10	0.17
K	1.89	1.88	1.99	1.89	1.95	1.94	1.89
Cr	0.00	0.00	0.00	0.01	0.00	0.00	0.01
Cl	0.00	0.00	0.00	0.00	0.00	0.01	0.00
P	0.02	0.01	0.00	0.02	0.01	0.00	0.00
Ba	0.00	0.00	0.00	0.01	0.00	0.01	0.00
F	0.99	0.97	1.18	1.15	1.47	1.35	1.12
OH	3.01	3.03	2.82	2.84	2.53	2.65	2.88
Tet	8.00	8.00	8.00	8.00	8.00	8.00	8.00
Oct	4.42	4.43	4.54	4.54	4.71	4.65	4.48
Dodec	2.08	2.01	2.08	2.02	2.04	2.05	2.08
Estimated Li content	1.17	0.46	0.20	0.25	0.27	0.26	0.93

Microprobe data for micas from the Lake Lewis Leucogranite.

Sample Analysis	LL99-12 12-3r	LL99-12 12-4c	LL99-12 12-4r	LLL2 III2-6	LLL2 III2-7	LLL3 III3a-4	LLL3 III3a-5	LLL3 III3a-6
Mineral	Li phengite	Li phengite	Li phengite	Li phengite	Li phengite	muscovite	muscovite	muscovite
Location	rim	core	rim			core	core	core
SiO ₂	45.29	44.95	44.69	51.74	51.56	49.00	46.19	45.61
TiO ₂	0.36	0.10	0.35	0.02	0.00	0.09	0.20	0.35
Al ₂ O ₃	28.74	29.56	29.07	26.15	26.70	32.79	34.70	34.38
FeO	8.46	7.41	8.49	3.52	2.81	2.47	2.74	3.07
MnO	0.20	0.16	0.04	0.00	0.00	0.02	0.17	0.00
MgO	0.45	0.34	0.40	2.40	2.20	1.07	0.47	0.48
CaO	0.00	0.03	0.03	0.11	0.07	0.09	0.03	0.00
Na ₂ O	0.37	0.40	0.45	0.09	0.05	0.36	0.44	0.41
K ₂ O	10.40	10.28	10.44	9.71	9.68	7.59	9.26	9.73
Cr ₂ O ₃	0.00	0.04	0.06	0.13	0.00	0.08	0.05	0.02
Cl	0.00	0.03	0.00	0.02	0.00	0.05	0.00	0.00
P ₂ O ₅	0.00	0.07	0.09	0.09	0.12	0.14	0.10	0.12
BaO	0.06	0.00	0.10	0.00	0.26	0.00	0.00	0.03
F	2.63	2.36	2.52	2.55	2.39	1.65	1.90	1.74
Total	96.96	95.74	96.72	96.52	95.85	95.40	96.25	95.93
Si	6.53	6.48	6.45	7.16	7.14	6.62	6.32	6.27
Ti	0.04	0.01	0.04	0.00	0.00	0.01	0.02	0.04
Al Total	4.88	5.02	4.94	4.27	4.36	5.22	5.59	5.57
Al IV	1.47	1.52	1.55	0.84	0.86	1.38	1.68	1.73
Al VI	3.40	3.51	3.39	3.43	3.50	3.84	3.92	3.85
Fe	1.02	0.89	1.02	0.41	0.33	0.28	0.31	0.35
Mn	0.02	0.02	0.00	0.00	0.00	0.00	0.02	0.00
Mg	0.10	0.07	0.09	0.50	0.45	0.22	0.10	0.10
Ca	0.00	0.00	0.00	0.02	0.01	0.01	0.00	0.00
Na	0.10	0.11	0.13	0.02	0.01	0.09	0.12	0.11
K	1.91	1.89	1.92	1.71	1.71	1.31	1.62	1.71
Cr	0.00	0.00	0.01	0.01	0.00	0.01	0.01	0.00
Cl	0.00	0.01	0.00	0.01	0.00	0.01	0.00	0.00
P	0.00	0.01	0.01	0.01	0.01	0.02	0.01	0.01
Ba	0.00	0.00	0.01	0.00	0.01	0.00	0.00	0.00
F	1.20	1.08	1.15	1.12	1.05	0.70	0.82	0.76
OH	2.80	2.92	2.85	2.88	2.95	3.28	3.18	3.24
Tet	8.00	8.00	8.00	8.00	8.00	8.00	8.00	8.00
Oct	4.59	4.51	4.55	4.35	4.29	4.36	4.37	4.34
Dodec	2.02	2.02	2.07	1.76	1.75	1.43	1.75	1.83
Estimated Li content	0.07	1.21	1.21	2.30	1.68	0.35	0.30	0.18

Microprobe data for micas from the Lake Lewis Leucogranite.

Sample Analysis	LLL3 III3a-7	LLL3 III3a-9	LLL3 III3a-10	LLL3 III3a-11	LLL3 III3a-12	LLL3 III3a-14	LLL3 III3a-16	LLL3 III3a-17	LLL3 III3a-18
Mineral	muscovite	phengite	phengite	phengite	phengite	phengite	phengite	phengite	muscovite
Location	rim	rim	rim	core	rim	rim	rim	rim	core
SiO ₂	46.37	51.75	51.88	52.59	51.73	52.27	51.60	50.42	47.05
TiO ₂	0.26	0.08	0.06	0.13	0.21	0.10	0.25	0.54	0.80
Al ₂ O ₃	34.66	26.06	28.75	26.06	25.51	27.81	23.60	25.55	32.45
FeO	2.85	4.90	2.71	5.26	5.29	3.58	7.30	6.44	3.63
MnO	0.03	0.00	0.06	0.11	0.01	0.02	0.02	0.07	0.13
MgO	0.71	1.21	2.22	1.10	1.42	2.17	1.10	1.09	0.63
CaO	0.00	0.11	0.03	0.03	0.00	0.08	0.03	0.16	0.02
Na ₂ O	0.58	0.09	0.03	0.00	0.00	0.09	0.00	0.00	0.25
K ₂ O	8.99	8.70	7.97	8.67	9.26	7.83	9.05	9.34	8.97
Cr ₂ O ₃	0.11	0.03	0.00	0.00	0.00	0.03	0.00	0.08	0.03
Cl	0.00	0.01	0.01	0.04	0.00	0.02	0.02	0.03	0.01
P ₂ O ₅	0.05	0.12	0.07	0.15	0.02	0.04	0.07	0.05	0.11
BaO	0.13	0.03	0.09	0.00	0.00	0.07	0.00	0.00	0.16
F	1.82	3.59	0.58	4.38	4.27	0.93	5.56	4.72	2.04
Total	96.56	96.67	94.46	98.53	97.71	95.04	98.61	98.51	96.28
Si	6.31	7.30	6.93	7.39	7.36	7.01	7.56	7.26	6.48
Ti	0.03	0.01	0.01	0.01	0.02	0.01	0.03	0.06	0.08
Al Total	5.56	4.33	4.53	4.32	4.28	4.40	4.07	4.34	5.26
Al IV	1.69	0.70	1.07	0.61	0.64	0.99	0.44	0.74	1.52
Al VI	3.87	3.63	3.46	3.71	3.64	3.41	3.63	3.60	3.74
Fe	0.33	0.58	0.30	0.62	0.63	0.40	0.89	0.78	0.42
Mn	0.00	0.00	0.01	0.01	0.00	0.00	0.00	0.01	0.01
Mg	0.14	0.25	0.44	0.23	0.30	0.43	0.24	0.23	0.13
Ca	0.00	0.02	0.00	0.00	0.00	0.01	0.01	0.02	0.00
Na	0.15	0.03	0.01	0.00	0.00	0.02	0.00	0.00	0.07
K	1.56	1.57	1.36	1.56	1.68	1.34	1.69	1.72	1.58
Cr	0.01	0.00	0.00	0.00	0.00	0.00	0.00	0.01	0.00
Cl	0.00	0.00	0.00	0.01	0.00	0.01	0.00	0.01	0.00
P	0.01	0.01	0.01	0.02	0.00	0.00	0.01	0.01	0.01
Ba	0.01	0.00	0.00	0.00	0.00	0.00	0.00	0.00	0.01
F	0.78	1.60	0.24	1.95	1.92	0.39	2.58	2.15	0.89
OH	3.22	2.40	3.75	2.04	2.08	3.60	1.42	1.84	3.11
Tet	8.00	8.00	8.00	8.00	8.00	8.00	8.00	8.00	8.00
Oct	4.37	4.49	4.22	4.59	4.59	4.27	4.80	4.70	4.39
Dodec	1.74	1.61	1.38	1.57	1.68	1.37	1.70	1.73	1.67
Estimated Li content	0.21	0.21	0.22	0.19	1.22	0.14	0.15	2.20	0.82

Microprobe data for micas from the Lake Lewis Leucogranite.

Sample	LLL3	LLL3						
Analysis	III3a-19	III3a-20	III3a-1	III3d-1	III3e-1	III3e-2	I3b-1	I3b-2
Mineral	muscovite	phengite						
Location	core	core	rim	core	core	rim	rim	rim
SiO ₂	47.38	46.42	44.12	43.94	44.39	44.25	45.74	50.72
TiO ₂	0.50	0.46	0.04	0.13	0.05	0.15	0.18	0.14
Al ₂ O ₃	32.51	33.46	33.98	34.18	33.75	33.90	33.18	23.71
FeO	3.71	3.11	2.58	2.86	2.91	2.88	3.30	6.03
MnO	0.17	0.02	0.00	0.00	0.13	0.00	0.16	0.06
MgO	0.65	0.47	0.59	0.46	0.37	0.41	0.35	0.71
CaO	0.04	0.00	0.04	0.00	0.05	0.04	0.03	0.00
Na ₂ O	0.33	0.38	0.66	0.68	0.51	0.63	0.61	0.11
K ₂ O	8.45	9.17	10.33	10.45	10.34	10.42	10.16	10.38
Cr ₂ O ₃	0.00	0.07	0.00	0.18	0.00	0.03	0.11	0.00
Cl	0.01	0.00	0.00	0.01	0.00	0.03	0.00	0.01
P ₂ O ₅	0.15	0.06	0.22	0.12	0.06	0.00	0.06	0.00
BaO	0.00	0.00	0.11	0.02	0.09	0.00	0.00	0.00
F	1.88	1.91	1.33	1.48	1.43	1.46	1.17	3.57
Total	95.78	95.53	94.01	94.51	94.08	94.19	95.06	95.43
Si	6.50	6.41	6.18	6.16	6.23	6.21	6.32	7.40
Ti	0.05	0.05	0.00	0.01	0.01	0.02	0.02	0.02
Al Total	5.26	5.44	5.61	5.64	5.59	5.61	5.40	4.08
Al IV	1.50	1.59	1.82	1.84	1.77	1.79	1.68	0.60
Al VI	3.76	3.85	3.79	3.80	3.82	3.82	3.72	3.48
Fe	0.43	0.36	0.30	0.33	0.34	0.34	0.38	0.74
Mn	0.02	0.00	0.00	0.00	0.02	0.00	0.02	0.01
Mg	0.13	0.10	0.12	0.10	0.08	0.09	0.07	0.15
Ca	0.01	0.00	0.01	0.00	0.01	0.01	0.00	0.00
Na	0.09	0.10	0.18	0.19	0.14	0.17	0.16	0.03
K	1.48	1.61	1.85	1.87	1.85	1.87	1.79	1.93
Cr	0.00	0.01	0.00	0.02	0.00	0.00	0.01	0.00
Cl	0.00	0.00	0.00	0.00	0.00	0.01	0.00	0.00
P	0.02	0.01	0.03	0.01	0.01	0.00	0.01	0.00
Ba	0.00	0.00	0.01	0.00	0.00	0.00	0.00	0.00
F	0.82	0.83	0.59	0.65	0.63	0.65	0.51	1.65
OH	3.18	3.17	3.41	3.34	3.37	3.34	3.49	2.35
Tet	8.00	8.00	8.00	8.00	8.00	8.00	8.00	8.00
Oct	4.40	4.35	4.22	4.24	4.27	4.27	4.21	4.39
Dodec	1.59	1.73	2.06	2.09	2.00	2.04	1.97	1.96
Estimated Li content	0.52	0.60	0.23	0.16	3.17	0.00	0.22	0.48

Microprobe data for micas from the Lake Lewis Leucogranite.

Sample Analysis	LLL3 I3b-3	LLL3 I3b-5	LLL3 I3b-6	LLL3 I3b-7	LLL3 I3b-11	LLL3 I3b-15	LLL3 I3b-16	LLL3 I3b-17	LLL3 I3c-1
Mineral Location	phengite rim	muscovite rim	phengite rim	phengite core	phengite rim	phengite rim	Li phengite core	muscovite core	zinnwaldite core
SiO ₂	48.20	45.83	46.94	47.48	49.35	45.46	45.83	46.49	46.38
TiO ₂	0.27	0.55	0.15	0.94	0.37	2.84	0.71	0.31	0.30
Al ₂ O ₃	29.76	32.96	24.35	26.37	25.84	26.83	30.91	31.38	21.18
FeO	3.56	3.23	9.31	7.12	5.39	6.64	4.71	3.90	11.91
MnO	0.06	0.10	0.08	0.00	0.11	0.00	0.19	0.10	0.00
MgO	0.86	0.18	0.41	0.35	0.67	0.28	0.27	0.22	0.75
CaO	0.20	0.07	0.06	0.00	0.13	0.09	0.02	0.04	0.03
Na ₂ O	0.23	0.48	0.31	0.04	0.24	0.26	0.44	0.41	0.24
K ₂ O	10.32	10.60	10.48	10.53	10.25	10.25	10.23	10.15	10.25
Cr ₂ O ₃	0.00	0.07	0.08	0.00	0.00	0.06	0.00	0.02	0.00
Cl	0.00	0.00	0.00	0.00	0.01	0.00	0.00	0.01	0.00
P ₂ O ₅	0.12	0.05	0.00	0.12	0.05	0.00	0.00	0.08	0.05
BaO	0.00	0.01	0.00	0.07	0.00	0.00	0.00	0.07	0.00
F	0.80	0.94	3.96	2.11	1.82	1.64	0.94	0.82	4.20
Total	94.38	95.06	96.13	95.13	94.22	94.34	94.26	93.99	95.29
Si	6.64	6.31	7.05	6.82	7.02	6.54	6.41	6.46	7.19
Ti	0.03	0.06	0.02	0.10	0.04	0.31	0.08	0.03	0.03
Al Total	4.83	5.35	4.31	4.46	4.33	4.55	5.09	5.14	3.87
Al IV	1.36	1.69	0.95	1.18	0.98	1.46	1.59	1.54	0.81
Al VI	3.47	3.66	3.36	3.28	3.35	3.09	3.50	3.59	3.05
Fe	0.41	0.37	1.17	0.85	0.64	0.80	0.55	0.45	1.54
Mn	0.01	0.01	0.01	0.00	0.01	0.00	0.02	0.01	0.00
Mg	0.18	0.04	0.09	0.07	0.14	0.06	0.06	0.04	0.17
Ca	0.03	0.01	0.01	0.00	0.02	0.01	0.00	0.01	0.01
Na	0.06	0.13	0.09	0.01	0.07	0.07	0.12	0.11	0.07
K	1.81	1.86	2.01	1.93	1.86	1.88	1.82	1.80	2.03
Cr	0.00	0.01	0.01	0.00	0.00	0.01	0.00	0.00	0.00
Cl	0.00	0.00	0.00	0.00	0.00	0.00	0.00	0.00	0.00
P	0.01	0.01	0.00	0.02	0.01	0.00	0.00	0.01	0.01
Ba	0.00	0.00	0.00	0.00	0.00	0.00	0.00	0.00	0.00
F	0.35	0.41	1.88	0.96	0.82	0.75	0.42	0.36	2.06
OH	3.65	3.59	2.12	3.04	3.18	3.25	3.58	3.64	1.94
Tet	8.00	8.00	8.00	8.00	8.00	8.00	8.00	8.00	8.00
Oct	4.12	4.14	4.66	4.31	4.21	4.27	4.21	4.14	4.81
Dodec	1.89	2.00	2.11	1.96	1.93	1.96	1.94	1.92	2.11
Estimated Li content	0.44	0.42	0.00	0.00	0.99	0.14	0.38	0.14	0.92

Microprobe data for micas from the Lake Lewis Leucogranite.

Sample Analysis	LLL3 I3c-2	LLL3 I3c-3	LLL3 I3c-7	LLL3 I3c-8	LLL3 I3c-9	LLL3 I3c-10	LLL3 I3c-11	LLL3 I3d-1	LLL3 I3d-2
Mineral	phengite	phengite	phengite	phengite	phengite	phengite	phengite	phengite	phengite
Location	core	core	core	core	core	core	core	rim	core
SiO ₂	50.88	50.47	50.47	50.35	50.56	50.41	50.07	45.37	50.83
TiO ₂	0.58	0.17	0.60	0.03	0.81	0.04	0.21	1.56	0.00
Al ₂ O ₃	26.54	25.79	24.16	24.76	24.13	28.24	28.39	25.00	27.80
FeO	4.26	4.92	5.82	5.87	5.51	3.38	3.58	8.56	3.08
MnO	0.00	0.11	0.01	0.10	0.13	0.00	0.15	0.10	0.03
MgO	1.32	1.15	1.05	1.10	1.17	1.15	1.18	0.65	1.45
CaO	0.12	0.00	0.10	0.07	0.03	0.11	0.10	0.00	0.06
Na ₂ O	0.09	0.20	0.15	0.09	0.07	0.09	0.13	0.19	0.09
K ₂ O	10.15	10.34	10.30	10.57	10.48	10.54	10.33	10.43	10.39
Cr ₂ O ₃	0.13	0.00	0.00	0.00	0.00	0.01	0.00	0.06	0.00
Cl	0.00	0.03	0.02	0.00	0.03	0.00	0.00	0.00	0.00
P ₂ O ₅	0.02	0.05	0.06	0.02	0.00	0.16	0.03	0.05	0.06
BaO	0.12	0.18	0.06	0.00	0.00	0.00	0.00	0.07	0.13
F	0.00	0.88	1.56	1.44	1.45	0.00	0.00	2.01	0.91
Total	94.20	94.29	94.35	94.41	94.37	94.12	94.17	94.05	94.83
Si	6.91	7.02	7.14	7.11	7.13	6.82	6.78	6.68	6.94
Ti	0.06	0.02	0.06	0.00	0.09	0.00	0.02	0.17	0.00
Al Total	4.25	4.23	4.03	4.12	4.01	4.50	4.53	4.34	4.47
Al IV	1.09	0.98	0.86	0.89	0.87	1.18	1.22	1.32	1.06
Al VI	3.16	3.24	3.17	3.23	3.15	3.32	3.31	3.02	3.42
Fe	0.48	0.57	0.69	0.69	0.65	0.38	0.41	1.05	0.35
Mn	0.00	0.01	0.00	0.01	0.02	0.00	0.02	0.01	0.00
Mg	0.27	0.24	0.22	0.23	0.25	0.23	0.24	0.14	0.29
Ca	0.02	0.00	0.02	0.01	0.00	0.02	0.01	0.00	0.01
Na	0.02	0.05	0.04	0.03	0.02	0.02	0.04	0.05	0.02
K	1.76	1.83	1.86	1.90	1.89	1.82	1.78	1.96	1.81
Cr	0.01	0.00	0.00	0.00	0.00	0.00	0.00	0.01	0.00
Cl	0.00	0.01	0.01	0.00	0.01	0.00	0.00	0.00	0.00
P	0.00	0.01	0.01	0.00	0.00	0.02	0.00	0.01	0.01
Ba	0.01	0.01	0.00	0.00	0.00	0.00	0.00	0.00	0.01
F	0.00	0.39	0.70	0.64	0.65	0.00	0.00	0.94	0.39
OH	4.00	3.60	3.30	3.36	3.35	4.00	4.00	3.06	3.61
Tet	8.00	8.00	8.00	8.00	8.00	8.00	8.00	8.00	8.00
Oct	3.99	4.08	4.16	4.18	4.15	3.96	4.01	4.41	4.08
Dodec	1.80	1.90	1.91	1.93	1.91	1.86	1.82	2.03	1.85
Estimated Li content	0.09	0.06	0.29	4.78	5.01	4.46	1.64	3.38	0.96

Microprobe data for micas from the Lake Lewis Leucogranite.

Sample Analysis	LLL3 I3d-3	LLL3 I3d-5	LLL3 I3d-7	LLL3 I3d-9	LLL3 I3d-10	LLL3 I3d-12	SC-20W 20w-1	SC-20W 20w-2
Mineral Location	phengite rim	Li phengite core	phengite core	muscovite core	muscovite core	phengite core	siderophyllite core	siderophyllite core
SiO ₂	50.34	46.73	47.72	46.03	45.85	50.32	35.62	35.79
TiO ₂	0.90	0.18	0.19	0.41	0.42	0.14	0.13	0.14
Al ₂ O ₃	25.87	30.97	26.51	32.29	32.84	27.06	23.00	23.17
FeO	4.51	4.15	6.89	3.44	3.06	4.13	25.15	24.82
MnO	0.00	0.23	0.02	0.05	0.12	0.00	0.40	0.53
MgO	1.08	0.71	0.38	0.26	0.25	0.49	0.16	0.14
CaO	0.02	0.00	0.03	0.00	0.00	0.13	0.00	0.00
Na ₂ O	0.16	0.36	0.19	0.45	0.49	0.05	0.50	0.51
K ₂ O	10.25	10.67	10.59	10.73	10.63	10.23	9.85	9.91
Cr ₂ O ₃	0.07	0.09	0.00	0.00	0.02	0.06	0.06	0.00
Cl	0.00	0.03	0.03	0.04	0.03	0.02	0.10	0.05
P ₂ O ₅	0.08	0.03	0.07	0.00	0.00	0.04	0.17	0.11
BaO	0.00	0.00	0.04	0.20	0.11	0.00	0.00	0.04
F	1.61	0.69	2.42	0.51	0.39	1.37	2.76	2.94
Total	94.88	94.84	95.07	94.41	94.21	94.03	97.91	98.17
Si	7.03	6.45	6.90	6.35	6.30	7.03	5.74	5.77
Ti	0.09	0.02	0.02	0.04	0.04	0.01	0.02	0.02
Al Total	4.26	5.04	4.52	5.25	5.32	4.45	4.37	4.40
Al IV	0.97	1.55	1.10	1.65	1.70	0.97	2.26	2.23
Al VI	3.29	3.49	3.41	3.59	3.62	3.48	2.11	2.17
Fe	0.53	0.48	0.83	0.40	0.35	0.48	3.39	3.34
Mn	0.00	0.03	0.00	0.01	0.01	0.00	0.05	0.07
Mg	0.23	0.15	0.08	0.05	0.05	0.10	0.04	0.03
Ca	0.00	0.00	0.00	0.00	0.00	0.02	0.00	0.00
Na	0.04	0.10	0.05	0.12	0.13	0.01	0.16	0.16
K	1.83	1.88	1.95	1.89	1.86	1.82	2.03	2.04
Cr	0.01	0.01	0.00	0.00	0.00	0.01	0.01	0.00
Cl	0.00	0.01	0.01	0.01	0.01	0.00	0.03	0.01
P	0.01	0.00	0.01	0.00	0.00	0.00	0.02	0.01
Ba	0.00	0.00	0.00	0.01	0.01	0.00	0.00	0.00
F	0.71	0.30	1.11	0.22	0.17	0.61	1.41	1.50
OH	3.29	3.69	2.89	3.77	3.83	3.39	2.56	2.49
Tet	8.00	8.00	8.00	8.00	8.00	8.00	8.00	8.00
Oct	4.13	4.16	4.35	4.09	4.08	4.10	5.61	5.63
Dodec	1.89	1.99	2.02	2.02	2.00	1.85	2.21	2.22
Estimated Li content	0.35	0.62	0.34	4.63	4.52	0.66	0.52	0.47

Microprobe data for micas from the Lake Lewis Leucogranite.

Sample Analysis	SC-20W 20w-3	SC-20W 20w-4	SC-20W 20w-5	SC-20W 20w-6	SC-20W 20w-7	SC-20W 20w-8	SC-20W 20w-9
Mineral	siderophyllite	protolithionite	protolithionite	phengite	muscovite	Li phengite	muscovite
Location	core	rim	rim	rim	rim	core	core
SiO ₂	35.84	39.52	36.57	47.79	44.77	45.24	44.50
TiO ₂	0.12	0.00	0.05	0.20	0.00	0.03	0.06
Al ₂ O ₃	23.15	24.25	23.03	27.26	33.83	32.08	33.73
FeO	24.43	19.08	23.90	7.99	4.22	5.72	4.44
MnO	0.67	0.41	0.37	0.04	0.12	0.10	0.16
MgO	0.17	0.58	0.17	0.22	0.00	0.05	0.01
CaO	0.00	0.06	0.00	0.00	0.00	0.00	0.05
Na ₂ O	0.57	0.33	0.30	0.05	0.66	0.50	0.60
K ₂ O	9.93	9.65	10.07	11.30	10.72	10.86	10.78
Cr ₂ O ₃	0.00	0.00	0.11	0.08	0.00	0.00	0.00
Cl	0.06	0.06	0.06	0.01	0.00	0.02	0.03
P ₂ O ₅	0.24	0.05	0.01	0.08	0.12	0.00	0.00
BaO	0.00	0.01	0.05	0.00	0.00	0.00	0.00
F	2.68	1.38	2.11	2.26	1.60	2.09	1.48
Total	97.85	95.38	96.80	97.27	96.03	96.68	95.84
Si	5.75	6.06	5.83	6.78	6.23	6.37	6.21
Ti	0.01	0.00	0.01	0.02	0.00	0.00	0.01
Al Total	4.38	4.38	4.33	4.56	5.55	5.32	5.55
Al IV	2.25	1.94	2.17	1.22	1.77	1.63	1.79
Al VI	2.13	2.44	2.16	3.34	3.77	3.69	3.75
Fe	3.28	2.45	3.19	0.95	0.49	0.67	0.52
Mn	0.09	0.05	0.05	0.01	0.01	0.01	0.02
Mg	0.04	0.13	0.04	0.05	0.00	0.01	0.00
Ca	0.00	0.01	0.00	0.00	0.00	0.00	0.01
Na	0.18	0.10	0.09	0.01	0.18	0.14	0.16
K	2.03	1.89	2.05	2.05	1.90	1.95	1.92
Cr	0.00	0.00	0.01	0.01	0.00	0.00	0.00
Cl	0.02	0.02	0.02	0.00	0.00	0.00	0.01
P	0.03	0.01	0.00	0.01	0.01	0.00	0.00
Ba	0.00	0.00	0.00	0.00	0.00	0.00	0.00
F	1.36	0.67	1.06	1.01	0.71	0.93	0.65
OH	2.63	3.32	2.92	2.98	3.29	3.07	3.34
Tet	8.00	8.00	8.00	8.00	8.00	8.00	8.00
Oct	5.55	5.08	5.44	4.36	4.28	4.39	4.30
Dodec	2.24	1.99	2.16	2.08	2.09	2.09	2.08
Estimated Li content	0.51	4.99	2.79	4.78	4.12	4.14	0.44

Microprobe data for micas from the Lake Lewis Leucogranite.

Sample	SC-20W	SC-20W	SC-20W	SC-20W	SC-20W	SC-20W	SC-20W
Analysis	20wb-1	20wb-2	20wb-6	20wb-7	20wb-8	20wb-9	20wb-10
Mineral	siderophyllite	siderophyllite	Li phengite	muscovite	muscovite	muscovite	muscovite
Location	core	core	rim	core	core	core	core
SiO ₂	35.36	35.40	45.04	44.59	44.29	45.09	44.93
TiO ₂	0.00	0.02	0.05	0.00	0.05	0.00	0.08
Al ₂ O ₃	23.04	23.42	31.52	33.24	33.63	33.82	33.25
FeO	24.23	24.91	5.57	4.80	4.65	4.21	4.58
MnO	0.46	0.50	0.08	0.08	0.00	0.07	0.13
MgO	0.06	0.14	0.23	0.07	0.04	0.01	0.03
CaO	0.02	0.01	0.00	0.06	0.00	0.00	0.02
Na ₂ O	0.50	0.59	0.43	0.62	0.82	0.73	0.80
K ₂ O	9.58	9.86	10.72	10.99	10.55	10.56	10.47
Cr ₂ O ₃	0.03	0.06	0.05	0.10	0.12	0.06	0.00
Cl	0.06	0.04	0.04	0.00	0.01	0.01	0.00
P ₂ O ₅	0.00	0.14	0.01	0.04	0.03	0.00	0.00
BaO	0.00	0.16	0.00	0.00	0.00	0.15	0.00
F	2.70	2.64	2.22	1.92	2.11	2.14	2.15
Total	96.05	97.88	95.96	96.52	96.30	96.87	96.44
Si	5.78	5.69	6.40	6.25	6.23	6.29	6.30
Ti	0.00	0.00	0.01	0.00	0.01	0.00	0.01
Al Total	4.44	4.44	5.28	5.49	5.57	5.56	5.50
Al IV	2.22	2.31	1.60	1.75	1.77	1.71	1.70
Al VI	2.22	2.13	3.69	3.74	3.80	3.85	3.80
Fe	3.31	3.35	0.66	0.56	0.55	0.49	0.54
Mn	0.06	0.07	0.01	0.01	0.00	0.01	0.02
Mg	0.01	0.03	0.05	0.01	0.01	0.00	0.01
Ca	0.00	0.00	0.00	0.01	0.00	0.00	0.00
Na	0.16	0.18	0.12	0.17	0.22	0.20	0.22
K	2.00	2.02	1.94	1.97	1.89	1.88	1.87
Cr	0.00	0.01	0.01	0.01	0.01	0.01	0.00
Cl	0.02	0.01	0.01	0.00	0.00	0.00	0.00
P	0.00	0.02	0.00	0.01	0.00	0.00	0.00
Ba	0.00	0.01	0.00	0.00	0.00	0.01	0.00
F	1.40	1.35	1.00	0.85	0.94	0.95	0.95
OH	2.58	2.64	2.99	3.15	3.06	3.05	3.05
Tet	8.00	8.00	8.00	8.00	8.00	8.00	8.00
Oct	5.62	5.59	4.41	4.34	4.36	4.35	4.37
Dodec	2.16	2.25	2.07	2.15	2.13	2.09	2.09
Estimated Li content	0.60	0.44	0.43	0.44	0.33	0.48	0.37

Microprobe data for micas from the Lake Lewis Leucogranite.

Sample Analysis	SC-20W 20wc-1	SC-20W 20wc-2	SC-20W 20wc-3	SC-20W 20wc-4	SC-20W 20wc-5	SC-20W 20wc-7	SC-20W 20wc-9
Mineral	siderophyllite	protolithionite	siderophyllite	protolithionite	protolithionite	muscovite	Li phengite
Location	core	core	core	rim	rim	rim	core
SiO ₂	35.41	36.62	35.72	36.09	36.83	44.71	44.67
TiO ₂	0.00	0.00	0.04	0.06	0.08	0.00	0.15
Al ₂ O ₃	23.26	22.92	22.83	23.21	23.70	33.49	32.42
FeO	24.58	24.08	25.46	23.99	22.96	4.55	5.40
MnO	0.45	0.47	0.48	0.53	0.35	0.20	0.08
MgO	0.08	0.20	0.08	0.11	0.18	0.05	0.05
CaO	0.04	0.07	0.00	0.00	0.07	0.00	0.00
Na ₂ O	0.46	0.38	0.28	0.36	0.40	0.73	0.52
K ₂ O	9.71	9.28	9.78	9.93	9.26	10.74	10.93
Cr ₂ O ₃	0.00	0.02	0.00	0.00	0.08	0.00	0.00
Cl	0.06	0.06	0.07	0.04	0.10	0.02	0.01
P ₂ O ₅	0.00	0.00	0.14	0.15	0.07	0.00	0.02
BaO	0.13	0.08	0.00	0.00	0.00	0.04	0.00
F	2.89	1.73	2.73	2.52	2.68	1.88	2.10
Total	97.09	95.91	97.62	96.99	96.75	96.40	96.35
Si	5.77	5.83	5.77	5.80	5.88	6.25	6.31
Ti	0.00	0.00	0.01	0.01	0.01	0.00	0.02
Al Total	4.46	4.30	4.35	4.39	4.46	5.52	5.40
Al IV	2.23	2.17	2.23	2.20	2.12	1.75	1.69
Al VI	2.23	2.13	2.12	2.19	2.34	3.78	3.71
Fe	3.35	3.21	3.44	3.22	3.07	0.53	0.64
Mn	0.06	0.06	0.07	0.07	0.05	0.02	0.01
Mg	0.02	0.05	0.02	0.03	0.04	0.01	0.01
Ca	0.01	0.01	0.00	0.00	0.01	0.00	0.00
Na	0.15	0.12	0.09	0.11	0.13	0.20	0.14
K	2.02	1.88	2.02	2.04	1.89	1.92	1.97
Cr	0.00	0.00	0.00	0.00	0.01	0.00	0.00
Cl	0.02	0.02	0.02	0.01	0.03	0.00	0.00
P	0.00	0.00	0.02	0.02	0.01	0.00	0.00
Ba	0.01	0.00	0.00	0.00	0.00	0.00	0.00
F	1.49	0.87	1.39	1.28	1.35	0.83	0.94
OH	2.49	3.11	2.59	2.71	2.62	3.16	3.06
Tet	8.00	8.00	8.00	8.00	8.00	8.00	8.00
Oct	5.67	5.46	5.66	5.52	5.52	4.34	4.38
Dodec	2.17	2.01	2.12	2.17	2.03	2.12	2.12
Estimated Li content	0.41	0.00	0.00	0.00	0.00	0.00	0.00

Microprobe data for micas from the Lake Lewis Leucogranite.

Appendix B

Microprobe data for plagioclase and K-feldspar from the Lake Lewis Leucogranite

Samples:

LL99-1

LL99-2

LL99-3

LL99-4

LL99-5

LL99-6

LL99-7

LL99-8

LL99-9

LL99-9

LL99-11

LL99-12

Microprobe data for feldspars from the Lake Lewis Leucogranite.

Sample	LL99-1							
Analysis	1k-1c	1k-1r	1k10c	1k10r	1k11c	1k11r	1k9c	1k9r
Location	core	rim	core	rim	core	rim	core	rim
Mineral	K-feldspar							
SiO ₂	64.12	64.58	65.47	63.76	63.73	63.26	63.57	62.23
TiO ₂	0.05	0.01	0.05	0.00	0.00	0.01	0.06	0.00
Al ₂ O ₃	18.84	19.00	18.29	18.82	18.77	18.47	18.20	20.75
FeO	0.00	0.00	0.00	0.00	0.00	0.02	0.00	0.70
MnO	0.03	0.03	0.17	0.05	0.03	0.10	0.03	0.00
MgO	0.02	0.00	0.02	0.06	0.00	0.05	0.00	0.32
BaO	0.00	0.00	0.03	0.00	0.01	0.01	0.00	0.00
CaO	0.05	0.00	0.00	0.02	0.00	0.09	0.00	0.01
Na ₂ O	0.62	1.49	0.12	0.69	0.32	0.88	0.40	0.20
K ₂ O	16.44	15.18	15.75	15.53	15.90	15.05	16.55	14.67
Total	100.17	100.29	99.90	98.93	98.76	97.94	98.81	98.88
Si	11.87	11.88	12.06	11.90	11.92	11.91	11.94	11.59
Al	4.11	4.12	3.97	4.14	4.13	4.10	4.03	4.55
Ti	0.01	0.00	0.01	0.00	0.00	0.00	0.01	0.00
Fe ₂	0.00	0.00	0.00	0.00	0.00	0.00	0.00	0.11
Mn	0.01	0.01	0.03	0.01	0.01	0.02	0.01	0.00
Mg	0.01	0.00	0.01	0.02	0.00	0.01	0.00	0.09
Ba	0.00	0.00	0.00	0.00	0.00	0.00	0.00	0.00
Ca	0.01	0.00	0.00	0.00	0.00	0.02	0.00	0.00
Na	0.22	0.53	0.04	0.25	0.12	0.32	0.15	0.07
K	3.88	3.56	3.70	3.70	3.79	3.62	3.97	3.49
Ab	5.40	13.00	1.10	6.30	3.00	8.10	3.60	2.00
An	0.20	0.00	0.00	0.10	0.00	0.50	0.00	0.10
Or	94.30	87.00	98.90	93.60	97.00	91.40	96.40	97.90

Microprobe data for feldspars from the Lake Lewis Leucogranite.

Sample	LL99-1	LL99-1	LL99-1	LL99-1	LL99-1	LL99-1	LL99-11	LL99-11
Analysis	1p-2c	1p-2r	1p-3c	1p-5c	1p-7c	1p-7r	11k4c	11k4r
Location	core	rim	core	core	core	rim	core	rim
Mineral	plagioclase	plagioclase	plagioclase	plagioclase	plagioclase	plagioclase	K-feldspar	K-feldspar
SiO ₂	68.79	69.17	69.48	67.46	64.65	68.98	64.11	63.44
TiO ₂	0.00	0.00	0.00	0.08	0.00	0.00	0.09	0.02
Al ₂ O ₃	19.83	19.64	19.74	18.83	21.15	19.73	18.89	18.94
FeO	0.00	0.00	0.03	0.00	0.06	0.00	0.01	0.02
MnO	0.01	0.00	0.00	0.00	0.01	0.06	0.03	0.00
MgO	0.10	0.00	0.02	0.03	0.07	0.10	0.02	0.00
BaO	0.00	0.00	0.00	0.00	0.00	0.00	0.00	0.08
CaO	0.33	0.00	0.04	0.04	0.93	0.18	0.00	0.00
Na ₂ O	12.00	12.03	10.03	10.46	9.19	9.90	1.19	0.79
K ₂ O	0.16	0.02	0.15	0.17	1.27	0.15	15.41	15.89
Total	101.22	100.86	99.49	97.07	97.33	99.10	99.75	99.18
Si	11.91	11.98	12.10	12.08	11.65	12.07	11.87	11.85
Al	4.04	4.01	4.05	3.97	4.49	4.06	4.12	4.17
Ti	0.00	0.00	0.00	0.01	0.00	0.00	0.01	0.00
Fe ₂	0.00	0.00	0.00	0.00	0.01	0.00	0.00	0.00
Mn	0.00	0.00	0.00	0.00	0.00	0.01	0.01	0.00
Mg	0.03	0.00	0.01	0.01	0.02	0.03	0.01	0.00
Ba	0.00	0.00	0.00	0.00	0.00	0.00	0.00	0.01
Ca	0.06	0.00	0.01	0.01	0.18	0.03	0.00	0.00
Na	4.03	4.04	3.39	3.63	3.21	3.36	0.43	0.29
K	0.04	0.00	0.03	0.04	0.29	0.03	3.64	3.79
Ab	97.70	99.90	98.80	98.70	87.20	98.00	10.50	7.00
An	1.50	0.00	0.20	0.20	4.90	1.00	0.00	0.00
Or	0.80	0.10	1.00	1.10	7.90	1.00	89.50	93.00

Micropore data for feldspars from the Lake Lewis Leucogranite.

Sample	LL99-11	LL99-11	LL99-11	LL99-11	LL99-11	LL99-11	LL99-11	LL99-11
Analysis	11k5r	11k9c	11k9r	11p2c	11p2r	11p3c	11p3r	11p6c
Location	rim	core	rim	core	rim	core	rim	core
Mineral	K-feldspar	K-feldspar	K-feldspar	plagioclase	plagioclase	plagioclase	plagioclase	plagioclase
SiO ₂	62.05	63.55	64.30	67.42	67.92	67.60	67.02	68.56
TiO ₂	0.00	0.03	0.00	0.00	0.01	0.01	0.00	0.00
Al ₂ O ₃	21.09	18.71	18.59	19.99	19.66	19.73	20.41	19.93
FeO	0.07	0.22	0.00	0.02	0.00	0.00	0.04	0.09
MnO	0.00	0.00	0.00	0.00	0.06	0.00	0.00	0.02
MgO	0.20	0.09	0.00	0.09	0.03	0.00	0.07	0.03
BaO	0.08	0.00	0.00	0.00	0.00	0.07	0.12	0.00
CaO	0.12	0.00	0.00	0.00	0.01	0.24	0.23	0.05
Na ₂ O	0.23	1.54	0.87	11.33	11.39	11.68	11.52	9.46
K ₂ O	15.23	14.51	15.33	0.05	0.02	0.15	0.30	0.14
Total	99.07	98.65	99.09	98.90	99.10	99.48	99.71	98.28
Si	11.55	11.87	11.96	11.90	11.96	11.90	11.79	12.07
Al	4.63	4.12	4.07	4.15	4.08	4.09	4.23	4.13
Ti	0.00	0.00	0.00	0.00	0.00	0.00	0.00	0.00
Fe ₂	0.01	0.03	0.00	0.00	0.00	0.00	0.01	0.01
Mn	0.00	0.00	0.00	0.00	0.01	0.00	0.00	0.00
Mg	0.06	0.03	0.00	0.02	0.01	0.00	0.02	0.01
Ba	0.01	0.00	0.00	0.00	0.00	0.01	0.01	0.00
Ca	0.02	0.00	0.00	0.00	0.00	0.05	0.04	0.01
Na	0.08	0.56	0.31	3.88	3.89	3.99	3.93	3.23
K	3.62	3.46	3.64	0.01	0.00	0.03	0.07	0.03
Ab	2.20	13.90	7.90	99.70	99.80	98.10	97.30	98.80
An	0.60	0.00	0.00	0.00	0.10	1.10	1.10	0.30
Or	97.10	86.10	92.10	0.30	0.10	0.80	1.70	0.90

Microprobe data for feldspars from the Lake Lewis Leucogranite.

Sample	LL99-11	LL99-11	LL99-11	LL99-12	LL99-12	LL99-12	LL99-12	LL99-12
Analysis	11p6r	11p7c	11p7r	12k10c	12k10r	12k4c	12k5c	12k5r
Location	plagioclase rim	plagioclase core	plagioclase rim	K-feldspar core	K-feldspar rim	K-feldspar core	K-feldspar core	K-feldspar rim
Mineral								
SiO ₂	67.82	68.43	66.25	64.24	64.18	63.69	63.50	63.42
TiO ₂	0.00	0.08	0.00	0.11	0.11	0.00	0.13	0.01
Al ₂ O ₃	20.23	20.13	20.43	18.98	19.17	19.16	18.89	19.33
FeO	0.03	0.17	0.06	0.00	0.00	0.00	0.00	0.00
MnO	0.00	0.05	0.00	0.04	0.05	0.07	0.00	0.00
MgO	0.04	0.00	0.06	0.02	0.05	0.01	0.00	0.00
BaO	0.15	0.00	0.02	0.02	0.01	0.15	0.00	0.00
CaO	0.13	0.00	0.39	0.00	0.01	0.06	0.04	0.00
Na ₂ O	9.92	10.74	11.50	1.02	0.40	1.95	1.42	0.85
K ₂ O	0.19	0.17	0.15	15.33	15.64	13.26	15.12	15.76
Total	98.51	99.77	98.86	99.76	99.62	98.35	99.10	99.37
Si	11.96	11.95	11.75	11.88	11.88	11.86	11.84	11.81
Al	4.20	4.14	4.27	4.13	4.18	4.20	4.15	4.24
Ti	0.00	0.01	0.00	0.02	0.02	0.00	0.02	0.00
Fe ₂	0.00	0.03	0.01	0.00	0.00	0.00	0.00	0.00
Mn	0.00	0.01	0.00	0.01	0.01	0.01	0.00	0.00
Mg	0.01	0.00	0.02	0.01	0.01	0.00	0.00	0.00
Ba	0.01	0.00	0.00	0.00	0.00	0.01	0.00	0.00
Ca	0.03	0.00	0.07	0.00	0.00	0.01	0.01	0.00
Na	3.39	3.64	3.96	0.37	0.14	0.70	0.51	0.31
K	0.04	0.04	0.03	3.62	3.69	3.15	3.60	3.74
Ab	98.00	99.00	97.30	9.20	3.80	18.20	12.50	7.60
An	0.70	0.00	1.80	0.00	0.10	0.30	0.20	0.00
Or	1.20	1.00	0.80	90.80	96.20	81.50	87.30	92.40

Microprobe data for feldspars from the Lake Lewis Leucogranite.

Sample	LL99-12	LL99-12						
Analysis	12k6c	12k6r	12k8c	12k8r	12k9c	12k9r	12p11c	12p11r
Location	core	rim	core	rim	core	rim	core	rim
Mineral	K-feldspar	K-feldspar	K-feldspar	K-feldspar	K-feldspar	K-feldspar	plagioclase	plagioclase
SiO ₂	63.49	63.23	63.93	63.71	63.42	63.73	66.60	67.17
TiO ₂	0.00	0.02	0.12	0.03	0.00	0.00	0.01	0.00
Al ₂ O ₃	19.27	19.03	18.91	18.75	18.79	18.81	20.76	20.07
FeO	0.04	0.00	0.07	0.00	0.04	0.02	0.00	0.04
MnO	0.00	0.00	0.00	0.00	0.00	0.02	0.01	0.10
MgO	0.00	0.05	0.00	0.00	0.06	0.03	0.02	0.05
BaO	0.07	0.05	0.06	0.00	0.04	0.00	0.00	0.00
CaO	0.05	0.00	0.00	0.00	0.00	0.00	0.83	0.24
Na ₂ O	0.55	0.27	0.85	0.84	0.35	1.03	10.65	10.18
K ₂ O	14.60	15.88	15.09	15.37	16.52	15.51	0.07	0.09
Total	98.07	98.53	99.03	98.70	99.22	99.15	98.95	97.94
Si	11.88	11.86	11.89	11.91	11.86	11.88	11.76	11.93
Al	4.25	4.20	4.14	4.13	4.14	4.13	4.32	4.20
Ti	0.00	0.00	0.02	0.00	0.00	0.00	0.00	0.00
Fe ₂	0.01	0.00	0.01	0.00	0.01	0.00	0.00	0.01
Mn	0.00	0.00	0.00	0.00	0.00	0.00	0.00	0.02
Mg	0.00	0.01	0.00	0.00	0.02	0.01	0.01	0.01
Ba	0.01	0.00	0.00	0.00	0.00	0.00	0.00	0.00
Ca	0.01	0.00	0.00	0.00	0.00	0.00	0.16	0.05
Na	0.20	0.10	0.31	0.30	0.13	0.37	3.65	3.51
K	3.49	3.80	3.58	3.66	3.94	3.69	0.02	0.02
Ab	5.40	2.50	7.90	7.70	3.10	9.20	95.50	98.20
An	0.30	0.00	0.00	0.00	0.00	0.00	4.10	1.30
Or	94.30	97.50	92.10	92.30	96.90	90.80	0.40	0.60

Microprobe data for feldspars from the Lake Lewis Leucogranite.

Sample	LL99-12						
Analysis	12p1r	12p2c	12p2r	12p3c	12p6c	12p6r	12p7c
Location	rim	core	rim	core	core	rim	core
Mineral	plagioclase						
SiO ₂	67.59	68.30	68.04	67.89	66.68	67.47	66.55
TiO ₂	0.00	0.01	0.00	0.05	0.00	0.00	0.08
Al ₂ O ₃	19.86	19.89	20.42	19.80	20.30	19.40	19.96
FeO	0.01	0.00	0.00	0.03	0.01	0.00	0.02
MnO	0.04	0.00	0.00	0.00	0.00	0.00	0.01
MgO	0.00	0.07	0.00	0.03	0.09	0.00	0.01
BaO	0.00	0.04	0.03	0.02	0.00	0.00	0.00
CaO	0.02	0.00	0.06	0.03	0.66	0.00	0.20
Na ₂ O	10.42	10.83	10.50	11.81	10.63	11.41	10.26
K ₂ O	0.08	0.08	0.16	0.03	0.20	0.27	0.21
Total	98.02	99.22	99.21	99.69	98.57	98.55	97.30
Si	11.98	11.98	11.93	11.91	11.82	11.96	11.91
Al	4.15	4.11	4.22	4.09	4.24	4.05	4.21
Ti	0.00	0.00	0.00	0.01	0.00	0.00	0.01
Fe ₂	0.00	0.00	0.00	0.00	0.00	0.00	0.00
Mn	0.01	0.00	0.00	0.00	0.00	0.00	0.00
Mg	0.00	0.02	0.00	0.01	0.02	0.00	0.00
Ba	0.00	0.00	0.00	0.00	0.00	0.00	0.00
Ca	0.00	0.00	0.01	0.01	0.13	0.00	0.04
Na	3.58	3.68	3.57	4.02	3.65	3.92	3.56
K	0.02	0.02	0.04	0.01	0.05	0.06	0.05
Ab	99.40	99.50	98.70	99.70	95.60	98.50	97.60
An	0.10	0.00	0.30	0.10	3.30	0.00	1.00
Or	0.50	0.50	1.00	0.20	1.20	1.50	1.30

Microprobe data for feldspars from the Lake Lewis Leucogranite.

Sample	LL99-12	LL99-2						
Analysis	12p7r	2k3c	2k3r	2k4c	2k4r	2k6c	2k6r	2k8c
Location	rim	core	rim	core	rim	core	rim	core
Mineral	plagioclase	K-feldspar						
SiO ₂	67.24	64.35	64.42	64.69	64.81	64.33	64.65	64.33
TiO ₂	0.11	0.02	0.05	0.00	0.06	0.00	0.00	0.00
Al ₂ O ₃	20.09	18.26	18.10	18.37	18.32	18.60	18.38	18.86
FeO	0.03	0.06	0.08	0.07	0.07	0.04	0.00	0.00
MnO	0.06	0.00	0.03	0.07	0.00	0.00	0.00	0.09
MgO	0.10	0.06	0.11	0.00	0.01	0.00	0.03	0.00
BaO	0.00	0.00	0.00	0.00	0.00	0.00	0.13	0.00
CaO	0.13	0.01	0.00	0.02	0.02	0.12	0.02	0.01
Na ₂ O	11.21	0.35	0.34	0.18	0.32	1.06	0.33	0.19
K ₂ O	0.16	16.76	16.51	16.61	16.61	14.56	16.01	16.05
Total	99.13	99.87	99.64	100.01	100.22	98.71	99.55	99.53
Si	11.86	11.96	11.98	11.98	11.98	11.97	12.00	11.93
Al	4.17	4.00	3.97	4.01	3.99	4.08	4.02	4.12
Ti	0.02	0.00	0.01	0.00	0.01	0.00	0.00	0.00
Fe ₂	0.00	0.01	0.01	0.01	0.01	0.01	0.00	0.00
Mn	0.01	0.00	0.01	0.01	0.00	0.00	0.00	0.01
Mg	0.03	0.02	0.03	0.00	0.00	0.00	0.01	0.00
Ba	0.00	0.00	0.00	0.00	0.00	0.00	0.01	0.00
Ca	0.03	0.00	0.00	0.00	0.00	0.02	0.00	0.00
Na	3.83	0.13	0.12	0.07	0.12	0.38	0.12	0.07
K	0.04	3.97	3.92	3.93	3.92	3.46	3.79	3.80
Ab	98.40	3.10	3.00	1.60	2.80	9.90	3.00	1.80
An	0.60	0.00	0.00	0.10	0.10	0.60	0.10	0.10
Or	0.90	96.90	97.00	98.30	97.10	89.50	96.90	98.20

Microprobe data for feldspars from the Lake Lewis Leucogranite.

Sample	LL99-2	LL99-2	LL99-2	LL99-2	LL99-2	LL99-2	LL99-2
Analysis	2k8r	2p1c	2p1r	2p2c	2p2r	2p5c	2p5r
Location	rim	core	rim	core	rim	core	rim
Mineral	K-feldspar	plagioclase	plagioclase	plagioclase	plagioclase	plagioclase	plagioclase
SiO ₂	65.97	68.14	68.25	68.47	68.33	68.87	68.46
TiO ₂	0.00	0.00	0.02	0.00	0.03	0.00	0.00
Al ₂ O ₃	18.59	19.33	19.28	19.30	19.18	19.37	19.37
FeO	0.12	0.00	0.00	0.00	0.04	0.14	0.04
MnO	0.03	0.09	0.00	0.00	0.00	0.00	0.00
MgO	0.00	0.12	0.00	0.02	0.02	0.04	0.16
BaO	0.00	0.04	0.00	0.00	0.01	0.49	0.00
CaO	0.00	0.03	0.05	0.04	0.00	0.01	0.03
Na ₂ O	0.10	12.25	10.53	11.10	11.71	11.63	11.81
K ₂ O	16.57	0.10	0.17	0.11	0.05	0.05	0.10
Total	101.38	100.10	98.30	99.04	99.37	100.60	99.97
Si	12.02	11.94	12.07	12.04	12.01	12.00	11.97
Al	3.99	3.99	4.01	4.00	3.97	3.97	3.99
Ti	0.00	0.00	0.00	0.00	0.00	0.00	0.00
Fe ₂	0.02	0.00	0.00	0.00	0.01	0.02	0.01
Mn	0.01	0.01	0.00	0.00	0.00	0.00	0.00
Mg	0.00	0.03	0.00	0.01	0.01	0.01	0.04
Ba	0.00	0.00	0.00	0.00	0.00	0.03	0.00
Ca	0.00	0.01	0.01	0.01	0.00	0.00	0.01
Na	0.04	4.16	3.61	3.79	3.99	3.93	4.01
K	3.85	0.02	0.04	0.03	0.01	0.01	0.02
Ab	0.90	99.30	98.70	99.10	99.70	99.70	99.30
An	0.00	0.10	0.20	0.20	0.00	0.10	0.10
Or	99.10	0.50	1.00	0.70	0.30	0.30	0.50

Microprobe data for feldspars from the Lake Lewis Leucogranite.

Sample	LL99-2	LL99-2	LL99-3	LL99-3	LL99-3	LL99-3	LL99-3	LL99-3
Analysis	2p7c	2p7r	3k1c	3k1r	3k2c	3k2r	3k3c	3k3r
Location	core	rim	core	rim	core	rim	core	rim
Mineral	plagioclase	plagioclase	K-feldspar	K-feldspar	K-feldspar	K-feldspar	K-feldspar	K-feldspar
SiO ₂	68.44	68.51	64.99	64.20	63.54	63.82	63.84	64.22
TiO ₂	0.00	0.00	0.00	0.06	0.05	0.07	0.00	0.00
Al ₂ O ₃	19.44	19.38	18.84	18.52	18.74	18.65	18.95	18.58
FeO	0.00	0.00	0.01	0.05	0.01	0.01	0.05	0.08
MnO	0.00	0.02	0.00	0.00	0.04	0.02	0.00	0.00
MgO	0.03	0.05	0.00	0.01	0.04	0.00	0.05	0.00
BaO	0.00	0.00	0.02	0.35	0.00	0.06	0.00	0.30
CaO	0.02	0.03	0.00	0.00	0.00	0.00	0.00	0.01
Na ₂ O	11.44	10.87	0.10	0.30	0.37	0.34	0.36	0.48
K ₂ O	0.22	0.00	16.23	16.46	16.44	16.20	16.42	16.01
Total	99.59	98.86	100.19	99.95	99.23	99.17	99.67	99.68
Si	12.00	12.05	11.97	11.93	11.87	11.91	11.87	11.94
Al	4.01	4.01	4.09	4.05	4.12	4.10	4.15	4.07
Ti	0.00	0.00	0.00	0.01	0.01	0.01	0.00	0.00
Fe ₂	0.00	0.00	0.00	0.01	0.00	0.00	0.01	0.01
Mn	0.00	0.00	0.00	0.00	0.01	0.00	0.00	0.00
Mg	0.01	0.01	0.00	0.00	0.01	0.00	0.01	0.00
Ba	0.00	0.00	0.00	0.03	0.00	0.00	0.00	0.02
Ca	0.00	0.01	0.00	0.00	0.00	0.00	0.00	0.00
Na	3.89	3.71	0.04	0.11	0.13	0.12	0.13	0.17
K	0.05	0.00	3.81	3.90	3.92	3.86	3.89	3.80
Ab	98.70	99.80	0.90	2.70	3.30	3.10	3.20	4.40
An	0.10	0.20	0.00	0.00	0.00	0.00	0.00	0.10
Or	1.20	0.00	99.10	97.30	96.70	96.90	96.80	95.60

Microprobe data for feldspars from the Lake Lewis Leucogranite.

Sample	LL99-3	LL99-3	LL99-3	LL99-3	LL99-3	LL99-3	LL99-4	LL99-4
Analysis	3p4c	3p4r	3p5c	3p5r	3p6c	3p6r	4k-3c	4k-3r
Location	core	rim	core	rim	core	rim	core	rim
Mineral	plagioclase	plagioclase	plagioclase	plagioclase	plagioclase	plagioclase	K-feldspar	K-feldspar
SiO ₂	69.20	68.80	68.64	68.75	68.70	69.45	64.56	63.34
TiO ₂	0.00	0.02	0.00	0.05	0.00	0.06	0.05	0.00
Al ₂ O ₃	19.81	19.75	19.68	19.78	19.96	19.69	18.87	18.43
FeO	0.00	0.00	0.00	0.00	0.03	0.00	0.15	0.04
MnO	0.00	0.00	0.02	0.07	0.05	0.00	0.01	0.00
MgO	0.04	0.02	0.03	0.03	0.03	0.09	0.00	0.00
BaO	0.45	0.00	0.00	0.20	0.00	0.09	0.00	0.02
CaO	0.16	0.14	0.10	0.10	0.43	0.00	0.00	0.08
Na ₂ O	9.00	9.36	9.62	9.67	10.28	10.99	1.54	0.53
K ₂ O	0.09	0.05	0.09	0.26	0.14	0.05	15.27	16.27
Total	98.75	98.14	98.18	98.91	99.62	100.42	100.45	98.71
Si	12.13	12.11	12.09	12.06	11.99	12.04	11.88	11.90
Al	4.09	4.09	4.08	4.09	4.10	4.02	4.09	4.08
Ti	0.00	0.00	0.00	0.01	0.00	0.01	0.01	0.00
Fe ₂	0.00	0.00	0.00	0.00	0.00	0.00	0.02	0.01
Mn	0.00	0.00	0.00	0.01	0.01	0.00	0.00	0.00
Mg	0.01	0.01	0.01	0.01	0.01	0.02	0.00	0.00
Ba	0.03	0.00	0.00	0.01	0.00	0.01	0.00	0.00
Ca	0.03	0.03	0.02	0.02	0.08	0.00	0.00	0.02
Na	3.06	3.19	3.29	3.29	3.48	3.69	0.55	0.19
K	0.02	0.01	0.02	0.06	0.03	0.01	3.58	3.90
Ab	98.40	98.90	98.80	97.70	96.90	99.70	13.30	4.70
An	1.00	0.80	0.60	0.60	2.20	0.00	0.00	0.40
Or	0.60	0.30	0.60	1.70	0.90	0.30	86.70	94.90

Microprobe data for feldspars from the Lake Lewis Leucogranite.

Sample	LL99-4	LL99-4	LL99-4	LL99-4	LL99-4	LL99-4	LL99-4	LL99-4
Analysis	4k-4c	4k-4r	4k-6c	4k-6r	4p-1c	4p-2c	4p-2r	4p-5c
Location	core	rim	core	rim	core	core	rim	core
Mineral	K-feldspar	K-feldspar	K-feldspar	K-feldspar	plagioclase	plagioclase	plagioclase	plagioclase
SiO ₂	64.46	63.55	63.74	64.99	68.23	67.95	68.34	67.10
TiO ₂	0.00	0.04	0.05	0.00	0.00	0.08	0.02	0.00
Al ₂ O ₃	18.90	18.86	18.63	19.06	19.88	20.00	20.02	20.62
FeO	0.00	0.03	0.02	0.00	0.00	0.00	0.10	0.00
MnO	0.00	0.00	0.00	0.00	0.00	0.00	0.00	0.00
MgO	0.00	0.04	0.12	0.06	0.10	0.00	0.05	0.02
BaO	0.00	0.00	0.03	0.00	0.00	0.00	0.00	0.01
CaO	0.03	0.00	0.01	0.00	0.18	0.17	0.00	0.51
Na ₂ O	1.79	0.60	1.46	1.11	11.71	11.48	11.89	11.88
K ₂ O	14.95	16.68	15.18	15.63	0.16	0.12	0.22	0.22
Total	100.13	99.80	99.24	100.85	100.26	99.80	100.64	100.36
Si	11.88	11.84	11.87	11.90	11.90	11.90	11.89	11.74
Al	4.10	4.14	4.09	4.11	4.09	4.12	4.10	4.25
Ti	0.00	0.01	0.01	0.00	0.00	0.01	0.00	0.00
Fe ₂	0.00	0.01	0.00	0.00	0.00	0.00	0.02	0.00
Mn	0.00	0.00	0.00	0.00	0.00	0.00	0.00	0.00
Mg	0.00	0.01	0.03	0.02	0.03	0.00	0.01	0.01
Ba	0.00	0.00	0.00	0.00	0.00	0.00	0.00	0.00
Ca	0.01	0.00	0.00	0.00	0.03	0.03	0.00	0.10
Na	0.64	0.22	0.53	0.39	3.96	3.90	4.01	4.03
K	3.52	3.96	3.61	3.65	0.04	0.03	0.05	0.05
Ab	15.40	5.20	12.70	9.70	98.30	98.50	98.80	96.50
An	0.10	0.00	0.00	0.00	0.80	0.80	0.00	2.30
Or	84.50	94.80	87.20	90.30	0.90	0.70	1.20	1.20

Microprobe data for feldspars from the Lake Lewis Leucogranite.

Sample	LL99-4	LL99-4	LL99-5	LL99-5	LL99-5	LL99-5	LL99-5	LL99-5
Analysis	4p-7c	4p-7r	5k-5c	5k-5r	5k6c	5k6r	5k7c	5k7r
Location	core	rim	core	rim	core	rim	core	rim
Mineral	plagioclase	plagioclase	K-feldspar	K-feldspar	K-feldspar	K-feldspar	K-feldspar	K-feldspar
SiO ₂	68.06	69.21	64.55	64.12	62.90	63.10	63.94	63.93
TiO ₂	0.11	0.09	0.00	0.08	0.00	0.00	0.00	0.06
Al ₂ O ₃	20.00	19.70	18.82	18.89	18.64	18.65	18.75	18.81
FeO	0.00	0.09	0.00	0.07	0.00	0.00	0.02	0.01
MnO	0.02	0.00	0.00	0.00	0.00	0.07	0.00	0.00
MgO	0.08	0.02	0.00	0.00	0.00	0.04	0.09	0.00
BaO	0.01	0.00	0.01	0.00	0.00	0.00	0.00	0.01
CaO	0.19	0.00	0.00	0.00	0.00	0.00	0.00	0.00
Na ₂ O	11.57	11.27	1.14	0.49	0.53	0.80	1.63	1.22
K ₂ O	0.27	0.12	15.31	15.82	16.02	15.25	14.24	15.22
Total	100.31	100.50	99.83	99.47	98.09	97.91	98.67	99.26
Si	11.88	12.00	11.92	11.90	11.88	11.89	11.91	11.89
Al	4.11	4.02	4.09	4.13	4.14	4.14	4.11	4.12
Ti	0.01	0.01	0.00	0.01	0.00	0.00	0.00	0.01
Fe ₂	0.00	0.01	0.00	0.01	0.00	0.00	0.00	0.00
Mn	0.00	0.00	0.00	0.00	0.00	0.01	0.00	0.00
Mg	0.02	0.01	0.00	0.00	0.00	0.01	0.03	0.00
Ba	0.00	0.00	0.00	0.00	0.00	0.00	0.00	0.00
Ca	0.04	0.00	0.00	0.00	0.00	0.00	0.00	0.00
Na	3.92	3.79	0.41	0.18	0.19	0.29	0.59	0.44
K	0.06	0.03	3.61	3.75	3.86	3.67	3.38	3.61
Ab	97.60	99.30	10.20	4.50	4.80	7.40	14.80	10.90
An	0.90	0.00	0.00	0.00	0.00	0.00	0.00	0.00
Or	1.50	0.70	89.80	95.50	95.20	92.60	85.20	89.10

Microprobe data for feldspars from the Lake Lewis Leucogranite.

Sample	LL99-5	LL99-5	LL99-5	LL99-5	LL99-5	LL99-5	LL99-5	LL99-5
Analysis	5k9c	5k9r	5p-1c	5p-1r	5p-2c	5p-2r	5p8c	5p8r
Location	core	rim	core	rim	core	rim	core	rim
Mineral	K-feldspar	K-feldspar	plagioclase	plagioclase	plagioclase	plagioclase	plagioclase	plagioclase
SiO ₂	63.95	63.65	67.56	68.79	69.20	67.60	66.80	67.53
TiO ₂	0.00	0.00	0.01	0.00	0.05	0.05	0.00	0.00
Al ₂ O ₃	18.56	18.44	19.34	19.30	19.40	20.20	19.63	19.56
FeO	0.00	0.06	0.01	0.03	0.00	0.00	0.01	0.00
MnO	0.00	0.01	0.00	0.00	0.00	0.00	0.00	0.00
MgO	0.00	0.03	0.00	0.03	0.11	0.08	0.03	0.00
BaO	0.00	0.10	0.02	0.00	0.00	0.02	0.00	0.42
CaO	0.03	0.00	0.15	0.08	0.00	0.22	0.22	0.05
Na ₂ O	1.61	0.56	11.50	10.56	11.90	11.54	12.12	11.51
K ₂ O	14.29	14.93	0.13	0.08	0.04	0.12	0.06	0.17
Total	98.44	97.78	98.72	98.87	100.70	99.83	98.87	99.24
Si	11.94	11.97	11.96	12.09	12.00	11.85	11.85	11.93
Al	4.08	4.09	4.03	3.99	3.96	4.17	4.10	4.07
Ti	0.00	0.00	0.00	0.00	0.01	0.01	0.00	0.00
Fe ₂	0.00	0.01	0.00	0.00	0.00	0.00	0.00	0.00
Mn	0.00	0.00	0.00	0.00	0.00	0.00	0.00	0.00
Mg	0.00	0.01	0.00	0.01	0.03	0.02	0.01	0.00
Ba	0.00	0.01	0.00	0.00	0.00	0.00	0.00	0.03
Ca	0.01	0.00	0.03	0.02	0.00	0.04	0.04	0.01
Na	0.58	0.20	3.95	3.60	4.00	3.92	4.17	3.94
K	3.40	3.58	0.03	0.02	0.01	0.03	0.01	0.04
Ab	14.60	5.40	98.60	99.10	99.80	98.30	98.70	98.80
An	0.20	0.00	0.70	0.40	0.00	1.00	1.00	0.20
Or	85.20	94.60	0.70	0.50	0.20	0.70	0.30	1.00

Microprobe data for feldspars from the Lake Lewis Leucogranite.

Sample	LL99-6	LL99-6						
Analysis	6k-1c	6k-1r	6k-7c	6k-7r	6k-8c	6k-8r	6p-2c	6p-2r
Location	core	rim	core	rim	core	rim	core	rim
Mineral	K-feldspar	K-feldspar	K-feldspar	K-feldspar	K-feldspar	K-feldspar	plagioclase	plagioclase
SiO ₂	62.51	63.86	63.70	63.49	63.50	63.45	66.82	66.68
TiO ₂	0.00	0.05	0.01	0.00	0.05	0.00	0.00	0.07
Al ₂ O ₃	18.50	18.49	18.72	18.54	18.87	19.07	20.63	20.17
FeO	0.04	0.00	0.00	0.00	0.00	0.11	0.00	0.00
MnO	0.00	0.00	0.00	0.00	0.02	0.00	0.00	0.04
MgO	0.00	0.00	0.02	0.01	0.03	0.00	0.00	0.00
BaO	0.00	0.00	0.00	0.04	0.00	0.00	0.00	0.00
CaO	0.00	0.00	0.00	0.00	0.00	0.00	0.82	0.70
Na ₂ O	0.43	0.27	1.33	0.49	1.56	1.27	10.94	10.07
K ₂ O	16.30	16.72	15.38	16.47	15.35	15.08	0.39	0.25
Total	97.78	99.39	99.16	99.04	99.38	98.98	99.60	97.98
Si	11.87	11.92	11.88	11.90	11.83	11.84	11.76	11.87
Al	4.14	4.07	4.11	4.09	4.14	4.19	4.28	4.23
Ti	0.00	0.01	0.00	0.00	0.01	0.00	0.00	0.01
Fe ₂	0.01	0.00	0.00	0.00	0.00	0.02	0.00	0.00
Mn	0.00	0.00	0.00	0.00	0.00	0.00	0.00	0.01
Mg	0.00	0.00	0.01	0.00	0.01	0.00	0.00	0.00
Ba	0.00	0.00	0.00	0.00	0.00	0.00	0.00	0.00
Ca	0.00	0.00	0.00	0.00	0.00	0.00	0.16	0.13
Na	0.16	0.10	0.48	0.18	0.56	0.46	3.73	3.47
K	3.95	3.98	3.66	3.94	3.65	3.59	0.09	0.06
Ab	3.80	2.40	11.60	4.30	13.40	11.30	93.90	94.80
An	0.00	0.00	0.00	0.00	0.00	0.00	3.90	3.60
Or	96.20	97.60	88.40	95.70	86.60	88.70	2.20	1.60

Microprobe data for feldspars from the Lake Lewis Leucogranite.

Sample	LL99-6	LL99-6	LL99-6	LL99-6	LL99-6	LL99-6	LL99-7	LL99-7
Analysis	6p-3c	6p-3r	6p-5c	6p-5r	6p-6c	6p-6r	7k10c	7k10r
Location	core	rim	core	rim	core	rim	core	rim
Mineral	plagioclase	plagioclase	plagioclase	plagioclase	plagioclase	plagioclase	K-feldspar	K-feldspar
SiO ₂	66.77	68.06	68.44	68.24	68.41	68.28	63.77	62.73
TiO ₂	0.00	0.00	0.00	0.00	0.00	0.00	0.05	0.02
Al ₂ O ₃	20.34	19.66	19.18	19.50	19.30	19.72	18.64	18.41
FeO	0.08	0.00	0.01	0.00	0.00	0.00	0.05	0.00
MnO	0.03	0.00	0.01	0.00	0.00	0.00	0.07	0.08
MgO	0.05	0.00	0.03	0.00	0.05	0.03	0.08	0.04
BaO	0.00	0.00	0.00	0.00	0.00	0.00	0.00	0.01
CaO	0.61	0.04	0.15	0.09	0.07	0.38	0.00	0.00
Na ₂ O	10.13	11.67	11.05	10.76	12.03	11.38	1.64	0.38
K ₂ O	0.19	0.14	0.02	0.12	0.12	0.16	14.44	14.93
Total	98.20	99.57	98.89	98.71	99.98	99.95	98.74	96.60
Si	11.85	11.95	12.05	12.03	11.97	11.94	11.89	11.94
Al	4.25	4.06	3.98	4.05	3.98	4.06	4.09	4.13
Ti	0.00	0.00	0.00	0.00	0.00	0.00	0.01	0.00
Fe ₂	0.01	0.00	0.00	0.00	0.00	0.00	0.01	0.00
Mn	0.01	0.00	0.00	0.00	0.00	0.00	0.01	0.01
Mg	0.01	0.00	0.01	0.00	0.01	0.01	0.02	0.01
Ba	0.00	0.00	0.00	0.00	0.00	0.00	0.00	0.00
Ca	0.12	0.01	0.03	0.02	0.01	0.07	0.00	0.00
Na	3.49	3.97	3.77	3.68	4.08	3.86	0.59	0.14
K	0.04	0.03	0.00	0.03	0.03	0.04	3.44	3.63
Ab	95.60	99.00	99.20	98.80	99.00	97.30	14.70	3.70
An	3.20	0.20	0.70	0.50	0.30	1.80	0.00	0.00
Or	1.20	0.80	0.10	0.70	0.70	0.90	85.30	96.30

Microprobe data for feldspars from the Lake Lewis Leucogranite.

Sample	LL99-7	LL99-7	LL99-7	LL99-7	LL99-7	LL99-7	LL99-7	LL99-7
Analysis	7k8c	7k8r	7k9c	7k9r	7p-1c	7p-3c	7p-3r	7p-4c
Location	core	rim	core	rim	core	core	rim	core
Mineral	K-feldspar	K-feldspar	K-feldspar	K-feldspar	plagioclase	plagioclase	plagioclase	plagioclase
SiO ₂	63.92	63.86	63.75	63.85	67.77	67.26	67.89	68.42
TiO ₂	0.00	0.02	0.00	0.00	0.00	0.06	0.06	0.00
Al ₂ O ₃	18.85	18.65	18.53	18.56	19.67	20.16	20.28	19.98
FeO	0.00	0.06	0.00	0.03	0.09	0.00	0.00	0.00
MnO	0.06	0.00	0.00	0.00	0.03	0.00	0.00	0.00
MgO	0.07	0.00	0.06	0.10	0.00	0.02	0.00	0.04
BaO	0.00	0.00	0.00	0.00	0.00	0.07	0.00	0.16
CaO	0.00	0.00	0.00	0.02	0.11	0.32	0.21	0.02
Na ₂ O	1.29	0.83	1.61	1.17	11.24	11.13	11.60	10.29
K ₂ O	15.29	15.10	14.68	15.40	0.08	0.13	0.15	0.07
Total	99.48	98.52	98.63	99.13	98.99	99.15	100.19	98.98
Si	11.87	11.94	11.91	11.90	11.95	11.86	11.85	12.01
Al	4.12	4.11	4.08	4.07	4.08	4.19	4.17	4.13
Ti	0.00	0.00	0.00	0.00	0.00	0.01	0.01	0.00
Fe ₂	0.00	0.01	0.00	0.01	0.01	0.00	0.00	0.00
Mn	0.01	0.00	0.00	0.00	0.00	0.00	0.00	0.00
Mg	0.02	0.00	0.02	0.03	0.00	0.01	0.00	0.01
Ba	0.00	0.00	0.00	0.00	0.00	0.01	0.00	0.01
Ca	0.00	0.00	0.00	0.00	0.02	0.06	0.04	0.00
Na	0.46	0.30	0.58	0.42	3.84	3.80	3.93	3.50
K	3.62	3.60	3.50	3.66	0.02	0.03	0.03	0.02
Ab	11.40	7.70	14.30	10.30	99.00	97.70	98.20	99.40
An	0.00	0.00	0.00	0.10	0.50	1.50	1.00	0.10
Or	88.60	92.30	85.70	89.60	0.50	0.70	0.80	0.50

Microprobe data for feldspars from the Lake Lewis Leucogranite.

Sample	LL99-7	LL99-7	LL99-7	LL99-8	LL99-8	LL99-8	LL99-8	LL99-8
Analysis	7p-4r	7p-7c	7p-7r	8k-30c	8k-30r	8k-7c	8k-7r	8k-8c
Location	rim	core	rim	core	rim	core	rim	core
Mineral	plagioclase	plagioclase	plagioclase	K-feldspar	K-feldspar	K-feldspar	K-feldspar	K-feldspar
SiO ₂	67.16	68.07	67.99	64.75	64.96	64.57	62.57	64.75
TiO ₂	0.00	0.00	0.04	0.00	0.00	0.07	0.01	0.00
Al ₂ O ₃	20.30	20.02	19.90	18.43	18.77	19.09	18.88	18.98
FeO	0.00	0.00	0.00	0.09	0.03	0.08	0.06	0.01
MnO	0.00	0.00	0.00	0.00	0.00	0.00	0.08	0.01
MgO	0.00	0.00	0.14	0.00	0.00	0.00	0.00	0.03
BaO	0.00	0.00	0.00	0.09	0.00	0.00	0.23	0.14
CaO	0.30	0.12	0.13	0.00	0.02	0.00	0.01	0.00
Na ₂ O	10.28	11.34	10.79	1.55	0.39	1.03	0.79	1.18
K ₂ O	0.11	0.16	0.11	14.91	15.94	15.34	15.42	14.90
Total	98.15	99.71	99.10	99.82	100.11	100.18	98.05	100.00
Si	11.90	11.92	11.95	11.96	11.97	11.89	11.82	11.92
Al	4.24	4.13	4.12	4.01	4.07	4.14	4.20	4.12
Ti	0.00	0.00	0.01	0.00	0.00	0.01	0.00	0.00
Fe ₂	0.00	0.00	0.00	0.01	0.01	0.01	0.01	0.00
Mn	0.00	0.00	0.00	0.00	0.00	0.00	0.01	0.00
Mg	0.00	0.00	0.04	0.00	0.00	0.00	0.00	0.01
Ba	0.00	0.00	0.00	0.01	0.00	0.00	0.02	0.01
Ca	0.06	0.02	0.02	0.00	0.00	0.00	0.00	0.00
Na	3.53	3.85	3.68	0.56	0.14	0.37	0.29	0.42
K	0.03	0.04	0.03	3.51	3.75	3.60	3.72	3.50
Ab	97.70	98.50	98.70	13.60	3.60	9.30	7.20	10.70
An	1.60	0.60	0.60	0.00	0.10	0.00	0.00	0.00
Or	0.70	0.90	0.70	86.40	96.30	90.70	92.70	89.30

Microprobe data for feldspars from the Lake Lewis Leucogranite.

Sample	LL99-8	LL99-8	LL99-8	LL99-8	LL99-8	LL99-8	LL99-8	LL99-8
Analysis	8k-8r	8k10c	8k10r	8p-1c	8p-1r	8p-20c	8p-20r	8p-21c
Location	rim	core	rim	core	rim	core	rim	core
Mineral	K-feldspar	K-feldspar	K-feldspar	plagioclase	plagioclase	plagioclase	plagioclase	plagioclase
SiO ₂	64.49	64.42	62.43	68.32	68.73	68.97	70.05	67.32
TiO ₂	0.00	0.02	0.11	0.00	0.05	0.09	0.00	0.00
Al ₂ O ₃	19.31	18.95	18.09	19.59	19.71	19.53	19.58	20.04
FeO	0.00	0.00	0.07	0.01	0.00	0.01	0.00	0.00
MnO	0.08	0.10	0.00	0.00	0.12	0.00	0.00	0.00
MgO	0.04	0.08	0.00	0.05	0.00	0.06	0.04	0.07
BaO	0.28	0.10	0.00	0.00	0.00	0.01	0.00	0.00
CaO	0.00	0.02	0.20	0.08	0.02	0.15	0.02	0.49
Na ₂ O	0.84	1.55	0.17	11.31	10.46	9.17	9.39	11.07
K ₂ O	15.29	14.77	16.31	0.16	0.08	0.22	0.11	0.22
Total	100.33	100.01	97.38	99.52	99.17	98.21	99.19	99.21
Si	11.87	11.88	11.90	11.98	12.04	12.13	12.18	11.86
Al	4.18	4.11	4.06	4.05	4.07	4.05	4.01	4.16
Ti	0.00	0.00	0.02	0.00	0.01	0.01	0.00	0.00
Fe ₂	0.00	0.00	0.01	0.00	0.00	0.00	0.00	0.00
Mn	0.01	0.02	0.00	0.00	0.02	0.00	0.00	0.00
Mg	0.01	0.02	0.00	0.01	0.00	0.02	0.01	0.02
Ba	0.02	0.01	0.00	0.00	0.00	0.00	0.00	0.00
Ca	0.00	0.00	0.04	0.02	0.00	0.03	0.00	0.09
Na	0.30	0.55	0.06	3.85	3.55	3.13	3.17	3.78
K	3.59	3.47	3.97	0.04	0.02	0.05	0.02	0.05
Ab	7.70	13.70	1.50	98.70	99.40	97.60	99.10	96.40
An	0.00	0.10	1.00	0.40	0.10	0.90	0.10	2.40
Or	92.30	86.20	97.40	0.90	0.50	1.50	0.80	1.20

Microprobe data for feldspars from the Lake Lewis Leucogranite.

Sample	LL99-8						
Analysis	8p-21r	8p-22c	8p-22r	8p-23c	8p-23r	8p-24c	8p-24r
Location	rim	core	rim	core	rim	core	rim
Mineral	plagioclase						
SiO ₂	68.96	69.41	68.90	68.38	69.58	66.86	69.16
TiO ₂	0.00	0.00	0.00	0.00	0.00	0.03	0.00
Al ₂ O ₃	19.61	20.05	19.73	19.91	19.82	20.45	19.48
FeO	0.01	0.00	0.03	0.00	0.00	0.15	0.07
MnO	0.00	0.11	0.00	0.00	0.00	0.08	0.10
MgO	0.00	0.03	0.05	0.00	0.01	0.00	0.00
BaO	0.00	0.00	0.00	0.13	0.00	0.00	0.00
CaO	0.04	0.14	0.11	0.25	0.00	0.85	0.05
Na ₂ O	11.43	9.75	10.38	10.26	9.88	10.51	11.83
K ₂ O	0.19	0.09	0.15	0.17	0.09	0.35	0.02
Total	100.24	99.58	99.35	99.10	99.38	99.28	100.71
Si	12.00	12.07	12.04	12.00	12.11	11.79	12.00
Al	4.02	4.11	4.06	4.12	4.06	4.25	3.98
Ti	0.00	0.00	0.00	0.00	0.00	0.00	0.00
Fe ₂	0.00	0.00	0.00	0.00	0.00	0.02	0.01
Mn	0.00	0.02	0.00	0.00	0.00	0.01	0.02
Mg	0.00	0.01	0.01	0.00	0.00	0.00	0.00
Ba	0.00	0.00	0.00	0.01	0.00	0.00	0.00
Ca	0.01	0.03	0.02	0.05	0.00	0.16	0.01
Na	3.86	3.29	3.52	3.49	3.33	3.59	3.98
K	0.04	0.02	0.03	0.04	0.02	0.08	0.00
Ab	98.70	98.60	98.50	97.60	99.40	93.70	99.70
An	0.20	0.80	0.60	1.30	0.00	4.20	0.20
Or	1.10	0.60	0.90	1.10	0.60	2.10	0.10

Microprobe data for feldspars from the Lake Lewis Leucogranite.

Sample	LL99-8						
Analysis	8p-25c	8p-25r	8p-26c	8p-26r	8p-27c	8p-27r	8p-28c
Location	core	rim	core	rim	core	rim	core
Mineral	plagioclase						
SiO ₂	66.32	68.80	67.80	68.93	67.00	69.24	67.93
TiO ₂	0.02	0.00	0.07	0.02	0.00	0.05	0.00
Al ₂ O ₃	21.33	19.66	20.63	19.69	20.88	19.74	21.52
FeO	0.01	0.00	0.00	0.00	0.06	0.02	0.00
MnO	0.00	0.05	0.07	0.04	0.01	0.00	0.00
MgO	0.02	0.05	0.00	0.06	0.04	0.12	0.03
BaO	0.00	0.00	0.00	0.00	0.00	0.00	0.00
CaO	1.71	0.01	0.80	0.13	1.28	0.12	1.53
Na ₂ O	9.36	11.14	9.36	10.65	9.58	10.36	7.95
K ₂ O	0.23	0.23	0.23	0.14	0.29	0.12	0.05
Total	99.00	99.94	98.96	99.66	99.14	99.77	99.01
Si	11.69	12.00	11.90	12.03	11.79	12.05	11.86
Al	4.43	4.04	4.26	4.05	4.33	4.05	4.42
Ti	0.00	0.00	0.01	0.00	0.00	0.01	0.00
Fe ₂	0.00	0.00	0.00	0.00	0.01	0.00	0.00
Mn	0.00	0.01	0.01	0.01	0.00	0.00	0.00
Mg	0.01	0.01	0.00	0.02	0.01	0.03	0.01
Ba	0.00	0.00	0.00	0.00	0.00	0.00	0.00
Ca	0.32	0.00	0.15	0.02	0.24	0.02	0.29
Na	3.20	3.77	3.19	3.60	3.27	3.50	2.69
K	0.05	0.05	0.05	0.03	0.07	0.03	0.01
Ab	89.50	98.60	94.10	98.50	91.40	98.60	90.10
An	9.00	0.10	4.40	0.70	6.70	0.60	9.60
Or	1.50	1.30	1.50	0.80	1.80	0.80	0.40

Microprobe data for feldspars from the Lake Lewis Leucogranite.

Sample	LL99-8						
Analysis	8p-28r	8p-29c	8p-29r	8p-2c	8p-3c	8p-3r	8p-9c
Location	rim	core	rim	core	core	rim	core
Mineral	plagioclase						
SiO ₂	69.08	67.51	69.37	66.34	66.82	67.96	61.52
TiO ₂	0.00	0.12	0.00	0.00	0.05	0.04	0.05
Al ₂ O ₃	20.16	19.37	19.46	20.75	21.03	20.78	24.78
FeO	0.09	0.00	0.00	0.07	0.00	0.00	0.05
MnO	0.11	0.00	0.00	0.04	0.00	0.02	0.03
MgO	0.00	0.04	0.02	0.00	0.09	0.12	0.03
BaO	0.01	0.00	0.02	0.00	0.01	0.00	0.00
CaO	0.03	0.27	0.00	0.62	0.61	0.16	5.78
Na ₂ O	9.60	11.38	10.52	9.57	9.59	10.25	8.13
K ₂ O	0.21	0.24	0.12	0.23	0.10	0.09	0.21
Total	99.29	98.93	99.51	97.62	98.30	99.42	100.58
Si	12.05	11.94	12.10	11.82	11.81	11.88	10.86
Al	4.14	4.03	4.00	4.36	4.38	4.28	5.15
Ti	0.00	0.02	0.00	0.00	0.01	0.01	0.01
Fe ₂	0.01	0.00	0.00	0.01	0.00	0.00	0.01
Mn	0.02	0.00	0.00	0.01	0.00	0.00	0.00
Mg	0.00	0.01	0.01	0.00	0.02	0.03	0.01
Ba	0.00	0.00	0.00	0.00	0.00	0.00	0.00
Ca	0.01	0.05	0.00	0.12	0.12	0.03	1.09
Na	3.25	3.90	3.56	3.31	3.29	3.47	2.78
K	0.05	0.05	0.03	0.05	0.02	0.02	0.05
Ab	98.40	97.40	99.20	95.10	95.90	98.60	70.90
An	0.20	1.30	0.00	3.40	3.40	0.90	27.90
Or	1.40	1.30	0.80	1.50	0.70	0.60	1.20

Microprobe data for feldspars from the Lake Lewis Leucogranite.

Sample	LL99-8	LL99-9						
Analysis	8p-9r	9k1c	9k1r	9k2c	9k2r	9k3c	9k3r	9p4c
Location	rim	core	rim	core	rim	core	rim	core
Mineral	plagioclase	K-feldspar	K-feldspar	K-feldspar	K-feldspar	K-feldspar	K-feldspar	plagioclase
SiO ₂	66.79	63.48	64.56	64.81	64.59	64.55	64.30	66.95
TiO ₂	0.00	0.07	0.00	0.00	0.00	0.02	0.04	0.00
Al ₂ O ₃	20.65	18.96	19.32	19.15	19.36	19.46	19.35	20.85
FeO	0.10	0.00	0.02	0.00	0.00	0.00	0.11	0.05
MnO	0.00	0.00	0.07	0.04	0.04	0.00	0.04	0.00
MgO	0.00	0.07	0.00	0.00	0.00	0.10	0.06	0.07
BaO	0.16	0.00	0.00	0.14	0.02	0.01	0.12	0.04
CaO	0.30	0.00	0.00	0.00	0.01	0.00	0.00	0.31
Na ₂ O	11.31	0.34	0.84	0.82	0.85	1.10	1.11	10.69
K ₂ O	0.26	15.55	14.71	14.96	14.63	14.48	14.72	0.09
Total	99.57	98.47	99.52	99.92	99.50	99.72	99.85	99.05
Si	11.76	11.88	11.90	11.93	11.90	11.87	11.85	11.79
Al	4.28	4.18	4.20	4.15	4.20	4.22	4.20	4.33
Ti	0.00	0.01	0.00	0.00	0.00	0.00	0.01	0.00
Fe ₂	0.02	0.00	0.00	0.00	0.00	0.00	0.02	0.01
Mn	0.00	0.00	0.01	0.01	0.01	0.00	0.01	0.00
Mg	0.00	0.02	0.00	0.00	0.00	0.03	0.02	0.02
Ba	0.01	0.00	0.00	0.01	0.00	0.00	0.01	0.00
Ca	0.06	0.00	0.00	0.00	0.00	0.00	0.00	0.06
Na	3.86	0.12	0.30	0.29	0.30	0.39	0.40	3.65
K	0.06	3.71	3.46	3.51	3.44	3.40	3.46	0.02
Ab	97.10	3.20	8.00	7.70	8.10	10.30	10.30	97.90
An	1.40	0.00	0.00	0.00	0.10	0.00	0.00	1.60
Or	1.50	96.80	92.00	92.30	91.80	89.70	89.70	0.50

Microprobe data for feldspars from the Lake Lewis Leucogranite.

Sample	LL99-9	LL99-9	LL99-9	LL99-9	LL99-9
Analysis	9p4r	9p5c	9p5r	9p6c	9p6r
Location	rim	core	rim	core	rim
Mineral	plagioclase	plagioclase	plagioclase	plagioclase	plagioclase
SiO ₂	68.61	68.22	67.92	66.97	67.96
TiO ₂	0.00	0.08	0.01	0.04	0.00
Al ₂ O ₃	20.22	20.90	20.30	20.59	20.16
FeO	0.04	0.00	0.00	0.08	0.00
MnO	0.00	0.00	0.01	0.07	0.00
MgO	0.10	0.00	0.02	0.01	0.08
BaO	0.00	0.22	0.00	0.00	0.00
CaO	0.06	0.18	0.13	0.14	0.00
Na ₂ O	10.59	8.51	8.68	11.20	11.47
K ₂ O	0.07	0.06	0.13	0.18	0.17
Total	99.69	98.17	97.20	99.28	99.84
Si	11.96	11.99	12.05	11.80	11.89
Al	4.15	4.33	4.24	4.27	4.15
Ti	0.00	0.01	0.00	0.01	0.00
Fe ₂	0.01	0.00	0.00	0.01	0.00
Mn	0.00	0.00	0.00	0.01	0.00
Mg	0.03	0.00	0.01	0.00	0.02
Ba	0.00	0.02	0.00	0.00	0.00
Ca	0.01	0.03	0.03	0.03	0.00
Na	3.58	2.90	2.99	3.83	3.89
K	0.02	0.01	0.03	0.04	0.04
Ab	99.30	98.40	98.20	98.30	99.00
An	0.30	1.20	0.80	0.70	0.00
Or	0.40	0.40	1.00	1.00	1.00

NOTES

NOTES